A tale of two nervous systems: mechanisms regulating glial migration across nervous system boundaries.

Taylor Garrett Welsh
Staunton, Virginia

B.S., Washington and Lee University, 2011

A Dissertation presented to the Graduate Faculty of the University of Virginia in Candidacy for the Degree of Doctor of Philosophy

Department of Biology

University of Virginia

July, 2018

Abstract

A functional nervous system consists of two halves: the central nervous system (CNS) and peripheral nervous system (PNS). Although these two halves are, for the most part, anatomically separate, their communication relies on specialized connections called transition zones (TZ) which form early in development. At these transition zones, axons cross in or out of the spinal cord, connecting CNS and PNS. Some glial cells migrate through TZs as part of normal nervous system development, while many others are restricted from migrating through, although they can send processes into the TZ and interact with glia on the other side. The mechanisms regulating TZ formation and migration of cells across TZ boundaries are not understood, although interactions between CNS and PNS cells are thought to play a major role. My research has discovered novel mechanisms regulating cell migration across TZs, focusing particularly on one type of glia, oligodendrocyte progenitor cells (OPCs). I have characterized a newly discovered cell type, motor exit point (MEP) glia, which are essential for preventing OPCs from migrating into the PNS. I have also discovered that neuronal modulation via adenosine signaling is an additional mechanism involved in regulating OPC migration. This work demonstrates the importance and specificity of cellular interactions in regulating cell migration and nervous system patterning.

Dedication

This work is dedicated to my loving, supportive, and strong husband, Daniel. You have prayed for and encouraged me, celebrated and sympathized with me. You even drove me over the mountain when I was sick so I wouldn't have to repeat an experiment, and you learned how to say "oligodendrocyte." To Mom and Dad, who always wanted to hear how experiments were going, and who encouraged me to "just keep swimming." To Ellie, who showed me in a way no one else could why all of this is so amazing.

Table of Contents

Figures and Tables

I. Nervous system development and introduction to transition zones

II. Materials and Methods

III. MEP glia: a novel cell involved in restricting OPC migration

IV. The neuromodulator adenosine regulates oligodendrocyte migration at motor exit point transition zones

Chapter 1

Nervous system development and introduction to transition zones

Introduction

A functional nervous system consists of two halves: the central nervous system (CNS) and peripheral nervous system (PNS). The PNS relays sensory information from peripheral organs to the spinal cord and brain in the CNS, which process the information and coordinate motor outputs. The motor outputs initiated in the CNS are sent through peripheral motor axons to reach peripheral targets such as skeletal muscle (Figure 1-1A). This summary simplifies the many complex abilities of vertebrate nervous systems, but it makes clear the important interrelation of the CNS and PNS. Although these two halves are, for the most part, anatomically separate, their communication relies on specialized connections which form early in development. At these specialized zones, called transition zones (TZ), axons penetrate through gaps in the basal lamina border of the spinal cord to connect the CNS and PNS. Although these sensory and motor axons form pathways into and out of the CNS, their cell bodies are restricted to the PNS and CNS, respectively (Figure 1-1B). Highly migratory glial precursors of the CNS and PNS associate with axons that cross through the TZ. Glial cells extend processes short distances into the transition zone, but with a few notable exceptions, the cell bodies are not permitted to migrate through. The interactions among glial cells at the TZ may be involved in regulating the segregation between CNS and PNS cells (Figure 1-1B).

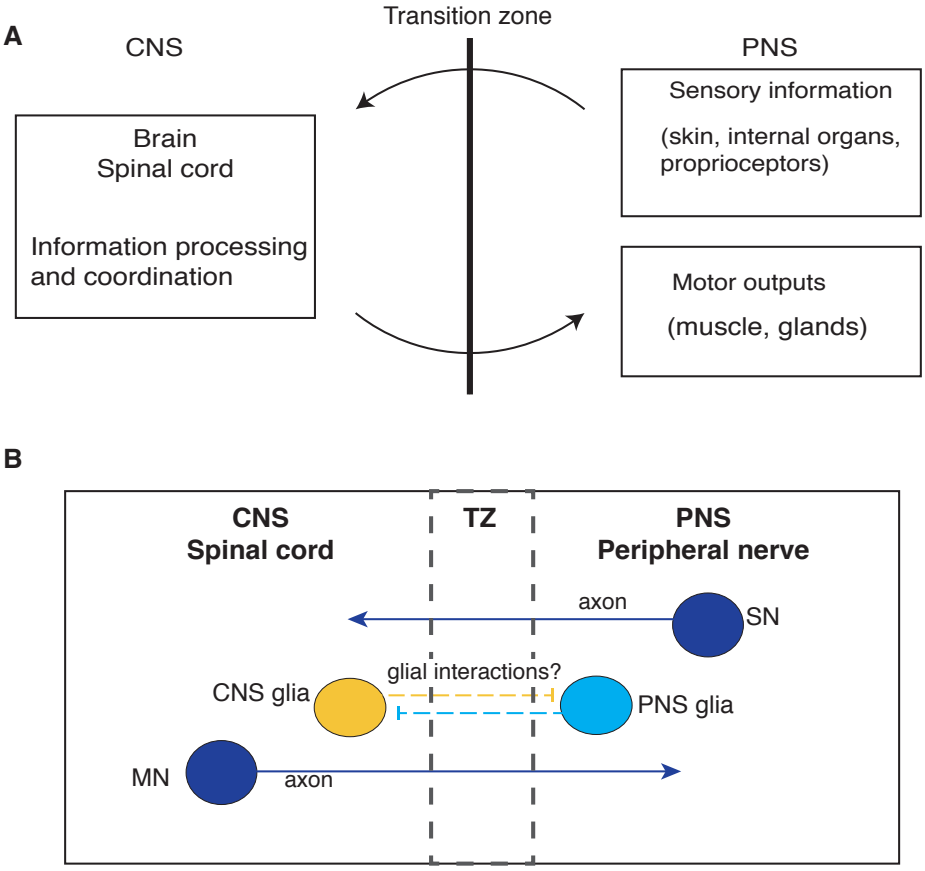

Figure 1-1 Summary of CNS/PNS interactions. (A) Peripheral tissues relay sensory information across transition zones (TZ) into the CNS. Information processing occurs within the CNS, and motor outputs are coordinated and initiated within the CNS. Motor signals from the CNS cross through TZs to reach targets in the PNS. (B) Motor neuron cell bodies reside within the spinal cord and extend axons through ventral TZs into the PNS. In contrast, sensory neuron cell bodies reside within the PNS and extend axons through dorsal TZs into the spinal cord. The TZ also forms a boundary separating CNS and PNS glia. Glial processes from the CNS and PNS extend into the TZ, but glial cell bodies do not migrate through. Interactions between CNS and PNS glia across TZs are not well understood, but are likely important for establishing and maintaining cell segregation at TZs.

CNS: motor neurons, oligodendrocytes, and other glia

The CNS consists of many types of neurons which transmit signals for motor control, sensory integration, and many higher-order processes such as sleep, learning, and memory. However, neurons cannot function properly without closely associated glial cells, which outnumber CNS neurons nearly 10:1 in the human brain (Rowitch, 2004). Oligodendrocytes, one type of glia, perform the essential role of wrapping neuronal axons with a membrane structure called myelin. Myelin is a lipid-rich structure that electrically insulates axons, promoting rapid conduction of action potentials. Myelin sheaths are also involved in exchange of nutrients and waste products between neurons and oligodendrocytes, so that oligodendrocytes provide essential metabolic support for neurons (Philips and Rothstein, 2017). The importance of oligodendrocytes and myelin for CNS function is underscored by the severe neurological defects observed in mouse mutants or human patients deficient in oligodendrocyte numbers or myelin production (Birey et al., 2017; Lemus et al., 2018). Recently, the groundbreaking discoveries that myelin is remodeled throughout adult life and that new myelin production is required for some types of learning emphasize the importance of oligodendrocytes and their precursors, oligodendrocyte progenitor cells (OPCs) not only during development, but throughout life (Almeida and Lyons, 2017).

My research has focused on CNS and PNS cell interactions across spinal cord TZs. Therefore, I will focus here on characteristics of CNS cells involved in these interactions.

Both motor and sensory neurons extend axons across TZs, which connect the CNS with peripheral targets, and many CNS and PNS glial cell types interact across TZs (Figure 1-2). Intriguingly, motor neurons, OPCs, and motor exit point (MEP) glia, which have important interactions in forming and maintaining MEP TZs, are all specified within a common progenitor domain within the spinal cord. Early patterning events in the embryonic neural tube establish transcriptional programs which are essential for the specification and differentiation of each cell type. Understanding these programs can give some clues toward how to study each cell type, and also how their interactions may be regulated. Early in development, a gradient of *sonic hedgehog* (*shh*) signaling establishes a dorsal-ventral axis of progenitor domains. Each domain has a unique transcriptional program and gives rise to distinct types of neurons and glia. For example, *shh* initiates expression of the transcription factor *oligodendrocyte transcription factor 2* (*olig2*) within a ventral region of the spinal cord called the motor neuron progenitor (pMN) domain (Rowitch, 2004). Olig2 represses expression of another transcription factor, *NK2 homeobox 2* (*nkx2.2*), which is expressed in and essential for establishing the more ventral p3 domain (Rowitch, 2004). Paracrine repression in this way establishes a distinct separation of *nkx2.2*-expressing cells in the ventral most p3 domain, and *olig2*-expressing cells in the pMN domain. *Olig2* is necessary for the specification of all cell types derived from pMN precursors (Rowitch, 2004). Since motor neurons, OPCs, and MEP glia are all specified in the pMN domain, they all express *olig2*, at least initially (Park et al., 2002; Smith et al., 2014).

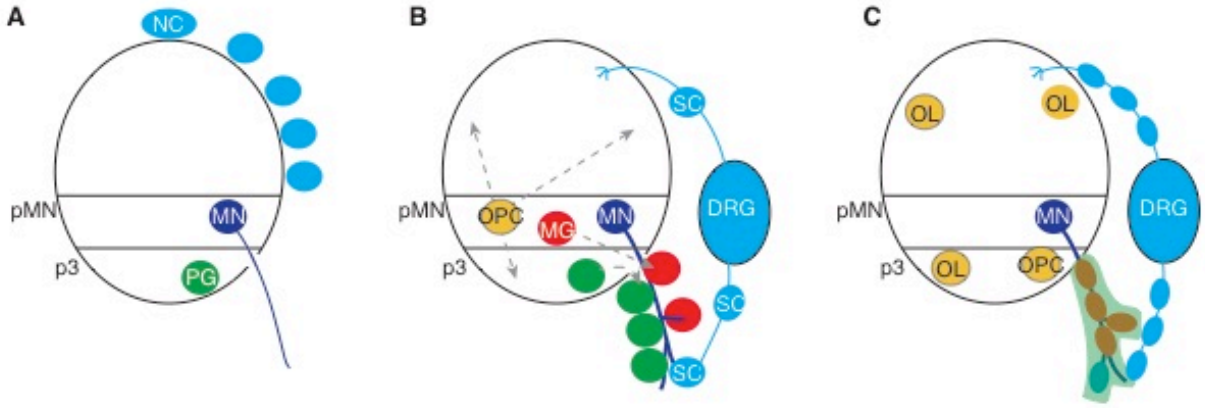

Figure 1-2 Development of zebrafish spinal nerves roots. (A) Motor neurons (MN) are specified in the spinal cord pMN domain. Motor axons extend through the motor exit point (MEP) into the PNS. Perineurial glia (PG) are specified from precursors in the p3 domain of the ventral spinal cord. The neural crest (NC) forms at the dorsal neural tube and neural crest cells (NCC) migrate ventrally. Migrating NCC reach the MEP soon after the first motor axons reach the periphery. (B) After neuronal specification, MEP glia (MG) and oligodendrocyte progenitor cells (OPCs) are specified within the pMN domain. OPCs migrate dorsally and ventrally (gray arrows) to disperse throughout the spinal cord and associate with CNS axons. MG migrate into the periphery through the MEP and associate with axons at the motor root. Perineurial glia extend processes out of the spinal cord through the MEP and eventually the entire cell body migrates into the PNS. Some NCCs at the motor root differentiate into sensory neurons and glia of the dorsal root ganglion (DRG). DRG neurons extend axons centrally into the spinal cord at the dorsal root entry zone (DREZ) and peripherally. Other NCCs differentiate into Schwann cells (SC) and associate with motor and sensory axons. (C) During differentiation, OPCs differentiate into oligodendrocytes (OL) and myelinate dorsal and ventral CNS axons. Some OPCs persist through development. MG (red) ensheathe proximal motor axon segments and produce myelin. SC (light blue) enseheathe more distal motor axon segments and sensory axons and form myelin sheaths. PG ensheath bundles of axons, MG, and SC and mature into the perineurium (green).

There is still some debate over whether neurons and glia specified in the pMN derive from common progenitor cells, or whether a mixture of fate-restricted cells separately differentiate into neurons or glia (Ravanelli and Appel, 2015; Rowitch, 2004). However, it is clear that neurons are specified first, and a temporal switch occurs when glial specification begins (Park et al., 2002; Richardson et al., 2000). In zebrafish, primary motor neurons are specified at the beginning of neural tube formation, and secondary neurogenesis continues past 24 hpf (Lewis and Eisen, 2003). The first motor axons emerge through the MEP at 18 hpf (Figure 1-2A) (Myers et al., 1986). OPC specification begins at 36 hpf, and at 48 hpf, OPCs begin to migrate and disperse from the pMN domain throughout the spinal cord (Kirby et al., 2006; Kucenas et al., 2008a). During this phase of active migration, some OPCs divide to produce two daughter OPCs (Figure 1-2B) (Kirby et al., 2006). At 72 hpf, some spinal cord OPCs stop migrating, differentiate into oligodendrocytes, and wrap axons with myelin (Figure 1-2C) (Kirby et al., 2006; Kucenas et al., 2008a). A subset of OPCs persists throughout adulthood and are capable of differentiating into oligodendrocytes to replace dying oligodendrocytes or to produce new myelin sheaths (Hughes et al., 2013). Some of the transcription factors and other signals regulating the processes of OPC specification and differentiation are known. I have already described *olig2*, which is required for motor neuron and OPC specification. In zebrafish, the transgenes *Tg(olig2:egfp)* and *Tg(olig2:dsred)*, which drive expression of fluorescent proteins in cells expressing *olig2*, can be used to visualize OPCs and oligodendrocytes throughout embryonic and larval stages. Additionally, OPCs are characterized by expression of the transcription factor and glial

master regulatory gene *SRY (sex determining region Y)-box 10* (*sox10*), which promotes OPC differentiation and expression of genes involved in myelin production (Emery and Lu, 2015). Zebrafish mutants lacking *sox10* have normal numbers of OPCs, but they do not form oligodendrocytes or myelin, indicating that *sox10* is not required for OPC specification, but is necessary for survival, differentiation and myelination (Takada et al., 2010). This is consistent with the role of *sox10* in regulating oligodendrocyte differentiation in mice (Stolt et al., 2002). Another transcription factor with an intriguing role in oligodendrocyte differentiation is *nkx2.2*. Although initially restricted to the floorplate and p3 domain, *Nkx2.2* (and its zebrafish ortholog *nkx2.2a*) expands its expression dorsally into the pMN domain around the time of OPC specification (Fu et al., 2002; Kucenas et al., 2008a; Zhou et al., 2001). Genetic deletion of *Nkx2.2* in mice or morpholino knock-down of *nkx2.2a* in zebrafish results in a decrease of differentiated, *myelin basic protein*$^{+}$ (*mbp*$^{+}$) oligodendrocytes (Kucenas et al., 2008a; Qi et al., 2001). Interestingly, *nkx2.2a* expression only marks a subset of OPCs in zebrafish, the ones that will go on to differentiate and produce myelin (Kucenas et al., 2008a). As oligodendrocytes differentiate and begin producing myelin, they initiate expression of various genes involved in myelin synthesis. These include *myelin basic protein* (*mbp*), *myelin oligodendrocyte protein* (*mog*), and *proteolipid protein* (*plp*). The factors driving myelination by oligodendrocytes are largely unknown. There is some evidence that oligodendrocytes will myelinate any axon of a given size, so that perhaps a pro-myelinating program is the default state for differentiated oligodendrocytes (Lee et al., 2012). There is also growing evidence for neuronal activity playing a role in regulating

oligodendrocyte myelination. *In vivo* and *in vitro* studies provide evidence that neuronal activity promotes oligodendrocyte differentiation and myelin production (Gibson et al., 2014; Hines et al., 2015; Mensch et al., 2015; Stevens et al., 2002). However, there is disagreement over whether neuronal activity is sufficient to drive myelination or rather fine-tunes myelin production that is primarily driven by other factors. The conclusions from many studies on the effects of neuronal activity are far from straightforward, as might be expected for a process as complicated as myelination. A general trend for increased neuronal activity increasing oligodendrogenesis/myelination and decreased activity decreasing oligodendrogenesis/myelination has been found in many studies. However, many exceptions to this trend exist, and even summary conclusions of "increased myelination" could involve changes in any of the myelin parameters from myelin sheath thickness, internode length, number of internodes produced by individual oligodendrocytes, overall amount of myelin in a given region or the percent of myelinated axons. Despite variations in experimental setups and the complexity of myelin itself contributing to different results, it is abundantly clear that changes in neuronal activity result in changes in OLs and myelin production (Almeida and Lyons, 2017). Since OPC migration, not myelination, has been the focus of much of my research, I will describe below studies that have directly tested the effects of neuronal activity on OPC behaviors.

Neuronal signals regulate OPC proliferation, migration, and differentiation

Even before the onset of myelination, OPCs have multiple processes that closely associate with axons (Ackerman et al., 2015; Cheli et al., 2015; Czopka et al., 2013; Kirby et al., 2006; Kucenas et al., 2008a; Schnädelbach et al., 2001; Ziskin et al., 2007). Recently, many studies provide evidence that OPCs rapidly detect changes in neuronal activity and respond with calcium signaling, changes in proliferation, migration, and/or differentiation (see Almeida and Lyons, 2017; Fields, 2015; Gallo et al., 2008 for reviews). An early study reported that transection of the optic nerve or injections of the sodium channel blocker tetrodotoxin (TTX) into the eye resulted in decreased proliferation of optic nerve OPCs (Barres and Raff, 1993). Since then, many more studies have used various methods to manipulate neuronal activity and observe effects on OPCs. In zebrafish, blocking synaptic vesicle release with tetanus toxin (TeNT) results in a decrease in OPC number, whereas increasing neuronal activity with the $GABA_A$ antagonist pentylenetetrazole (PTZ) resulted in increased numbers of oligodendrocytes (Mensch et al., 2015). Also supporting a role for neuronal signals in influencing oligodendrocyte number, zebrafish mutants with reduced numbers of spinal cord axons have reduced OPC proliferation and reduced numbers of mature oligodendrocytes compared to WT (Almeida and Lyons, 2016). Similarly, optogenetic stimulation of mouse neurons resulted in increased OPC proliferation and differentiation, and training in a complex motor learning task promotes differentiation of new oligodendrocytes (Gibson et al., 2014; Xiao et al., 2016). However, the effects of neuronal activity on oligodendrocytes may be context-dependent or depend on patterns of activity. Two experiments used sensory deprivation to ablate evoked neuronal firing.

One study observed increased differentiation of OPCs into oligodendrocytes, and the other observed increased numbers of OPCs (Etxeberria et al., 2016; Mangin et al., 2012). Interestingly, *in vivo* electrical stimulation promoted OPC proliferation at high frequencies, and differentiation at low frequencies (Nagy et al., 2017).

How do OPCs detect and respond to changes in neuronal activity? Light microscopy studies using various methods to label OPC processes have made clear the extensive physical contacts between OPC processes and axons, so that OPCs are well positioned to detect axonal signals (Ackerman et al., 2015; Cheli et al., 2015; Czopka et al., 2013; Kirby et al., 2006; Schnädelbach et al., 2001; Ziskin et al., 2007) Furthermore, OPCs express glutamate receptors both *in vitro* and *in vivo*, and *in vitro* activation of AMPA-type glutamate receptors decreases OPC proliferation and differentiation (Barres et al., 1990; Berger, 1995; Gallo et al., 1996). A breakthrough in answering this question came from ultrastructural studies of the connections between OPC processes and axons. A landmark study described synaptic structures between OPCs and axons *in vivo* (Bergles et al., 2000). OPC and axonal membranes were separated by a synaptic cleft, with specialized synaptic structures on both axonal and OPC membranes. Within the axon, synaptic vesicles were clustered near the axonal presynaptic membrane. Within the OPC, electron-dense structures resembling post-synaptic densities were observed. Live imaging studies in zebrafish have even enabled observations of synaptic vesicle release from axonal segments in contact with OPC processes (Hines et al., 2015). Electrophysiological recordings from OPCs in slice culture systems have revealed that

stimulation of glutamatergic neurons or bath application of glutamate receptor agonists directly results in post-synaptic currents in the OPC (Bergles et al., 2000; De Biase et al., 2010; Kukley et al., 2007; Lin et al., 2005; Wake et al., 2011; Ziskin et al., 2007). These results demonstrate that OPCs detect neuronal release of glutamate with active ionotropic glutamate receptors, which cause membrane depolarizations on the OPCs. Although OPCs are not electrically active in the sense that they do not fire action potentials or propagate electrical activity to other cells, these membrane depolarizations resulting from neuronal neurotransmitter release can affect expression or activation of ion channels involved in migration or differentiation, or other downstream signaling events (De Biase et al., 2010; Lin and Bergles, 2004). Follow-up studies have discovered that OPCs express active AMPA, NMDA, $GABA_A$, norepinephrine, and acetylcholine receptors, and synapses between OPCs and GABAergic interneurons have also been identified (Lin and Bergles, 2004a, 2004b). In fact, synapses have been identified between OPCs and glutamatergic and GABAergic neurons of various brain regions including hippocampus, corpus callosum, and optic nerve (reviewed in Bergles et al., 2010). Activation of AMPA, NMDA, or acetylcholine receptors has been shown to stimulate OPC migration *in vitro* (Gudz et al., 2006; Xiao et al., 2013). OPCs, with many branched processes, can potentially detect changes in activity from many neurons at once. Some researchers have hypothesized that the effects of modifying neuronal activity on OPCs may not be cell autonomous, that is, OPCs may respond to relative changes in activity of some neurons compared to other nearby neurons, rather than responding to increases or decreases in activity of a single neuron like an on/off switch

for differentiation (Gallo et al., 2008; Hines et al., 2015). This hypothesis is supported by the finding that silencing activity from the axon tracts of one eye altered myelination of those axons, but also affected myelination of nearby axons from the opposite eye, which are bundled into the same tract (Etxeberria et al., 2016). Similarly, manipulating activity levels of certain kinds of neurons, but not others, reduced myelination of those axons (Koudelka et al., 2016). It is an intriguing thought that OPCs may integrate information from many axons in making decisions about proliferation, migration, and ultimately myelination. Theoretically, similar populations of neurons would need similar myelination and conduction levels, so an ability of OPCs to detect and respond to similar or dissimilar firing patterns could be an efficient way to promote circuit formation. This idea could also explain some of the variability between *in vitro* and *in vivo* studies, since *in vitro* studies typically use global modifications to activity. It is a difficult question to test, however, with current technology. It is difficult to precisely control or measure changes in neuronal activity of more than one population of neurons. This is something that zebrafish, with the ability to transgenically label different neuronal populations and image in real time the behavior of OPCs associated with those neurons, could be a powerful system for addressing.

Perineurial glia are PNS glia with CNS origins

While it was long believed that only axons, but never whole cells, crossed through vertebrate TZs during normal development, work by Kucenas et al. proved that in

zebrafish, perineurial glia (PG) are specified within the spinal cord and migrate through the MEP TZ to reach the periphery (Kucenas et al., 2008b). PG are peripheral glial cells that form an essential component of the blood-nerve barrier. Concentric layers of these cells encircle axon-Schwann cell bundles in the mature nerve, beginning proximally at the motor root and extending as far distally as the neuromuscular junction (NMJ). PG are specified in the p3 progenitor domain of the spinal cord and are characterized by expression of the transcription factor *nkx2.2a* (Figure 1-2A). At 45 hpf, they begin migrating through the MEP to enter the PNS (Figure 1-2B). A more recent study showed the central origin of PG in mice, suggesting that the development and migration of these cells is conserved in mammals and fish (Clark et al., 2014). PG precursors within the ventral spinal cord may also be involved in determining the location of the presumptive MEP and/or guiding pioneer motor axons through the proper exit points. In support of this, morpholino knockdown of *nkx2.2a* results in motor axons exiting the spinal cord at irregular, ectopic positions along the anterior-posterior axis (Kucenas et al., 2008b). Motor neuron cell bodies were also observed to be incorrectly positioned outside of the spinal cord along peripheral motor nerves, suggesting that PG or their precursors may also prevent motor neuron cell bodies from exiting the spinal cord along their axons (Kucenas et al., 2008b). As a caveat to these experiments, *nkx2.2a* knockdown disrupts all ventral neuroepithelial cell development, so it is unclear whether the effects on motor neurons are specific to PG. Once in the periphery, PG have important functions in peripheral nerve development, which will be discussed below in the section on the PNS.

MEP glia, another PNS cell with CNS origins

Our lab recently identified another PNS glial cell type that originates within the spinal cord. We have named these cells motor exit point glia (MEP glia), because they stay closely associated with the MEP after migrating into the periphery. Similar to OPCs, MEP glia are specified within the pMN domain, and they express *olig2* and *sox10* (Smith et al., 2014). However, differences in morphology and expression of other markers clearly distinguish MEP glia from OPCs. MEP glia migrate into the periphery at around 56 hpf. They closely associate with the most proximal portions of the peripheral motor roots, and they myelinate the motor root axons (Figure 1-2B&C) (Smith et al. 2014). MEP glia have an important role in maintaining glial segregation at the TZ, and further characterization and details about their function will be the focus of Chapter 3.

PNS: Schwann cells and other neural crest-derived cells

The majority of PNS cells are derived from a progenitor population known as the neural crest, and neural crest cells additionally contribute to tissues in the skin, heart, and cartilage (Lewis and Eisen, 2003; Raible and Eisen, 1994). The neural crest is a transient population of multipotent progenitor cells located at the dorsal neural tube. From their initial location in the dorsal neuroepithelium, streams of neural crest cells delaminate and migrate to various target tissues. In zebrafish, trunk neural crest migration occurs between 15 and 23 hpf, and at around 18 hpf, a subset of cells reaches the MEP, soon after motor axons have extended into periphery (Figure 1-2A) (McGraw et al., 2012; Raible and Eisen, 1994; Vaglia and Hall, 2000). Once at the MEP,

these neural crest cells continue to proliferate. Some continue migrating distally along the nerve and differentiate into proliferative Schwann cell precursors (SCPs), while others cluster near the MEP and become the sensory neurons and glia of the DRG (Figure 1-2B) (Honjo et al., 2008; McGraw et al., 2008). Sensory neurons in the DRG extend peripheral axonal projections to innervate the skin and other peripheral organs. They also extend central axonal projections through the dorsal root entry zone (DREZ) and into the spinal cord (Smith et al., 2017). Thus, sensory axon entry into the spinal cord through the DREZ always occurs after motor axon exit out of the spinal cord through the MEP. From around 24 to 60 hpf, SCPs proliferate, migrate along axons, and continue to differentiate (Lyons et al., 2005; Perlin et al., 2011). While SCPs are associating with motor axons, PG migrate out of the spinal cord and onto the peripheral nerve (Figure 1-2B). Beginning at 72 hpf, mature myelinating Schwann cells wrap individual axons with myelin, or mature nonmyelinating Schwann cells ensheath bundles of small, unmyelinated axons (Figure 1-2C). PG also differentiate and form a sheath of cells around axon-Schwann cell bundles (Figure 1-2C). PG sort bundles of Schwann cells and axons into fascicles, and tight junctions between adjacent PG are an essential component of the blood-nerve barrier (Kucenas et al., 2008b; Morris et al., 2017).

Once they have reached their targets (and in some cases, perhaps while migrating) neural crest cells turn on expression of genes involved in their differentiation. Although the precise timing and regulation of gene expression differs among species, the genes involved in specification and migration are very similar (Raible et al., 1992; Stuhlmiller

and García-Castro, 2012). *neuregulin 1* (*Nrg1*) signaling is critical for neural crest migration to the MEP, as mutants for *Nrg1* or its receptors *erb-b2 receptor tyrosine kinase 2* (*erbb2*) and *erb-b2 receptor tyrosine kinase 3b* (*erbb3*) have absent or misplaced DRGs, and Schwann cells are missing from the nerve (Honjo et al., 2008; Jessen, 2004; Lyons et al., 2005; Meyer et al., 1997). Neural crest cells differentiate into SCPs, which are highly migratory and proliferative, but require *nrg1 type III* from axons to survive. In fact, studies in mice and zebrafish have shown that the *nrg1 type III* isoform expressed by neurons is specifically required for Schwann cell differentiation and survival (Garratt et al., 2000; Perlin et al., 2011; Wolpowitz et al., 2000). The transcription factor *sox10* is required for peripheral glia differentiation and also controls *erbb3* expression in neural crest cells. Zebrafish *colourless (cls)* mutants, which lack *sox10* function, and mice homozygous for a targeted *sox10* null mutation, do not form Schwann cells or satellite glia (Britsch et al., 2001; Dutton et al., 2001). At around E12-13 in the mouse, migrating neural crest cells become tightly associated with axons and turn on expression of *Desert hedgehog* (*Dhh*), *Myelin protein zero* (*Mpz*, also known as *P0*), and *Peripheral myelin protein 22* (*Pmp22*), among others (Jessen and Mirsky, 2002).

Beginning at E13 in mice, SCPs become immature Schwann cells, which have a flattened morphology and begin to wrap around bundles of axons. Immature Schwann cells continue to express many SCP markers, but also turn on *S100 calcium binding protein* (*S100*) and *Glial fibrillary acidic protein* (*Gfap*) expression (Jessen and Mirsky,

2002). In addition, immature Schwann cells do not require *nrg1 type III* for survival, but it is still important for regulating their proliferation and differentiation. Depending on the level of *nrg1 type III* signaling from axons, immature Schwann cells will differentiate into either pro-myelinating or non-myelinating Schwann cells (Jessen and Mirsky, 2002). Not much is known about the genetic regulation of non-myelinating Schwann cells. Unlike myelinating Schwann cells, they envelop bundles of multiple small caliber axons. Both non-myelinating and myelinating Schwann cells are terminally differentiated but can revert to an immature-like state after nerve injury. Promyelinating Schwann cells associate with large caliber axons and begin radially sorting them into a 1:1 relationship. At this stage they begin to express the transcription factors *early growth response 2* (*egr2*, also known as *krox20*) and *POU class 3 homeobox 1* (*pou3f1*, also known as *oct6*), which are necessary for differentiation of myelinating Schwann cells, and are eventually downregulated in terminally differentiated, myelinating Schwann cells (Jessen and Mirsky, 2002). Recent studies have identified a G-protein coupled receptor, *g-protein receptor 126 (gpr126)*, that is required cell autonomously in mice and zebrafish for Schwann cells to initiate myelination (Monk et al., 2009, 2011). Early stages of Schwann cell differentiation in *gpr126*$^{-/-}$ larvae are normal, and Schwann cells form normal associations with axons. However, Schwann cells are arrested at the pro-myelinating stage and never produce myelin. Mutations in the ligand for *Gpr126*, *Laminin 211*, have been identified in human peripheral neuropathy patients, supporting the importance of this conserved pathway for myelination in zebrafish, mice, and humans (Hewitt et al., 2009; Petersen et al., 2015). Schwann cell development is a

complex, multi-step process with distinct morphologies and gene expression associated with the different stages.

Boundary cap cells (BCC)

First described as clusters of neural crest cells located at the DREZ and MEP, BCCs are multipotent progenitors with numerous roles in nervous system development (Radomska and Topilko, 2017). Most BCCs are believed to originate as neural crest cells and migrate to the MEP or DREZ. Fate mapping studies using quail-chick chimeras have supported the neural crest origin of dorsal BCCs (Niederländer and Lumsden, 1996). However, more recent evidence suggests some BCCs located at the MEP may come from ventral spinal cord progenitors (Radomska and Topilko, 2017). BCCs are found clustered at the chick dorsal spinal cord before sensory axons cross through the DREZ. They are hypothesized to help guide sensory axons through the DREZ, or to provide a permissive substrate for axons to cross through and enter the spinal cord (Golding and Cohen, 1997). Another study tested whether BCCs were necessary to guide axons through the DREZ by knocking down *Semaphorin* expression in chick embryos. *Semaphorin 6A (SEMA6A)* and *Semaphorin 6D* (*SEMA6D*) are guidance molecules expressed by BCCs. They observed disorganized DREZs in embryos with knocked-down *SEMA6A* or *SEMA6D*, with some axons misrouting into the wrong DREZ, and irregular spacing between DREZ (Mauti et al., 2007). This supports a conclusion that BCCs are involved in guiding axons to the DREZ. However, the animals without BCCs in this study did, for the most part, form DREZ at the proper locations

along the spinal cord, even if the nerve roots had irregular morphologies or the DREZ area was larger than normal. The results from this study suggest that even though BCCs are important for guiding axons through the DREZ, they do not determine the DREZ location, and other mechanisms can also guide axons into the spinal cord.

BCC clusters have also been observed at the MEP, associated with peripheral motor axons. However, it is unlikely that BCCs are involved in guiding motor axons through the MEP, because unlike dorsal BCCs, ventral BCCs do not appear at the MEP until after motor axons have crossed through (Fraher et al., 2007). While dorsal BCCs cluster adjacent to the spinal cord, ventral BCCs are located a short distance distal to the MEP (Fraher et al., 2007). Differences in morphologies and expression of certain markers have also been observed between dorsal and ventral BCCs, leading to the hypothesis that they may be unique populations or even have separate origins (Radomska and Topilko, 2017). For example, the genes *WNT inhibitory factor 1* (*Wif1)*, *Sema6a*, and *Sema6d* are expressed by both dorsal and ventral BCCs, but only dorsal BCCs express *Hey2* (Coulpier et al., 2009). Both dorsal and ventral BCCs express *Krox20*, at stages earlier than this gene can be detected in pro-myelinating Schwann cells (Vermeren et al., 2003). After remaining clustered at the MEP for a few days, BCCs migrate distally along the nerve and can differentiate into a variety of cell types, from Schwann cells to DRG neurons to pericytes (Radomska and Topilko, 2017).

Transition zones

A common theme arises in TZ organization in invertebrate and vertebrate nervous system development (Fontenas and Kucenas, 2017; Parker and Auld, 2006). Where motor axons extend out of the CNS, CNS-derived glia follow the motor axons into the PNS. On the other hand, sensory axons and their associated glia derive from common peripheral neuroglial precursors. Sensory axons grow into the CNS, and sensory glia assist with pathfinding into the entry points (Smith et al., 2017). Our knowledge of the structure of the developing and mature TZ comes primarily from transmission electron microscopic (TEM) studies. During development, bundles of axons extend through the immature glia limitans. When axon bundles are beginning to emerge through the MEP, radial glia processes form an incomplete layer, and motor axons cross through gaps between the processes (Figure 1-3A) (Fraher et al., 2007). As development progresses, glial endfeet form a tight barrier around the spinal cord, with very little space between glial endfeet and axons. At the mature transition zone, the basal lamina surrounding the spinal cord is continuous with the basal lamina around peripheral nerve roots (Figure 1-3B). Furthermore, motor axon rootlets emerge from the MEP before sensory axons are observed crossing into the DREZ (Fraher et al., 2007). After motor axons have crossed through the TZ, OPC processes extend peripherally along these axons into the TZ, while peripheral glial processes extend centrally into the TZ (Figure 1-3A). Where these processes meet, a transitional node forms, with oligodendrocyte myelin on one side and Schwann cell or MEP glia myelin on the other (Figure 1-3B) (Fraher et al., 2007). As the transition zone matures, central and peripheral glia form a tighter and tighter meshwork around motor axons, so that a clear boundary between CNS and PNS forms.

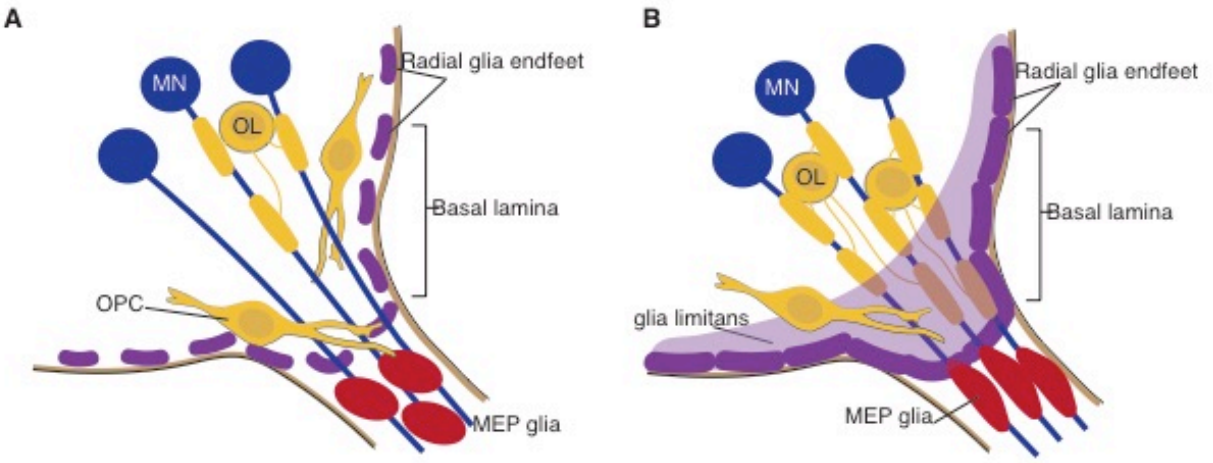

Figure 1-3 Structure of developing and mature motor exit point (MEP) transition zones. (A) Motor neurons (MN) within the spinal cord extend axons through the MEP into the PNS. Immature radial glia endfeet (purple) form an incomplete border around the spinal cord and delineate the boundary between CNS and PNS. Oligodendrocyte progenitor cells (OPCs) extend processes through the TZ and contact MEP glia positioned along motor axons just outside the spinal cord. Differentiated oligodendrocytes (OL) begin to wrap central portions of motor axons with myelin sheaths. MEP glia also begin to differentiate and ensheathe peripheral motor axon segments. (B) Mature radial glial endfeet (dark purple) form a tight barrier around the entire spinal cord. A meshwork of glial processes known as the glia limitans (light purple) is thickened at TZs, and there is no space between glial processes and axons. Differentiated OLs and MEP glia wrap central and peripheral portions of motor axons, respectively, with myelin sheaths, with a transitional node of Ranvier between them.

Motor axons cross through specialized MEP TZs

For motor neurons to innervate their peripheral targets, their axons must grow out of the spinal cord at the MEP. This is no trivial task, as many neuronal cell bodies are located some distance anterior or posterior to the MEP, requiring their axons to pathfind through the spinal cord along the anterior-posterior axis and then turn ventrally at the correct location to cross through the MEP at specialized openings in the basal lamina. These MEPs occur at regular intervals along the spinal cord, corresponding with spinal cord segments. Whether pioneer axons create the MEP by penetrating the basal lamina or are guided to a pre-formed MEP is still debated (Bravo-Ambrosio and Kaprielian, 2011). It is clear, however, that guidance cues within the spinal cord are necessary to direct growing motor axons through the MEP. Absence of these cues results in axonal failure to exit the spinal cord or exit at ectopic locations. *neuropilin1a* morpholino oligonucleotide (MO) knockdown causes ectopic exit of axons, and zebrafish with mutations in the *plexina3* gene have axon guidance defects including ectopic axon exit points (Feldner et al., 2005; Noma et al., 2017; Palaisa and Granato, 2007; Sato-Maeda et al., 2008; Tanaka et al., 2007). These studies have led to a proposed model that *neuropilin1a* and *plexina3* expressed by motor neurons interact with secreted class 3 semaphorins to guide motor axons to the correct exit points. In *Drosophila* embryos, clusters of CNS-derived peripheral glia called “exit glia” form cone-like arrangements at sites of axon exit from the CNS. These cells are thought to act as intermediate targets guiding axons to and through the proper exit points (Sepp et al., 2001). Could cells positioned at the vertebrate MEP have a similar role in guiding motor axon growth?

BCCs at the MEP are unlikely to fill this role. Although neural crest-derived BCCs have been identified at the MEP of chick and mouse embryos, these clusters of cells are only seen after axons have already crossed through the MEP into the PNS, making it unlikely that BCCs are involved in determining the location of the MEP (Fraher et al., 2007). However, PG, which have some similarities to *Drosophila* exit glia because of both being CNS-derived, may be involved in determining the MEP location or guiding axons through the MEP, since MO knockdown of *nkx2.2a*, a gene essential for PG specification, results in ectopic exit of motor axons from the spinal cord (Kucenas et al., 2008b).

Ectopic migration of CNS cells

The primary evidence for the existence of active mechanisms for restricting cell migration across transition zones comes from observations of CNS cells ectopically positioned along peripheral nerve roots in genetic mutants. In fact, the first known role for BCCs positioned at the MEP was to prevent motor neurons from migrating through the MEP and into the motor nerve root (Vermeren et al., 2003). In chick embryos, when the neural crest precursors to BCCs were surgically ablated, motor neurons were observed to be ectopically positioned outside of the spinal cord along peripheral nerve roots (Vermeren et al., 2003). Similarly, ectopic motor neuron migration was observed when mouse BCCs were genetically ablated with diphtheria toxin driven by the *Krox20* promoter in BCCs (Vermeren et al., 2003). The ability of BCCs to prevent ectopic motor neuron migration involves *Semaphorin-Plexin* signaling (Bron et al., 2007; Mauti et al.,

2007). Although BCCs have not been identified in zebrafish, *semaphorin* signaling may still be involved in gating motor neurons. In one study, knocking down *neuropilin1* expression, a receptor for *semaphorin*, resulted in ectopic exit of motor neurons from the spinal cord (Feldner et al., 2005).

Not only motor neurons, but also CNS glia have been observed to ectopically migrate out of the spinal cord onto peripheral nerves. In mice, BCCs seem to also play a role in repelling OPCs from migrating out of the spinal cord. When BCCs are genetically ablated, OPCs and myelinating oligodendrocytes can be found along the peripheral nerve roots (Coulpier et al., 2010). Mice with null mutations in *Krox20* do not have any BCCs and also have peripherally-migrated OPCs (Coulpier et al., 2010). It has not been tested whether the BCCs responsible for repelling OPCs are the same cells that repel motor neurons, or a different subpopulation. The glial master regulatory gene *Sox10*, while not necessary for BCC specification and survival, is also important for their ability to repel OPCs. When *Sox10* was selectively deleted from BCCs and Schwann cells, OPCs were observed along the peripheral nerve roots, although BCC clusters were still present (Fröb et al., 2012). Similarly, *sox10* is involved in repelling peripheral OPC migration in zebrafish, as *colourless* mutants, which have a mutation in *sox10*, also have peripherally migrated OPCs (Kucenas et al., 2009). Peripherally-migrated OPCs have also been observed in zebrafish larvae with mutations in *erbb3*, and in zebrafish larvae with mutations in both *forkhead box D3* (*foxd3)* and *transcription factor AP-2 alpha* (*tfap2a)* (Kucenas et al., 2009; Morris et al., 2017; Smith et al., 2014). While it

was initially hypothesized that these mutations resulted in peripheral OPC migration because of effects on neural crest-derived Schwann cells, my research and work by others in the lab has discovered that an entirely different mechanism is responsible for preventing OPC migration out of the spinal cord. Work from our lab recently discovered that MEP glia, a cell population similar in many ways to mouse BCCs, are necessary to prevent peripheral OPC migration (Smith et al., 2014). The mechanisms involved in regulating OPC migration across TZs will be the subject of Chapters 3 and 4.

Conclusions

The development and maintenance of the vertebrate TZ is an intriguing topic because of the unique interactions of many cell types that do not occur anywhere else. Motor and sensory axons pathfind out of and into the spinal cord at precise locations, and MEP glia and PG follow motor axons into the PNS. What are the mechanisms guiding or allowing these cells to exit the spinal cord? In contrast, OPCs and Schwann cells also migrate along axons, but are prevented from crossing through TZs. All of these cell types are in close proximity to each other and even physically contact each other at TZs. How are these interactions important for maintaining cell boundaries at the TZ? In mice, chicks, and fish, CNS cells have been observed ectopically positioned at the PNS motor roots, evidence for a breakdown in the mechanism(s) normally responsible for restricting their migration. Studies in mice have shown that BCCs prevent motor neurons and OPCs from migrating into the PNS (Coulpier et al., 2010; Fröb et al., 2012; Vermeren et al.,

2003). Work from our lab has also revealed that MEP glia are necessary to prevent peripheral migration of OPCs in zebrafish (Smith et al., 2014). Not much is known about mechanisms regulating the differentiation and function of these cells, or the signals involved in restricting OPC migration. My research has focused on uncovering the mechanisms that restrict cell migration across TZs. I have characterized some of the signals required for specification and differentiation of MEP glia. I have also discovered that neuronal activity, particularly modulation of neuronal activity through neuronal adenosine receptors, is an important regulator of OPC migration at TZs. This work has found some intriguing similarities between MEP glia and mammalian BCCs. The discovery of new mechanisms regulating OPC migration at the MEP opens exciting possibilities for understanding how OPCs reach their final destinations during development and identifies mechanisms that could promote their migration in disease.

Chapter 2

Materials and Methods

Fish Husbandry

All animal studies were approved by the University of Virginia Institutional Animal Care and Use Committee. Zebrafish strains used in these studies were: AB*, *Tg(sox10(4.9):eos)*^{w9}, *Tg(sox10(4.9):nls-eos)*^{w18} (Prendergast et al., 2012), *Tg(olig2:egfp)*^{vu12}, *Tg(olig2:dsred)*^{vu19} (Shin et al., 2003), *Tg(neurod:gal4)*, *Tg(nkx2.2a:megfp)*^{vu17} (Kucenas et al., 2008), *Tg(mbp:egfp-CAAX)* (Almeida et al., 2011), *Tg(sox10(7.2):mRFP)*^{vu234} (Kirby et al., 2006), *Tg(sox10:megfp)*, *plexina3*^{p55emcf} (*plxna3*, also called *sidetracked* or *set*) (Palaisa and Granato, 2007), *Gt(foxd3:mcherry)*^{ct110a} (Hochgreb-Hägele and Bronner, 2012), *colourless*^{m241} (*cls*) (Dutton et al., 2001), *mont blanc*^{m610} (*mob*) (Montero-Balaguer et al., 2006), *mother superior*^{m188} (*mos*) (Barrallo-Gimeno et al., 2004), *krox20*^{fh227} and *gpr126*^{st49} (Monk et al., 2009), *adora2aa*^{ct845}. Table 2-1 denotes abbreviations used for each strain and summarizes what each transgene labels. Embryos were raised at 28.5°C in egg water and staged by hours or days post fertilization (hpf and dpf, respectively). Embryos of either sex were used for all experiments (Kimmel et al., 1995). Phenylthiourea (PTU) (0.004%) in egg water was used to reduce pigmentation for imaging. Stable, germline transgenic lines were used in all experiments with the exception of the F0 CRISPR data.

Table 2-1. Transgenic and mutant lines used in these studies, with abbreviations and descriptions.

Transgene name	Abbreviation	Description
Tg(sox10(4.9):eos)^{w9}	*sox10:eos*	Photoconvertible (green to red) Eos protein expressed by OPCs, Schwann cells, MEP glia and some interneurons
Tg(sox10(4.9):nls-eos)^{w18}	*sox10:nls-eos*	Photoconvertible (green to red) Eos protein expressed in the nucleus of Sox10-expressing cells
Tg(sox10(7.2):mRFP)^{vu234}	*sox10:mrfp*	Membrane-tethered RFP expressed by OPCs, MEP glia, and Schwann cells
Tg(sox10:megfp)	*sox10:megfp*	Membrane-tethered GFP expressed by OPCs, MEP glia, and Schwann cells
Tg(olig2:egfp)^{vu12}	*olig2:egfp*	GFP expressed by motor neurons and axons, OPCs, MEP glia and some interneurons
Tg(olig2:dsred)^{vu19}	*olig2:dsred*	DsRed expressed by motor neurons and axons, OPCs, MEP glia and some interneurons
Gt(foxd3-mcherry)^{ct11aR}	*foxd3:mcherry*	Mcherry expressed by Schwann cells and MEP glia
Tg(nkx2.2a:megfp)^{vu17}	*nkx2.2a:megfp*	Membrane-tethered GFP expressed by perineurial glia and myelinating OPCs
Tg(mbp:egfp-CAAX)	*mbp:megfp*	Membrane-tethered GFP expressed by myelinating glia
Tg(neurod:gal4)	*neurod:gal4*	GAL4 transcriptional activator expressed by neurons
plxna3^{p55emcf}	*plxna3*	Misrouted motor axons create ectopic MEPs
colourless^{m241}	*cls*	*sox10* mutation impairs Schwann cell and OPC differentiation and survival
mont blanc^{m610}; mother superior^{m188}	*mob;mos*	*tfap* and *foxd3* mutations block all neural crest specification
krox20^{fh227}	*krox20*	Schwann cells fail to differentiate and do not produce myelin
gpr126^{st49}	*gpr126*	Schwann cells radially sort peripheral axons, but do not produce myelin
adora2aa^{ct845}	*adora2aa*	Mutation in *adora2aa* receptor characterized in this research

Chemical treatments

All chemical stocks were ordered from Sigma unless otherwise noted. Stock solutions were dissolved in DMSO or distilled water and stored as frozen aliquots at -20C. 100x working stocks were prepared fresh on the day of use. For drug treatments: one *olig2:dsred* embryo per well was placed in the wells of a 96 well plate with 198 μl of water. 2 μl of compound from the working stock was added to the water for a final concentration of 1% DMSO (for drugs dissolved in DMSO) Various concentrations of chemicals were used, as noted in the text. For drugs dissolved in DMSO, 1% DMSO served as the negative control for each experiment. For drugs dissolved in water, 1 row of embryos with 2 μl of distilled water added to each well was used as the negative control. Plates were covered with a low evaporation lid and placed in a 28.5°C incubator until analysis at 72 hpf. Plates were analyzed on a Zeiss AxioObserver inverted microscope equipped with epifluorescence using a 10x objective (NA = 0.3). At 72 hpf, the number of peripheral *olig2*$^{+}$ cells was quantified for each larva, excluding the first (anterior) 2 somites which are obscured by the yolk, and the last (posterior) 4 somites in the tail, which develop more slowly than the rest of the trunk.

In vivo imaging

Embryos were anesthetized with 0.01% 3-aminobenzoic acid ester (Tricaine), immersed in 0.8% low-melting point agarose and mounted laterally in glass-bottomed 35 mm petri dishes (Electron Microscopy Sciences). After mounting, the petri dish was filled with egg water containing PTU and Tricaine. For some experiments, chemical compounds were

also dissolved in the water. A 25X multi-immersion objective (NA = 0.8), 40X oil objective (NA= 1.4) and a 40X water objective (NA = 1.1) mounted on a motorized Zeiss AxioObserver ZI microscope equipped with a Quorum WaveFX-XI spinning disc confocal system (Quorum Technologies Inc.) were used to capture images. Image processing was performed with MetaMorph and Photoshop to enhance brightness and contrast of images. The Fiji plugin MTrackJ was used to annotate time-lapse movies (Meijering et al., 2012).

We used fate mapping with photoconversion of the *sox10:eos* transgenic line to identify MEP glia in some experiments. The nascent Eos protein exists in a green fluorescent state, but when exposed to ultraviolet (UV) light, it permanently shifts to a red fluorescent state. When exposed to UV light at 48 hpf, neural crest-derived cells are photocenverted to red fluorescence. MEP glia, which are not neural crest-derived and begin expressing *sox10:eos* after 48 hpf, are not photoconverted and can be identified as green fluorescent cells on the nerve root (Smith et al., 2014). For photoconversion, the entire trunk of *sox10:eos* larvae was exposed to 30 secords of UV light through a DAPI filter using a 20X objective (NA = 0.8). Single cell ablations were performed with a nitrogen-pulsed MicroPoint laser using a coumarin dye (435nm) with either 40x (Schwann cell ablation) or 63x (MEP glia ablation) water immersion objectives. After pre ablation images were acquired, a region of interest (ROI) was created based on the merged-color image around Schwann cells or MEP glia to selectively laser ablate single cells.

Calcium imaging

We injected the calcium indicator UAS:GcAMP5 DNA construct into stable transgenic zebrafish embryos *neuroD:gal4*. The combination of UAS:GcAMP5 and *neuroD:gal4* leads to mosaic expression of GcAMP5 in CNS neurons. Prior to imaging, larvae expressing GcAMP5 in the ventral spinal cord were treated with 800μM 4-aminopyridine (4-AP) (Sigma A78403) diluted in egg water for 15 minutes to induce neuronal activity (Ellis, Seibert et al. 2012), then immediately paralyzed using the neuromuscular junction (NMJ) blocking nicotinic receptor antagonist pancuronium bromide (Sigma P1918) for 10 minutes, which was dissolved in egg water (0.3 mg/mL) (Baraban, Koudelka et al. 2018). Larvae were then embedded in 0.8% low melting point agarose for imaging.

To record Ca^{2+} dynamics, individual neurons of the ventral spinal cord were imaged every 250 ms for 2 minutes, using an exposure time of 100 ms on single z-planes.

Images were captured with a 63x water immersion objective (na = 1.2) mounted on a motorized Zeiss AxioObserver ZI microscope equipped with a Quorum Wave FX-XI spinning disc confocal system (Quorum Technologies Inc.). Single-plane time-lapses were processed in MetaMorph with no intensity averaging.

GcAMP5 analysis

Fluorescence intensity measurements were extracted from ROIs using ImageJ and imported to Excel. $\Delta F/F_0$ were measured by applying the following formula $\Delta F/F_0 = (F_t - F_0)/(F_0 - F_{background})$, where F_t is the fluorescence intensity in the ROI in which the calcium transient was observed at time *t*, F_0 is the average fluorescence intensity of first three

frames of the timelapse in the same ROI, and $F_{background}$ is the fluorescence intensity of the background at time *t* (Baraban, Koudelka et al. 2018). For each individual neuron, the average baseline fluorescence was determined by averaging the $\Delta F/F_0$ of all 500 timepoints. For fold change quantification, all $\Delta F/F_0$ values one standard deviation or more above the baseline were considered firing events, and their average was compared to the baseline.

Immunohistochemistry and fluorescent antagonist treatment

Embryos were fixed and stained using the procedure previously described (Smith et al., 2014). Antibodies used were: rabbit anti-A2a (1:100 GeneTex (Andersson et al., 2012)) rabbit anti-Sox10 (1:5000 (Binari et al., 2013)), rabbit anti-MBP (1:250 (Kucenas et al., 2009)), and Alexa 647 goat anti-rabbit (1:600) (ThermoFisher). Fluorescent SCH-58261 (SCH-red) was purchased from CisBio. 25 hpf embryos were immersed in 7.14 μM SCH-red in 30% DMSO for 30 minutes, then fixed in 4% PFA at 25°C for 3 hours. Embryos were mounted in glass-bottomed petri dishes for imaging as described above.

Morpholino and mRNA injections

Antisense morpholino oligonucleotides (MO) were purchased from Gene Tools. *adora2aa*^{MO1} (CATTGTTCAGCATGGTGAGGTCGCT) (Haas et al., 2013) is complementary to the region spanning the translation start codon of *adora2aa* mRNA, and *adora2ab*^{MO1} (GTGCTATCAACCAGTGTGAAAGGAT) is complementary to the region immediately 5' to the start codon of *adora2ab* mRNA. *Adora2ab*^{MO2}

(GCTGTTGTACCTTAGGAAGACAAAA) is complementary to the junction of intron 2 and exon 3. *Wif1*^{MO} (5' TCTGTTTGTCTGCGCTCGGTTCAGT 3') targets exon 1, just 5' of the translational start codon. Embryos were injected with 2 to 3 nl of injection solution (distilled water, 4 mg/ml phenol red, diluted MO) at the 1-cell stage. Any embryos damaged during the injection procedure were removed, and the rest were incubated at 28.5°C. RT-PCR was performed to detect incorrectly spliced *adora2ab* transcripts in embryos injected with *adora2ab*^{MO2}. Total RNA was extracted from 30 pooled embryos at 25 hpf using the protocol previously described (Peterson and Freeman, 2009). Embryos were lysed with TRIzol® (ThermoFisher) and homogenized using pellet pestles (Fisher), and total RNA was purified using phenol:chloroform extraction. First strand cDNA was generated from total RNA using the High-Capacity cDNA Reverse Transcription Kit (ThermoFisher). PCR was performed with the primers TGGATGCCTCTTCATCGCTT, CCGAACATGGGGGTCAGTC, and TGGAAGGGGAAAAGCCATTGA to detect WT and incorrectly spliced transcripts. TGGATGCCTCTTCATCGCTT and CCGAACATGGGGGTCAGTC amplify a 201 bp region of WT *adora2ab* cDNA, whereas TGGAAGGGGAAAAGCCATTGA and CCGAACATGGGGGTCAGTC amplify a 695 bp region spanning intron 2 and exon 3 in the splice-blocked transcript. Data presented for *adora2aa* and *adora2ab* MOs are combined from at least 3 independent experiments. Uninjected controls and phenol red control injections were performed at least twice for each data set.

For Tetanus Toxin experiments, TeNT cDNA was prepared from plasmid pGEMTEZ-TeTxLC (a gift from Marcel Tawk) as previously described (Fontenas et al., 2016). TeNT mRNA was prepared using the mMessage mMachine SP6 *in vitro* transcription kit (ThermoFisher). Injections of mRNA encoding Tetanus Toxin Light Chain (TeNT) were performed at the 1 to 2 cell stage. A 2 nl volume of 175 ng/μl mRNA in DEPC-treated distilled water was used. All embryos were manually dechorionated at 2 dpf and evaluated for paralysis at that time. The startle reflex was also analyzed at 3 dpf as further evidence that TeNT expression caused inhibition of neuronal firing.

Adora2ab CRISPR injections

sgRNA targeting *adora2ab* was designed using CHOPCHOP (http://chopchop.cbu.uib.no/) and the protocol from http://www.schierlab.fas.harvard.edu/resources/ (Gagnon et al., 2014). The sgRNA target for *solute carrier family 45 member 2* (*slc45a2*) has been previously published (Irion et al., 2014). The sgRNA target for *tyrosinase* (*tyr*) has been previously published (Jao et al., 2013). Each sgRNA was tested for somatic mutation efficiency, and all efficiencies were greater than 85% (Table 2-2). We annealed the 5' gene-specific oligo and the 3' constant oligo using the PCR protocol described in (Nakayama et al., 2014). We transcribed sgRNA using Ambion Megascript T7 kit and injected 2 nl of 200-400 ng/μl sgRNA with 500 ng/μl Cas9 protein (PNA Bio) dissolved in nuclease-free water into cells of *olig2:dsred or olig2:egfp* embryos at the 1 cell stage. Larvae were analyzed at 3 dpf for peripheral OPCs and then DNA was extracted from individual larvae for

Table 2-2. CRISPR sgRNA efficiency. Individual injected larvae were randomly chosen for sequencing and detection of mutations in the target gene to determine sgRNA efficiency. Control sgRNA efficiency was quantified as the number of injected larvae with defects in pigment formation.

	Target	**Mutation efficiency (%)**	**Total injected**
adora2ab sgRNA 6	GATGGTGACGGCAAATGGAA	11 (91.7%)	12
adora2ab sgRNA 7	GAAGCCGATGCTGATGGTGA	13 (86.7%)	15
scl45a2 sgRNA	GGTTTGGGAACCGGTCTGAT	34 (94.4%)	36
tyr sgRNA	CCCCAGAAGTCCTCCAGTCC	29 (87.9%)	33

sequencing. The primers CAACTATGTGTGTCCCTGAGGA and ATGAAGAGGCATCCATGAAAAT were used to PCR amplify a 279 base pair region of genomic *adora2ab*, and Sanger sequencing with the primer CAACTATGTGTGTCCCTGAGGA was used to identify CRISPR-induced mutations. Sequence trace files were analyzed with ApE or SnapGene. Because mutations are mosaic in F0 animals, we cloned single mutated DNA fragments using TOPO cloning. To analyze the CRISPR induced-mutations, DNA from 3 dpf individual embryos was extracted and amplified by PCR using the *adora2ab* forward (5'-CAACTATGTGTGTCCCTGAGGA-3') and reverse (5'-ATGAAGAGGCATCCATGAAAAT-3') primers. PCR was done with GoTaq green master mix (Promega) and conditions were as follows: 95°C for 3 min, followed by 35 cycles at 95°C for 30 s, 60°C for 30 s and 72°C for 1 min. Final extension was at 72°C for 20 min. PCR products from individual embryos were TOPO TA cloned into pCR8/GW vectors (Invitrogen). For each embryo, 8 clones were sequenced using the M13 forward primer. Sequences were aligned to WT genomic DNA using BLAST global alignment tool. All F0 CRISPR data presented in this manuscript has been confirmed via sequencing and the gRNAs have been verified to induce reproducible cuts within the target gene.

In situ hybridization and sectioning

Larvae were fixed in 4% PFA at 4°C overnight and stored in 100% methanol at -20°C and processed for in situ RNA hybridization. Plasmids were linearized with appropriate restriction enzymes and cRNA preparation was carried out using Roche DIG-labeling

reagents and RNA polymerases (NEB). We used a previously published probe for *wif1* (Smith et al., 2014). After in situ hybridization, embryos were embedded in 1.5% agarose/30% sucrose and frozen in 2-methylbutane chilled by immersion in liquid nitrogen. We collected 20 μm transverse sections on microscope slides using a cryostat microtome and covered with 75% glycerol. Images were obtained using a Zeiss AxioObserver inverted microscope using a 40x oil immersion objective. All images were imported into Adobe Photoshop. Adjustments were limited to levels, contrast, and cropping.

Genotyping

The primers used for genotyping *gpr126*^{st49} have previously been published (Monk et al., 2009). The primers AAGCCATCCCATGTGAACTC and TCACATTCAGGGCAGAACAG were used to amplify a 151 bp product within *adora2aa*. Because the mutation is a 7 bp deletion, which is difficult to resolve on an agarose gel, we performed Sanger sequencing using the primer TCACATTCAGGGCAGAACAG to identify WT, heterozygous, and homozygous mutants.

Statistics

GraphPad Prism was used for all statistical analysis. Unpaired student's t-test or, for multiple comparisons, 1-way ANOVA followed by Bonferonni post test was used for quantifications of OPCs, MEP glia, Eos^{+} peripheral cells, A2a antibody expression, and heart rate. Chi-squared analysis was used for quantification of paralysis and startle

reflex, and survival test was used for analyzing mutant survival and hatching. A p value less than 0.05 was considered statistically significant. For dose response experiments, 10 to 12 embryos were treated per dose, and n is reported as the range of larvae analyzed per dose. To quantify A2a antibody expression, a region of interest was drawn around the peripheral nerve roots using ImageJ, and integrated density was calculated for this region of interest. To correct for background fluorescence, integrated density was calculated for an identical region of interest adjacent to the nerve roots, and this value was subtracted from the nerve root value to achieve the corrected total fluorescence for each nerve root.

Chapter 3

MEP glia: a novel cell involved in restricting OPC migration

Introduction

The CNS and PNS are often thought of as two separate nervous systems. They are anatomically distinct and have unique glial populations. The zebrafish CNS contains oligodendrocytes, OPCs, and radial glia, whereas Schwann cells, perineurial glia, and satellite glia are the glial cells of the PNS. There are even separate types of myelin for central and peripheral axons: CNS axons are myelinated by oligodendrocytes, and PNS axons are myelinated by Schwann cells. However, the CNS and PNS must interact and communicate in order to function effectively as a whole nervous system. The regions where axons traverse in and out of the spinal cord to connect the CNS and PNS are known as transition zones (TZ). Two TZ are present within each spinal cord hemisegment: a ventral motor exit point (MEP), where motor axons extend out of the spinal cord to become peripheral nerves, and a dorsal root entry zone (DREZ), where sensory axons from the periphery grow into the spinal cord to eventually synapse on central targets. Although axons cross through these specialized structures, the transition zone is impermeable to most cell types. Thus, it serves as the dividing line for CNS and PNS cell types. Motor neuron cell bodies, radial glia, oligodendrocyte lineage cells, and astrocytes remain in the CNS, whereas sensory neuron cell bodies, Schwann cells, and satellite glia reside in the PNS. However, in addition to axons, the MEP TZ is selectively permeable to two types of glia that we know of: perineurial glia (PG) and MEP glia. Both

are specified in the spinal cord and subsequently migrate through the MEP TZ to associate with peripheral axons (Kucenas et al., 2008; Smith et al., 2014). This chapter will describe the discovery of MEP glia, their role in regulating glial migration across the MEP TZ, and other characteristics and unanswered questions regarding this novel cell type.

Identification of Motor Exit Point Glia

MEP glia are a newly discovered type of peripheral glial cell that resides on the peripheral spinal motor root at the MEP. They are not present along the motor root until after 48 hpf. Similar to Schwann cells, MEP glia express the master glial regulatory gene *sox10*. However, although MEP glia and Schwann cells are *sox10*-expressing glia found on peripheral nerves, they have unique lineages. We can prove that MEP glia are a distinct cell population by performing fate mapping with the photoconvertible transgenic line *sox10:eos*. In this line, green Eos protein is expressed in all *sox10*-expressing cells, including MEP glia, Schwann cells, and oligodendrocytes. The nascent Eos protein exists in a green fluorescent state, but when exposed to UV light, it permanently shifts to a red fluorescent state. Thus, UV exposure at a given time point converts all *sox10*$^{+}$ cells to red fluorescence, and any progeny of those cells will also inherit the red Eos protein. At 48 hpf, neural crest cells have finished migrating to the peripheral nerves and have begun differentiating into Schwann cells and other PNS cell types. However, MEP glia do not appear on the nerve until after 48 hpf. Therefore, when we exposed whole zebrafish embryos to UV light at 48 hpf, neural crest-derived

Schwann cells were photoconverted to red fluorescence. As photoconverted Schwann cells proliferate and populate the nerve, the daughter cells continue to express red photoconverted Eos at later stages (Smith et al., 2014). However, MEP glia are not derived from a neural crest or Schwann cell lineage, since they initiate *de novo* expression of *sox10* after 48 hpf, and do not express any photoconverted red Eos protein. They can be identified as green fluorescent cells on the nerve root by 54 hpf (Smith et al., 2014).

In order to characterize these cells, we performed time-lapse imaging of MEP glia using *sox10:eos*. We observed them originate within the spinal cord, turn on *sox10* expression, and migrate through the MEP at around 56 hpf (Smith et al., 2014). Within the spinal cord, MEP glia are specified within the pMN domain, the same domain that gives rise to motor neurons and oligodendrocyte progenitor cells (OPCs). Like all cells from this domain, MEP glia express the transcription factor *olig2* (Smith et al., 2014). They continue to express *olig2* even after exiting the spinal cord, up to 3 dpf, and can thus be distinguished from Schwann cells, which are also present at the motor root. As *sox10*$^{+}$*/olig2*$^{+}$ glia specified within the pMN domain, MEP glia have many similarities to OPCs. However, like Schwann cells, MEP glia express the transcription factor *foxd3* (Smith et al., 2014). We commonly use *sox10:eos;olig2:dsred* transgenic zebrafish to identify *sox10*$^{+}$*/olig2*$^{+}$ MEP glia on the nerve, distinct from *sox10*$^{+}$*/olig2*$^{-}$ Schwann cells. I discovered that *WNT inhibitory factor 1* (*wif1)*, another BCC marker, selectively labels MEP glia in 54 and 72 hpf larvae, developmental stages when *olig2*$^{+}$*/sox10*$^{+}$ MEP glia

can be identified via live imaging of transgenic embryos (Figure 3-1A) (Smith et al., 2014). Since MEP glia are specified within the pMN domain and, like OPCs, express *sox10* and *olig2*, we also tested whether Notch signaling was involved in their specification. Notch is one signal known to be important in the developmental switch from neuronal to glial specification that is essential for OPC development, and blocking Notch signaling with the inhibitor DAPT prevents OPC specification (Kim et al., 2008; Park et al., 2003). When I analyzed zebrafish treated with DAPT, they had significantly reduced *wif1*$^{+}$ MEP glia, suggesting that MEP glia also require Notch for specification from pMN precursors (Figure 3-1B&E. $p = 0.01$, $n = 7$) (Smith et al., 2014).

Signals regulating MEP glia specification and migration

MEP glia are essential for repelling OPCs from migrating into the PNS. While OPCs are migrating throughout the spinal cord, their processes extend through the MEP TZ and contact MEP glia. When this happens, the OPC process retracts and the cell migrates away from the MEP (Smith et al., 2014). However, when MEP glia are ablated, OPC processes extend long distances into the PNS, and OPC cell bodies migrate through the MEP and onto peripheral nerves (Smith et al., 2014). Based on their positioning at motor exit points and their role in repelling peripheral OPC migration, MEP glia are similar to mammalian boundary cap cells (BCC). Like BCCs, MEP glia express *sox10* and *wif1* (Coulpier et al., 2009; Smith et al., 2014). However, MEP glia and BCCs are not entirely homologous, as BCCs are hypothesized to be neural crest-derived, and they do not share all of the same markers with MEP glia (Smith et al., 2014). In addition,

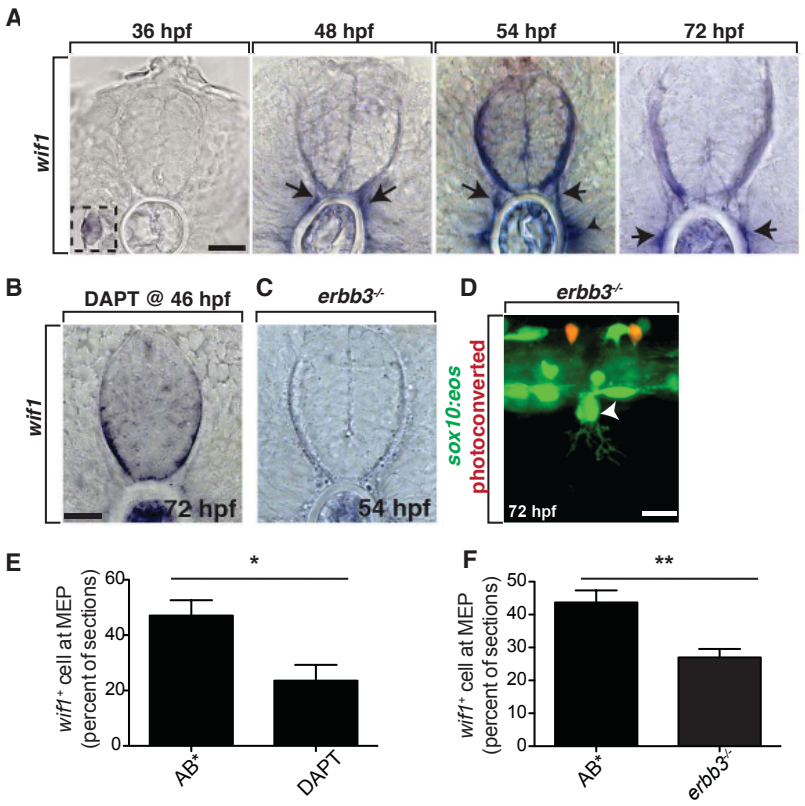

Figure 3-1 MEP glia originate from ventral spinal cord progenitors and express *wif1*. (A) *In situ* hybridization with *wif1* riboprobe at 36, 48, 54, and 72 hpf shows timing of *wif1* expression at the nerve root denoted by arrows. Arrowhead denotes the horizontal myoseptum staining. Inset at 36 hpf shows *wif1*$^{+}$ staining is expressed at the lateral line, as has been previously described. (B) Embryos treated with DAPT at 46 hpf do not have any *wif1* staining at the nerve root at 72 hpf. (C) *Erbb3*$^{-/-}$ embryos do not have any *wif1* staining at the motor root at 54 hpf. (D) *Erbb3*$^{-/-}$ larvae expressing sox10:eos and photoconverted at 48 hpf do not have any green (unconverted) MEP glia. Arrowhead points to *sox10*$^{+}$, multipolar OPC that has migrated onto the peripheral nerve root. (E) Quantification of *wif1* expression at 54 hpf in WT and *erbb3*$^{-/-}$ embryos. Analyzed by student's t-test. p = 0.003(F) Quantification of *wif1* expression at 72 hpf in WT larvae and larvae treated from 48 to 72 hpf with DAPT. Analyzed by student's t-test. p = 0.01. Scale bars, 25 μm. Panels A-D are from Smith et al., 2014 Figure 6 and Supplemental Figure 5.

BCCs at the MEP are involved in preventing ectopic positioning of motor neuron cell bodies, whereas MEP glia do not share this role (see Appendix I for details). Intriguingly, there is some evidence for heterogeneity among BCCs. Fate mapping studies using the markers *krox20* and *prss56* have revealed at least two populations of BCCs (Radomska and Topilko, 2017). Although *krox20*-expressing BCCs were initially characterized as being neural crest-derived, a recent review has suggested that a subset of BCCs, like MEP glia, have origins in the ventral spinal cord (Radomska and Topilko, 2017). If there is a subset of CNS-derived BCCs, they may have more in common with MEP glia than originally thought, and further studies of MEP glia may help reveal more mechanisms for mammalian TZ boundary maintenance.

We wanted to further characterize signals important for MEP glial differentiation and migration to the motor root. I looked at *neuregulin 1 (nrg1)/ erb-b2 receptor tyrosine kinase 3b (erbb3)* signaling, because this pathway is required for Schwann cells to associate with and migrate along peripheral axons. The ligand, *nrg1*, expressed by axons, binds to *erbb3* receptors expressed by Schwann cells to initiate downstream signaling. Without either *nrg1* or *erbb3*, Schwann cell precursors fail to associate with peripheral axons and are missing from the spinal nerve roots (Brinkmann et al., 2008; Honjo et al., 2008; Lyons et al., 2005). I used *erbb3b* mutant zebrafish to test whether MEP glia similarly require *nrg1* signaling to associate with the motor root. There is a significant reduction in *wif1* expression at the motor root in 54 hpf *erbb3*$^{-/-}$ larvae, suggesting that MEP glia are missing from the motor root (Figure 3-1C&F. $p = 0.003$, n

= 5 (WT) n = 8 (*erbb3*$^{-/-}$)) (Smith et al., 2014). I also used photoconversion of larvae expressing *sox10:eos* to look for MEP glia in *erbb3*$^{-/-}$ larvae. At 72 hpf, *erbb3*$^{-/-}$*;sox10:eos* larvae do not have unconverted Eos^{+} MEP glia (Figure 3-1D) (Smith et al., 2014). I also observed a lack of photoconverted (red) Eos^{+} neural crest-derived cells along the nerves of *erbb3*$^{-/-}$ larvae, which is consistent with the previously published phenotype of these mutants (Figure 3-1D) (Lyons et al., 2005; Smith et al., 2014). As a result of the loss of MEP glia, OPCs migrate into the PNS in *erbb3* mutant larvae (Smith et al., 2014). These results suggest that, like neural crest-derived Schwann cells, *nrg1/erbb3* signaling is required for MEP glia to associate with the motor root.

Our discovery that OPCs migrate onto peripheral nerves in *erbb3*$^{-/-}$ mutant larvae because MEP glia are missing from the nerve root reminded me of a previous study showing OPC migration into the periphery in zebrafish mutants. Kucenas et al. showed that OPCs ectopically exit the spinal cord and migrate onto peripheral nerves in *cls*$^{-/-}$ and *mob*$^{-/-}$*;mos*$^{-/-}$ mutant larvae (Kucenas et al., 2009). *Cls* is a mutation in *sox10*, and since *sox10* is necessary for Schwann cell differentiation and survival, Schwann cells die and are missing from the peripheral nerves early in development (Dutton et al., 2001; Kucenas et al., 2009). *Mob* is a mutation in *tfap2a*, and *mos* is a mutation in *foxd3* (Barrallo-Gimeno et al., 2004; Montero-Balaguer et al., 2006). Both genes are important for neural crest specification, and *mob*$^{-/-}$*;mos*$^{-/-}$ double mutants completely lack all neural crest cells and their derivatives (Arduini et al., 2009; Wang et al., 2011). Before the discovery of MEP glia, it was hypothesized that the lack of Schwann cells was

responsible for peripheral OPC migration. However, since MEP glia express the transcription factors *foxd3 and sox10*, I wondered whether the ectopic peripheral OPC migration observed in *cls*$^{-/-}$ and *mob*$^{-/-}$;*mos*$^{-/-}$ larvae could be the result of effects of these genes on MEP glia development or function. I first tested whether *cls*$^{-/-}$ and *mob*$^{-/-}$;*mos*$^{-/-}$ embryos had *wif1*$^{+}$ MEP glia present at the motor root by performing in situ hybridization for *wif1*. At 54 hpf, *wif1*$^{+}$ MEP glia can be observed at the motor root in WT and *cls*$^{-/-}$ embryos, but not in *mob*$^{-/-}$;*mos*$^{-/-}$ embryos (3- 2A). In order to more selectively test the effects of *foxd3*, I used the gene trap line *Gt*(*foxd3-mcherry*)^{ct110aR}, which has mcherry coding sequence knocked into the *foxd3* locus, resulting in a loss of function (Hochgreb-Hägele and Bronner, 2012). Embryos homozygous for *Gt*(*foxd3-mcherry*)^{ct110aR}, hereafter referred to as *foxd3*$^{-/-}$, are lacking *foxd3* expression because of the knock-in at the *foxd3* locus. I also did not observe any *wif1*$^{+}$ MEP glia in 54 hpf *foxd3*$^{-/-}$ embryos (3-2A). Since both *mob*$^{-/-}$;*mos*$^{-/-}$ and *foxd3*$^{-/-}$ embryos did not have any *wif1*$^{+}$ MEP glia at the motor root, this suggests that *foxd3* is required for MEP glia specification. In contrast, *wif1*$^{+}$ MEP glia were present in *cls*$^{-/-}$ embryos at 54 hpf, and remained present at the nerve root in 72 hpf larvae (Figure 3-2A-C). I observed no differences in motor root *wif1* expression between WT and *cls*$^{-/-}$ larvae at 72 hpf (Figure 3-2C $p = 0.99$, $n = 6$). This result suggests that *sox10* is not required for MEP glia specification or initial association with the motor root. I then wanted to confirm my *in situ* results using live imaging of transgenic zebrafish. I used photoconversion of *sox10:eos* to identify MEP glia in WT larvae compared to *foxd3* mutant larvae. By exposing zebrafish embryos to UV light at 48 hpf, all neural crest-derived cells along the nerve

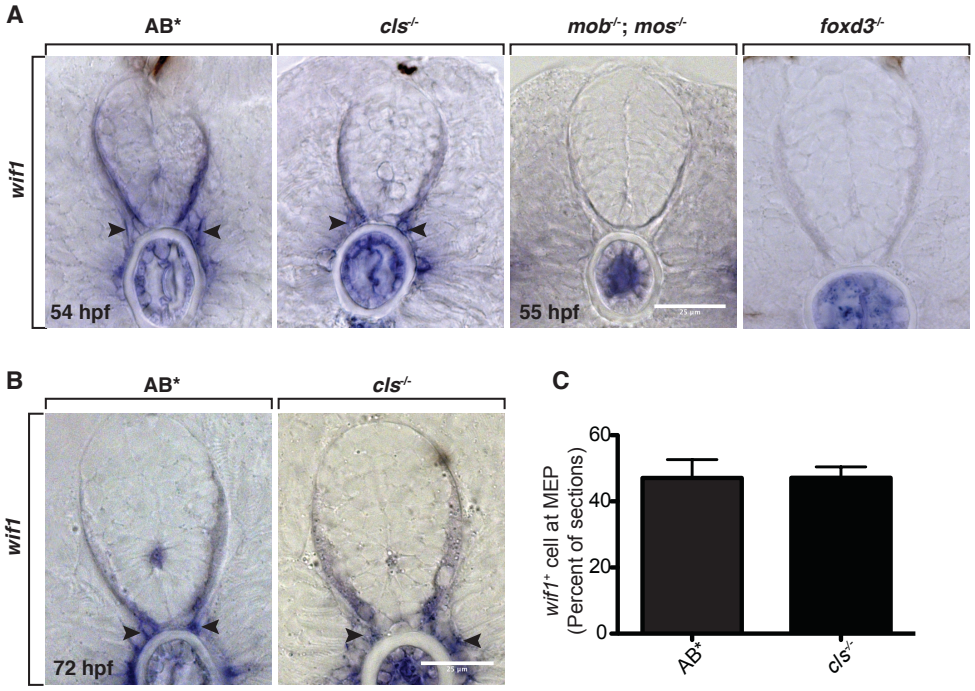

Figure 3-2 *Foxd3* is required for MEP glia specification. (A) *in situ* hybridization for *wif1* to label MEP glia in 54 hpf embryos. Arrowheads point to MEP glia. (B)*in situ* hybridization for *wif1* to label MEP glia in 72 hpf larvae. Arrowheads point to MEP glia.(C) Quantification of *wif1*$^{+}$ MEP glia in72 hpf WT and *cls*$^{-/-}$ larvae. Analyzed by student's t-test. p = 0.99 Scale bars 25 μm.

are converted to red fluorescence, whereas MEP glia, which do not initiate *sox10* expression until after 48 hpf, are green. At 52 hpf, green (unconverted) Eos^{+} MEP glia can be seen at the motor root of WT embryos, but I did not observe any green Eos^{+} MEP glia in *foxd3*$^{-/-}$ embryos (Figure 3-3A). However, in 54 hpf *cls*$^{-/-}$ embryos, *olig2*$^{+}$/*sox10*$^{+}$ MEP glia can be identified, but they have a clearly abnormal morphology compared to WT (Figure 3-3B). I conclude from these experiments that *foxd3* is required for MEP glial specification, since MEP glia are completely absent in *foxd3* mutant embryos. *Sox10*, on the other hand, is not required for specification of MEP glia, but may be required for their survival or differentiation, since MEP glia have abnormal morphology in *cls*$^{-/-}$ embryos lacking *sox10*. This is similar to the role of *sox10* in OPCs, as initial specification and OPC numbers are normal in *cls*$^{-/-}$ embryos and larvae, and OPC migration into the dorsal spinal cord after specification is also normal (Takada et al., 2010). However, OPCs in *cls*$^{-/-}$ larvae fail to differentiate and make myelin, and differentiating oligodendrocytes that have begun the process of wrapping axons soon die (Takada et al., 2010). *Sox10* is therefore required for differentiation of OPCs and survival following differentiation. Similarly, *sox10* is not required for initial neural crest cell specification in zebrafish, but Schwann cells do not differentiate in *cls*$^{-/-}$ mutants, and Schwann cells die during embryonic stages (Dutton et al., 2001; Kucenas et al., 2009). It is possible that *foxd3* functions upstream of *sox10* in the MEP glia lineage. This is consistent with our lab's previous observation that *foxd3* expression is initiated as early as 46 hpf, before MEP glia exit the spinal cord, whereas *sox10* expression is initiated after *foxd3* and *olig2*, just as MEP glia exit the spinal cord (Smith et al., 2014).

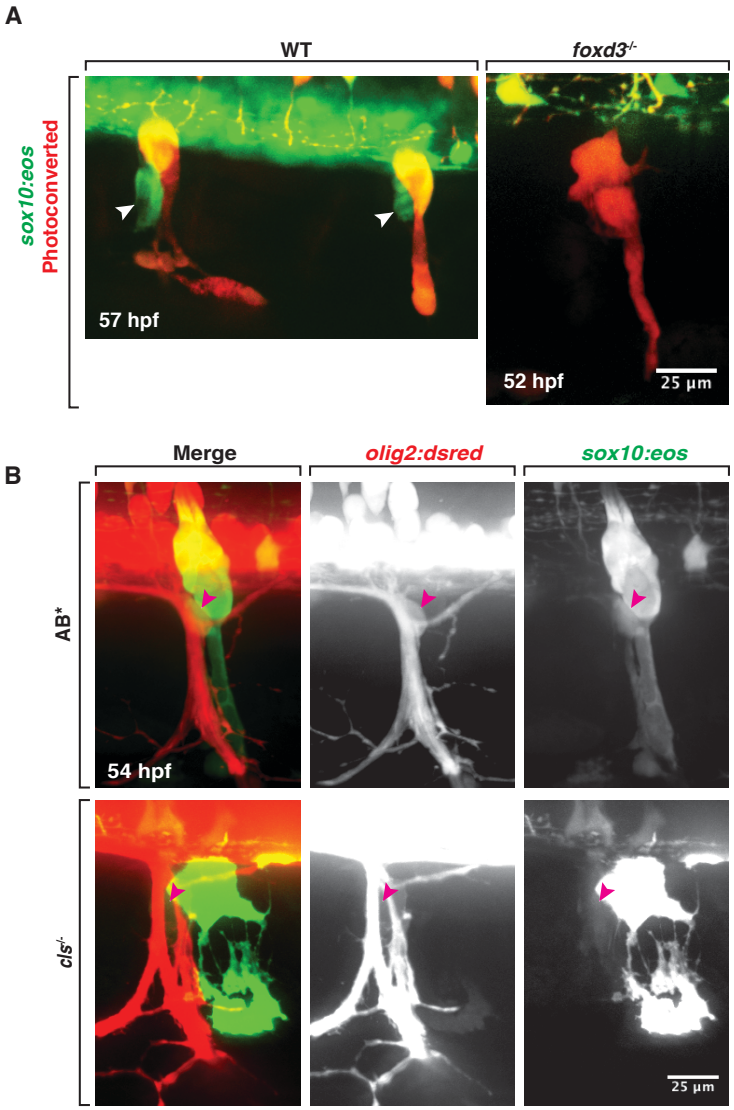

Figure 3-3 MEP glia have abnormal morphology in *cls*$^{-/-}$ embryos. (A) Sox10:eos embryos were photoconverted at 48 hpf to identify MEP glia. MEP glia (green cells, arrowheads) are present in WT, but not *foxd3*$^{-/-}$ embryos. Arrowhead points to MEP glia. (B) Images of *olig2:dsred;sox10:eos* larvae identifying MEP glia. MEP glia are the only *olig2*$^{+}$/*sox10*$^{+}$ cells at the motor nerve. Arrowheads point to MEP glia. Scale bars, 25 μm.

Sox10 and *wif1* are required for MEP glia to repel peripheral OPC migration

I next tested whether these genes expressed by MEP glia were necessary for their ability to prevent ectopic OPC migration. A previous study reported ectopic OPC migration in *cls*$^{-/-}$ and *mob*$^{-/-}$*;mos*$^{-/-}$ larvae (Kucenas et al., 2009). However, *mob*$^{-/-}$*;mos*$^{-/-}$ mutant larvae have mutations in *foxd3* and *tfap2a* and lack all neural crest cells, so it is unclear whether the effects on neural crest cells or on MEP glia result in peripheral OPC migration. I therefore tested whether a mutation in *foxd3* alone was sufficient to result in ectopic OPCs. I imaged *foxd3*$^{-/-}$*;sox10:eos* embryos from 49 to 54 hpf to test whether OPCs migrated into the periphery in these mutants. As described above, *foxd3*$^{-/-}$ mutant embryos lacked MEP glia. Because *foxd3* is also required early in Schwann cell development, many nerves also lacked Schwann cells (28/39 nerves) or had *sox10*$^{+}$ neural crest-derived cells with abnormal morphology (11/39 nerves). Not surprisingly, since *foxd3*$^{-/-}$ embryos completely lack MEP glia, I observed *sox10*$^{+}$ OPCs extend processes through the MEP on almost every nerve imaged (34/39), and on many of these nerves, the entire OPC cell body was in the periphery (18/39) (Figure 3-4A). Interestingly, nerves without any neural crest-derived “Schwann cells” were far more likely to have OPC processes and/or cell bodies (Figure 3-4B. $p = 0.0096$, $n = 39$ nerves). It is unclear whether the absence of Schwann cells somehow promotes OPC migration into the PNS, or if the absence of Schwann cells correlates with other factors, such as an improperly formed MEP, which may be more directly linked to OPC migration. We believe the latter option is more likely, because experiments performed

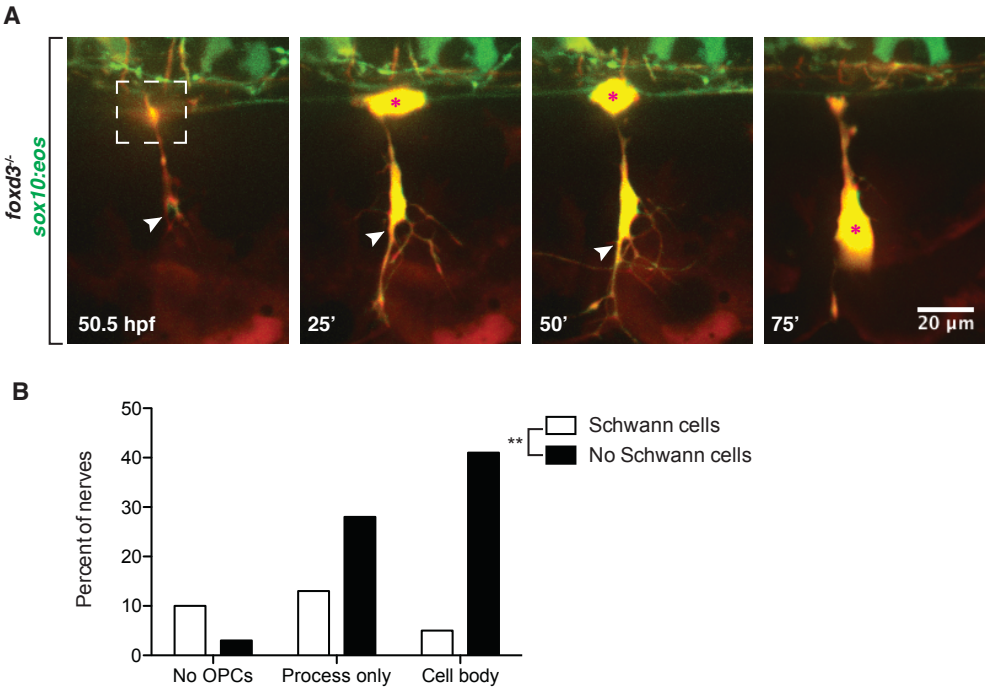

Figure 3-4 OPCs migrate into the PNS in *foxd3*$^{-/-}$ embryos lacking MEP glia. (A) Single frames captured from a time-lapse movie of a *foxd3*$^{-/-}$ embryo. A long *sox10*$^{+}$ process (arrowheads) can be seen protruding through the motor exit point (box), followed by the *sox10*$^{+}$ OPC cell body (asterisk). (B) Quantification of peripheral OPC processes and cell bodies on nerves with or without Schwann cells in *foxd3*$^{-/-}$ embryos. Analyzed by Chi-square test, p= 0.0096. Scale bar, 20 mm

by others in the lab using laser ablation to remove all Schwann cells along a single nerve did not result in any peripheral OPC migration (See Chapter 4 Figure 4-6). The factors regulating the formation of the MEP, and how this could affect MEP glia function and/or OPC exit are not understood. Previous studies of neural crest migration have made clear, however, that neural crest cell migration is directed toward an already-formed MEP once motor axons have emerged, so a role for neural crest cells in forming the MEP in zebrafish is unlikely (Honjo et al., 2008).

I also performed time-lapse imaging using *cls*$^{-/-}$ mutant larvae, to test whether MEP glia are able to repel OPCs from migrating into the periphery in mutants lacking *sox10*. As described above, *cls*$^{-/-}$ larvae have MEP glia, identified by co-expression of the transgenes *sox10:eos* and *olig2:dsred*, as well as by expression of the marker *wif1*. However, the MEP glia in *cls*$^{-/-}$ larvae have abnormal morphology. Because *sox10* is required for oligodendrocyte and Schwann cell differentiation and survival, I hypothesized that MEP glia would not be functional and would fail to repel OPC exit from the spinal cord in *cls* mutants larvae. I performed time-lapse imaging on *sox10:eos;olig2:dsred;cls*$^{-/-}$ larvae from 51 to 72 hpf. At least one OPC migrated through the MEP and onto the peripheral nerve in 100% (3/3) of nerves imaged (Figure 3-5). On one nerve, I observed 3 OPCs exit the spinal cord. These observations of OPCs migrating onto peripheral nerves in *cls*$^{-/-}$ larvae are consistent with previous data (Kucenas et al., 2009). These results indicate that even though MEP glia are present in

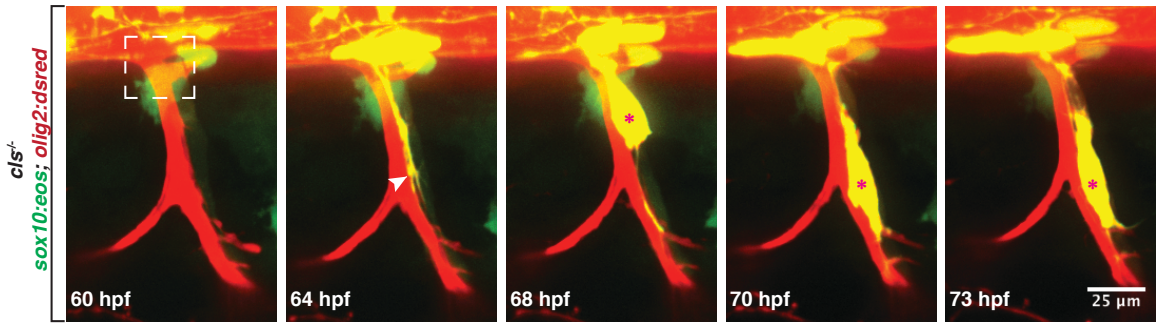

Figure 3-5 OPCs migrate onto peripheral nerves in *cls*$^{-/-}$ larvae. Single frames captured from a time-lapse movie of a *cls*$^{-/-}$ larva. A long *sox10*$^{+}$*/olig2*$^{+}$ process (arrowhead) can be seen protruding through the motor exit point (box), followed by the *sox10*$^{+}$*/olig2*$^{+}$ OPC cell body (asterisk). Scale bar, 25 μm

cls mutant larvae, they do not repel peripheral OPC migration. It is likely that, similar to OPCs, *sox10* is not required for MEP glia specification, but is necessary for their differentiation and function. This role of *sox10* is another similarity between MEP glia and mammalian BCCs. When *sox10* was conditionally deleted from *krox20*-expressing BCCs, BCCs were still found in normal numbers at the nerve roots, but OPCs migrated into the PNS despite the presence of BCCs (Fröb et al., 2012). It would be interesting to further test the hypothesis that *sox10* is required for MEP glia differentiation using markers for MEP glia differentiation, such as *myelin basic protein* (*mbp*) in *cls*$^{-/-}$ larvae. The abnormal morphology of *cls*$^{-/-}$ MEP glia in my experiments may also be an indication of poor health, and it is possible that *sox10* is important for MEP glial survival like it is for both OPCs and Schwann cells. I did not test for markers of cell death in my experiments, and this analysis would likely need to be continued at stages past 72 hpf to definitively test whether *sox10* is important for MEP glia survival.

We have previously shown that the gene *wif1* is a selective marker for MEP glia (Figure 3-1A) (Smith et al., 2014). Expression of *wif1* can be observed in MEP glia as soon as they are present on the motor root at 54 hpf. I hypothesized that *wif1* may be involved in the function of MEP glia to prevent peripheral OPC migration. I tested this hypothesis by knocking down expression of *wif1* using a morpholino oligonucleotide (MO). I injected zebrafish embryos at the 1-cell stage with an antisense MO targeting *wif1*. The MO binds to *wif1* mRNA a few bases upstream of the translation start site and blocks initiation of translation. *Wif1* MO injection resulted in some defects in gross

morphological development of the larvae with varying severity, so I categorized injected larvae as having mild, moderate, or severe phenotypes (Figure 3-6A). Mild phenotypes looked WT or had slight curvature of the tail without any other defects. Moderate phenotypes had some brain necrosis or edema, with or without body curvature. Severe phenotypes had pronounced microcephaly and truncated tails. I hypothesized that *wif1* would be important for MEP glial specification, and that MO-injected larvae would not have MEP glia at the motor root. I tested this hypothesis by injecting *wif1* MO into embryos expressing *olig2:dsred* and quantified the number of *olig2*$^{+}$ MEP glia present in the periphery at 76 hpf. The curved and shortened trunks of larvae in the "severe" category prevented imaging, so quantification was only performed for uninjected, mild, and moderate categories. Surprisingly, I observed no differences in the numbers of nerves that had MEP glia among uninjected, mild, and moderate MO injected larvae (Figure 3-6B. n = 4 WT, n = 7 mild, n =.12 moderate. p = 0.75). This result suggests that *wif1* is not required for MEP glia specification, and that MEP glia are able to migrate to and associate with the motor root without *wif1* expression. However, even though normal numbers of MEP glia were present at the motor root in *wif1* MO-injected larvae, the MEP glia were impaired in their ability to prevent peripheral OPC migration. In these larvae, I also quantified the number of *olig2*$^{+}$ OPCs on the peripheral nerves, and I observed significant numbers of peripherally-migrated OPCs in *wif1* MO-injected larvae in the moderate category compared to uninjected controls (Figure 3-6C. n = 4 WT, n = 7 mild, n = 12 moderate. p = 0.002.)

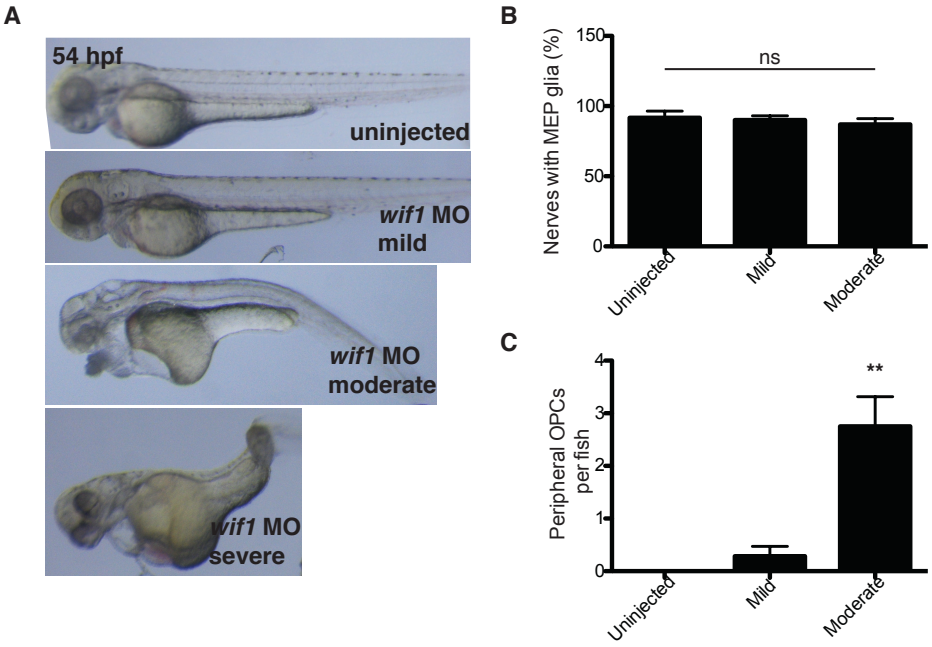

Figure 3-6 *wif1* MO results in peripheral OPC migration. (A) Morphology of uninjected control and *wif1* MO-injected larvae in mild, moderate, and severe categories at 54 hpf. (B) Quantification of the percent of nerves per larvae with MEP glia at 76 hpf. Analyzed by 1-way ANOVA. p = 0.75. (C) Quantification of the number of peripherally migrated OPCs at 3 dpf. Analyzed by 1-way ANOVA. p = 0.002 compared to uninjected.

MEP glia myelinate the motor root in peripheral myelin mutants

During development, a single MEP glial cell migrates through each motor exit point, and each MEP glial cells proliferates at least once to ensheath the proximal portions of the motor nerve (Smith et al., 2014). Similar to Schwann cells, MEP glia are closely associated to the nerves they ensheath, and, beginning at around 4 dpf, they wrap these axons with MBP^{+} membranes (Smith et al., 2014). Although morphologically, myelinating MEP glia resemble myelinating Schwann cells, they do not use the same signaling cascades implicated in Schwann cell myelination. For Schwann cells, the transcription factors *krox20* and *g protein coupled receptor 126*, *gpr126*, are necessary for myelination. Zebrafish with mutations in either gene do not have peripheral myelin (Monk et al., 2009). However, these proteins are not involved in the production of CNS myelin, as myelination in the CNS is completely normal in these mutant larvae. I tested whether these proteins were required for MEP glia to myelinate the motor root. Both *krox20* and *gpr126* mutant embryos have *wif1*$^{+}$ MEP glia at 54 hpf, and MEP glia can also be identified at 72 hpf in both *gpr126*$^{-/-}$ and *krox20*$^{-/-}$ mutant larvae using *sox10:eos* photoconversion (Figure 3-7 and Chapter 4 Figure 4-14). *Sox10*$^{+}$ MEP glia are green because, unlike neural crest derived Schwann cells, they initiate *sox10* expression after photoconversion at 48 hpf. I next tested whether MEP glia myelinate the motor root in *krox20* and *gpr126* mutant larvae. Expression of MBP antibody has previously been observed along the motor root in *gpr126*$^{-/-}$ larvae at 5 dpf (Monk et al., 2009). Using an antibody for MBP and *sox10:eos* transgenic larvae, I observed MBP expression along the motor root in *gpr126* mutant larvae at 91 hpf, but did not observe any peripheral

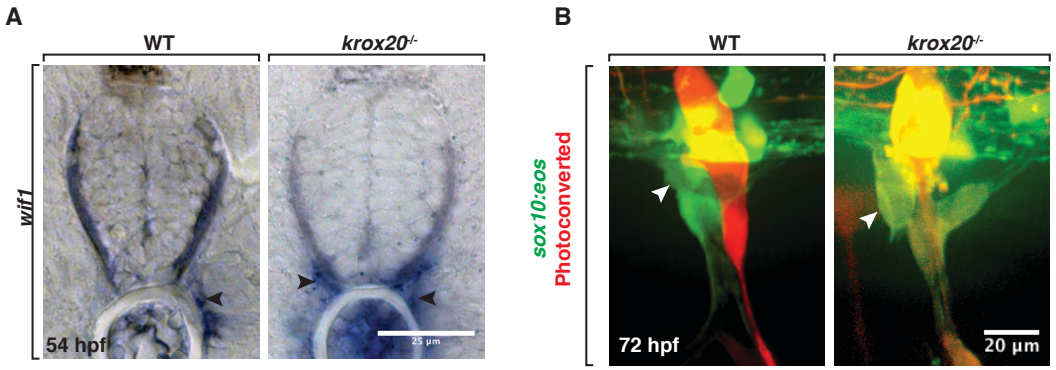

Figure 3-7 MEP glia are present in WT and *krox20*$^{-/-}$ larvae. A) Cross section of the spinal cord stained for *wif1* by *in situ* hybridization. B) Lateral view of *sox10:eos* larvae photoconverted at 48 hpf. Unconverted (green) cells are MEP glia and their derivatives, whereas converted (red) cells are neural crest derived. Arrowheads point to MEP glia. Scale bar, 25 μm (A) 20 μm (B).

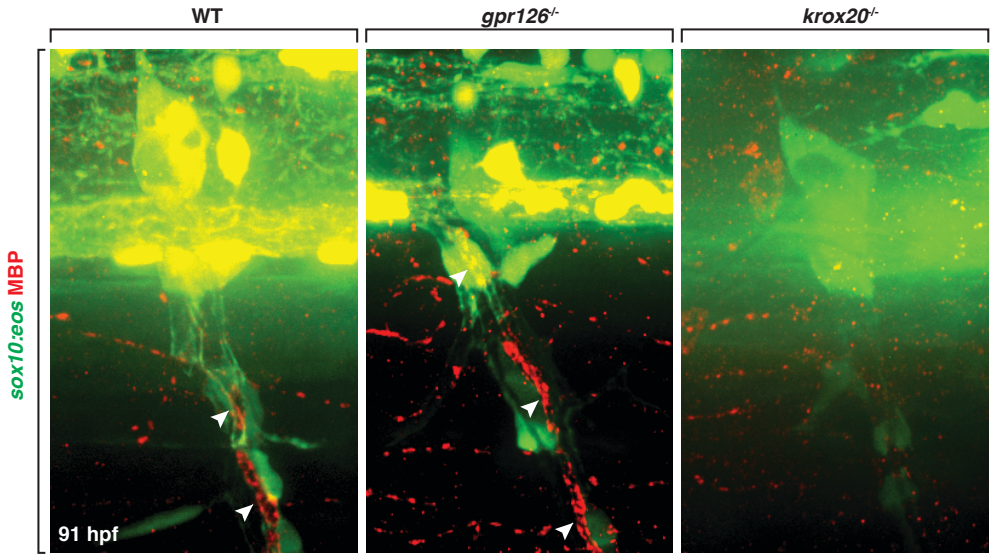

Figure 3-8 MEP glia myelinate the motor root in *gpr126*$^{-/-}$ larvae. Images of MBP antibody labeling in 91 hpf *sox10:eos*-expressing larvae. Arrowheads point to MBP expression on the motor root.

MBP expression in *krox20* mutant larvae (Figure 3-8). This result suggests that MEP glia do not require *gpr126* for myelin initiation, and may instead follow myelination cues similar to oligodendrocytes. However, MEP glia do not myelinate in *krox20* mutant larvae, so this transcription factor may be involved in their differentiation. This hypothesis requires further testing.

Conclusions

We have sought to answer the question of how migratory OPCs within the spinal cord are restricted from migrating into the PNS, despite motor axons being able to penetrate through exit points in the spinal cord and enter the PNS. We discovered a novel glial cell population, MEP glia, which is responsible for preventing peripheral OPC migration by repelling OPCs at the MEP (Smith et al., 2014). We wanted to know more about how these cells function, so I undertook characterization of the signals regulating MEP glia specification, differentiation, and function. The previously published BCC marker *wif1* selectively labels MEP glia at the motor root at all stages investigated so far, and it is a useful tool for assessing the presence of MEP glia in genetic mutants or other manipulations hypothesized to affect MEP glia. Furthermore, *wif1* is important for the functioning of MEP glia, as MO knockdown of *wif1* expression results in ectopic peripheral migration of OPCs. The expression of *wif1* in MEP glia and BCCs is a similarity between these two cell types, and ongoing work in the lab is testing whether *wif1* functions similarly in BCCs to prevent peripheral OPC migration. Another similarity between MEP glia and BCCs is the requirement for *sox10* for differentiation and/or

function, but not for specification or positioning at the MEP. In zebrafish *cls*$^{-/-}$ larvae lacking *sox10*, MEP glia were present at the motor root, and previously published results demonstrated that *wif1*-knockout BCCs were present at the mouse MEP, but OPCs were ectopically positioned along the motor root in zebrafish *cls*$^{-/-}$ larvae and *sox10* conditional knockout mice (3- 5) (Fröb et al., 2012; Kucenas et al., 2009). MEP glia have many obvious similarities to OPCs, since both originate from the pMN domain of the spinal cord, express *olig2* and *sox10*, require *notch* for specification, and require *sox10* for differentiation. However, MEP glia also have some signaling pathways in common with Schwann cells. Both require *erbb3* signaling to migrate and associate with the peripheral motor root, and MEP glia and Schwann cells are missing from the nerve in *erbb3* mutant larvae (Figure 3-1) (Lyons et al., 2005; Smith et al., 2014). *Foxd3* is also involved in early specification of both cell types, since *foxd3* mutant embryos do not have MEP glia, and *foxd3* mutant embryos also have impaired neural crest specification (Figure 3-3) (Montero-Balaguer et al., 2006).

Our discovery that MEP glia are a novel glial population positioned specifically at spinal cord motor exit points to repel ectopic OPC migration is a significant step forward in understanding mechanisms regulating boundary formation in nervous system development. Our findings and studies of BCCs show that deployment of discrete cell populations at boundary locations to repel ectopic migration by other cells is a conserved mechanism from fish to mammals (Coulpier et al., 2010; Fröb et al., 2012; Smith et al., 2014; Vermeren et al., 2003). MEP glia, which are easy to identify and

image live, can help us learn more about BCCs and boundary mechanisms in mammals. BCC interactions are more difficult to study because of heterogeneity within the population and because cell-cell interactions and migration cannot be imaged live at the mouse MEP. We are also intrigued by the interactions between MEP glia and OPCs as a potential model for studying contact-mediated repulsion (CMR) as a regulator of cell migration and spacing. It has recently been hypothesized that a subset of BCCs may originate from the ventral spinal cord like MEP glia (Radomska and Topilko, 2017). It would be interesting to test whether some of what we know about MEP glia have similar applications to BCCs. For example, is *wif1* required to repel peripheral OPC migration in mice like it is in zebrafish? Are any ventral BCCs derived from *olig2*-expressing progenitors? More thorough analysis of MEP glia would also be facilitated by a specific transgene driven by *wif1* expression or another selective marker, and ongoing efforts in the lab are working toward this goal.

Chapter 4

The neuromodulator adenosine regulates oligodendrocyte migration at motor exit point transition zones

Summary

During development, OPCs migrate extensively throughout the spinal cord, but their migration is restricted at transition zones (TZ). At these specialized locations, unique glial cells in both zebrafish and mice are at least partially responsible for preventing peripheral OPC migration, but the mechanisms of this regulation are not understood. In order to elucidate the mechanisms that mediate OPC segregation at motor exit point (MEP) TZs, we performed an unbiased small molecule screen. Using chemical screening and *in vivo* imaging, we discovered that inhibition of A2a adenosine receptors (AR) causes ectopic OPC migration out of the spinal cord. In our studies, we provide *in vivo* evidence that endogenous neuromodulation by adenosine regulates OPC migration along motor axons, specifically at the MEP TZ. This work opens exciting possibilities for understanding how OPCs reach their final destinations during development and identifies mechanisms that could promote their migration in disease.

Introduction

Oligodendrocyte progenitor cells (OPC) are migratory, proliferative cells with multiple functions in central nervous system (CNS) development and disease (Bergles and Richardson, 2015; Emery and Lu, 2015; Zuchero and Barres, 2015). These progenitors differentiate into oligodendrocytes (OL), the myelinating glia of the CNS, which ensheath axons in an insulating layer of myelin that is essential for rapid propagation of action potentials (Simons and Nave, 2016). During gliogenesis, OPCs are specified from discrete precursor domains within the brain and spinal cord, but they migrate extensively to become distributed throughout the entire CNS (Miller, 2002; Rowitch, 2004). In the spinal cord, the majority of OPCs are specified from ventral pMN precursors that also give rise to motor neurons during neurogenesis (Richardson et al., 2000). These motor neurons extend axons ventrally toward the motor exit point (MEP) transition zone (TZ) and cross into the peripheral nervous system (PNS), where they ultimately innervate targets including skeletal muscle (Lewis and Eisen, 2003; Bonanomi and Pfaff, 2010). As OPCs disperse from the pMN domain to populate the spinal cord, a subset extends membrane processes into the MEP TZ (Fraher and Kaar, 1984; Smith et al., 2014). However, OPC cell bodies are normally restricted from migrating through the MEP TZ and onto peripheral nerves.

The mechanisms allowing selective migration of motor axons and other glial populations, but not OPCs, through the MEP TZ are not understood. Recently, work from our lab and others shows that OPCs are capable of migrating into the PNS in

zebrafish and mouse mutants with PNS defects, and peripheral OPCs have even been described in human peripheral neuropathy patients (Coulpier et al., 2010; Fröb et al., 2012; Kucenas et al., 2009; Smith et al., 2014). Based on these studies, we hypothesize that active regulation of OPC migration restricts them to the CNS.

Although the molecular mechanisms that mediate OPC restriction to the CNS have not yet been elucidated, previous work from our lab identified a population of CNS-derived peripheral glial cells called motor exit point (MEP) glia, which are essential for preventing OPC migration onto spinal motor nerves (Smith et al., 2014). A similar population known as boundary cap cells (BCC) located at TZs also exists in mice and is hypothesized to regulate OPC migration at MEP TZs (Coulpier et al., 2010; Fröb et al., 2012). Specific ablation of MEP glia or BCC without any other damage to the nerve results in OPC migration onto spinal motor nerves.

In order to identify mechanisms regulating OPC migration at the MEP TZ, we performed an unbiased chemical screen of pharmacologically active compounds. This screen identified 10 small molecules that resulted in peripherally-located OPCs. We focused further testing on one of these compounds, an adenosine receptor (AR) antagonist, because adenosine is a well-known modulator of neuronal activity, and neuronal activity has been implicated in regulating OPC differentiation, proliferation, and migration (Etxeberria et al., 2016; Gibson et al., 2014; Gudz et al., 2006; Hines et al., 2015;

Mangin et al., 2012; Mensch et al., 2015; Stevens et al., 2002; Xiao et al., 2016, 2013 reviewed in Almeida and Lyons, 2017; Fields, 2015).

Purinergic signaling modulates neuronal firing

Adenosine triphosphate (ATP) and its derivatives, adenosine diphosphate (ADP), adenosine monophosphate (AMP), and adenosine, important players in cell metabolism, can also act as extracellular "purinergic" signaling ligands for a variety of cell types (Burnstock and Knight, 2004; Stone, 1985). Cell membrane receptors for these ligands, known as purinergic receptors, initiate a variety of downstream signaling events (Dunwiddie and Masino, 2001). Members of the purinergic receptor family have nearly ubiquitous expression in many different tissues, including the nervous system, where they regulate processes as diverse as inflammation, vasodilation, and neurotransmission (Burnstock and Knight, 2004). In the CNS, purinergic signaling is implicated in processes ranging from sleep and arousal, locomotor activity, and pain processing (Burnstock, 2013).

Purinergic receptors are divided into two main classes: P1 receptors, which are activated by adenosine, and P2 receptors, which are activated by ATP and/or ADP (Figure 4-1) (Abbracchio et al., 2006; Welsh et al., 2018). P2 receptors are further subdivided into P2X or P2Y subtypes, according to whether the receptor is ionotropic (P2X) or metabotropic (P2Y). Four mammalian P1 receptors have been identified, A1, A2a, A2b and A3, all of which are G protein coupled receptors. A1 and A3 work by the

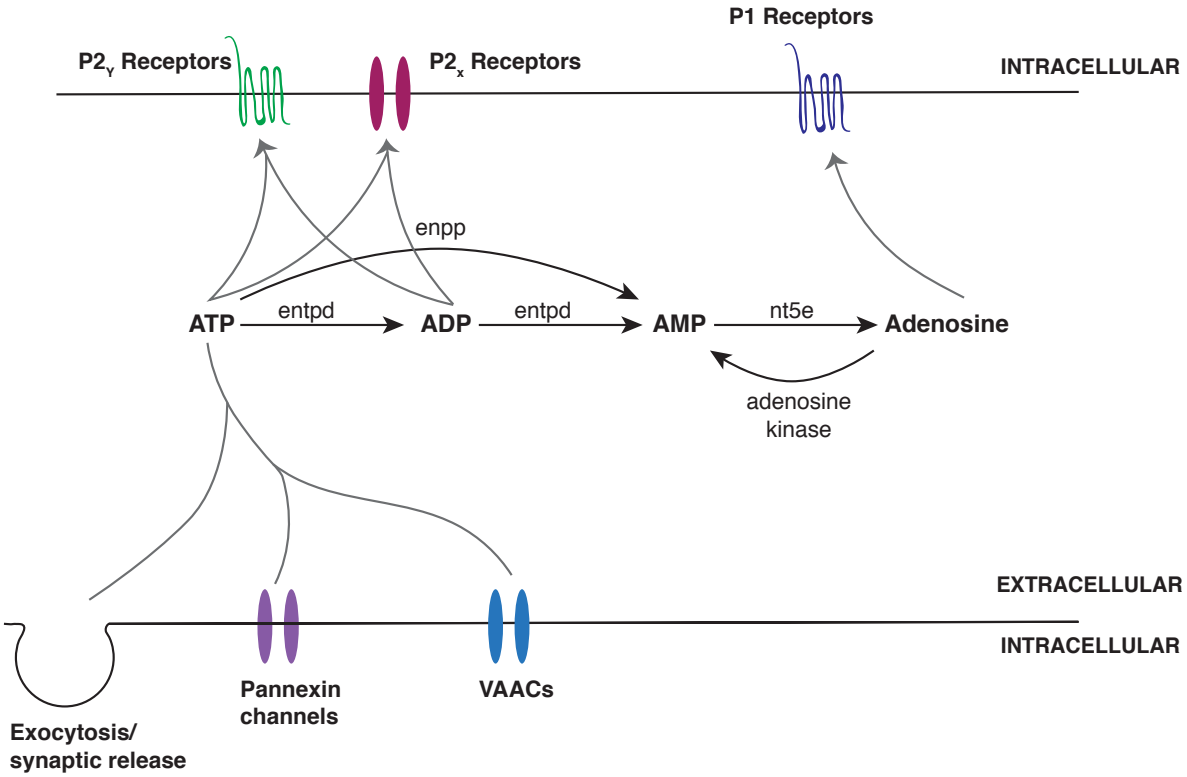

Figure 4-1 Purinergic release, receptors, and degradation. Adenosine triphosphate (ATP) can be released into the extracellular space via membrane channels or exocytosis. In neurons, ATP is released in high concentrations from synaptic vesicles. Extracellular enzymes rapidly degrade ATP into adenosine diphosphate (ADP), adenosine monophostphate (AMP), and adenosine. ATP and ADP activate metabotropic $P2_Y$ and/or ionotropic $P2_X$ receptors. Adenosine activates P1 receptors. Figure is from Welsh and Kucenas, 2017 J Neurochem.

same mechanism, inhibiting adenylate cyclase and decreasing intracellular cAMP. A2a and A2b both activate adenylate cyclase, increasing cAMP (Fredholm et al., 2000; Schulte and Fredholm, 2003). In the CNS, P1 signaling via A1 and/or A2a receptors has been implicated in regulating neuronal firing in a variety of circuits (Chen et al., 2014; Cunha, 2001; Sebastiao and Ribeiro, 2015). Generally, A1 receptors inhibit neuronal activity, although the mechanism differs depending on whether A1 receptors are expressed on presynaptic or postsynaptic membranes. At presynaptic terminals, A1 decreases neurotransmitter releases by affecting calcium channels (Gundlfinger et al., 2007; Wu and Saggau, 1994, 1997). Presynaptic neuronal inhibition by A1 receptors has been reported for excitatory inputs to the visual cortex, spinal cord dorsal horn, amygdala, subiculum, basal forebrain, and tegmentum (Arrigoni et al., 2001; Bannon et al., 2014; Deuchars and Brooke, 2001; Hargus et al., 2009; Hawryluk et al., 2012; Patel et al., 2001; Rau et al., 2015). In addition to presynaptic inhibition, A1 can act postsynaptically to inhibit excitatory post synaptic currents (EPSCs), either by modulating glutamate receptors, or by hyperpolarizing membrane potentials to make cells less excitable (Arrigoni et al., 2001; Trussell and Jackson, 1985). Although this mechanism seems to be less common than presynaptic inhibition, postsynaptic A1 inhibition has been identified in the visual cortex and also in the subiculum (Arrigoni et al., 2001; Bannon et al., 2014). Most studies of A1 inhibition have focused on excitatory neurotransmission, but in some cases A1 also inhibits GABAergic currents (Arrigoni et al., 2001; Rombo et al., 2014; Zhang et al., 2015). However, others have reported no effect of A1 signaling on GABAergic currents, so whether and how A1 receptors

modulate neuronal activity varies with types of neurons and in different parts of the brain (Deuchars and Brooke, 2001). Interstingly, many studies note that application of A1 antagonists alone, without any exogenously applied adenosine, results in significant facilitation of EPSCS (Bannon et al., 2014; Hargus et al., 2009; Hawryluk et al., 2012). These results suggest that in many areas of the brain, basal levels of endogenous adenosine are high enough to exert a tonic inhibitory effect, which can be relieved by application of A1 antagonists.

Because A2a expression is less widespread in the CNS, and because selective agonists and antagonists have more recently been developed, A2a effects on neurotransmission have been less extensively studied. Generally, A2a activation facilitates neuronal activity through a variety of mechanisms (Cunha, 2001; Dunwiddie and Masino, 2001; Sebastiao and Ribeiro, 2015). A2a activation can facilitate excitatory neurotransmitter release from presynaptic terminals, as well as GABA release from GABAergic projections (Bannon et al., 2014; Ciruela et al., 2015; Quarta et al., 2004; Rombo et al., 2014; Zhang et al., 2015). Postsynaptic facilitation of excitatory synapses has also been observed in neurons of the hippocampus and amygdala (Dias et al., 2012; Rau et al., 2015; Rebola et al., 2008; Tebano et al., 2005). A2a receptors can also affect neuronal activity through interactions with other neurotransmitter receptors. A2a activation has been shown to modulate A1, dopamine D2, and metabotropic glutamate mGluR receptors (Lopes et al., 2002; Shen et al., 2008; Tebano et al., 2005).

Sources of extracellular adenosine in the nervous system

Most extracellular adenosine in the CNS is thought to come from hydrolysis of extracellular ATP (Cunha, 2001). All cells synthesize ATP as part of their metabolism and, therefore, are capable of releasing large quantities into the extracellular space if damaged (Casano et al., 2016; Davalos et al., 2005; Elliott et al., 2009). Additionally, multiple mechanisms exist for the regulated release of ATP during normal nervous system physiology, and the most well characterized is via ATP packaged into synaptic vesicles (Figure 4-1) (Abbracchio et al., 2009; Burnstock, 1972; Fields and Burnstock, 2006). Most, if not all, neurons use ATP transporters to concentrate neurotransmitters into synaptic vesicles (Abbracchio et al., 2009). ATP is therefore released in high concentrations (up to 1000 mM) as a co-transmitter with neurotransmitters such as glutamate and acetylcholine (Fields and Burnstock, 2006). In some PNS and CNS neurons, ATP is even released as a bona fide neurotransmitter (Burnstock, 1972; Edwards et al., 1992; Holton and Holton, 1954). One study has also reported activity-dependent release of adenosine directly from neurons, although it is unclear whether synaptic vesicles or some other mechanism is the route of release (Wall and Dale, 2007).

However, axon terminals are not the only sites of ATP release in the nervous system. Multiple studies demonstrate ATP release from axonal segments remote from synaptic terminals or from cultured neurons that haven't formed any synapses (Edstrom et al., 1992; Fields and Ni, 2010; Kriegler and Chiu, 1993; Stevens and Fields, 2000). This

ATP may come from “extrasynaptic” vesicles released from premyelinated/unmyelinated segments of axons. Another proposed mechanism for axonal ATP release is via volume activated anion channels (VAACs). These channels can be activated by cell swelling and/or mechanical stress and are a well-characterized mechanism of ATP release in non-neuronal cells (Burnstock, 1999; Sabirov and Okada, 2005). One *in vitro* study demonstrated that axonal swelling and mechanical stress as a result of firing action potentials can activate VAACs, leading to ATP leaking out of VAACs (Fields and Ni, 2010). Whether VAACs are involved in axonal ATP release *in vivo* remains to be determined. VAAC-mediated versus vesicular release of ATP from axons may not necessarily be mutually exclusive, since both of these mechanisms involve activity-dependent release from pre-myelinated and/or unmyelinated axons In addition to activity-dependent release, there is also evidence for ATP release via ATP-binding cassette transporters and pannexin channels expressed by neurons and glia. Additionally, astrocytes can release ATP via vesicular release or through gap junction hemichannels (Abbracchio et al., 2009; Boué-Grabot and Pankratov, 2017). The relative contributions of neurons and astrocytes to extracellular adenosine levels are unclear. However, many studies have shown that endogenous adenosine levels are high enough to tonically activate CNS A1 receptors (Bannon et al., 2014; Hargus et al., 2009; Hawryluk et al., 2012).

After release, extracellular ATP is rapidly hydrolyzed by extracellular enzymes (Abbracchio et al., 2009; Dunwiddie and Masino, 2001) . The extracellular enzymes

ectonucleotide pyrophosphatase/phosphodiesterase (*enpp*) and *ectonucleoside triphosphate diphosphohydrolase* (*entpd*) hydrolyze ATP to ADP and AMP. Nt5e, also known as CD73, is the main enzyme that converts AMP to adenosine, and its expression is enriched in OPCs compared to other neural cell types, suggesting a potential role for OPCs in regulating extracellular adenosine concentrations (Zhang et al., 2014; Zimmermann, 2000). The function of ectonucleotidases in nervous system development is unclear, although there is some evidence for their involvement in regulating neuronal excitability (Carlsen and Perrier, 2014; Sowa et al., 2010) . Because of adenosine's involvement in regulating neuronal activity and the recent evidence for neuronal activity affecting OPCs, we hypothesized that adenosinergic regulation of neuronal activity at spinal motor roots may be crucial for restricting OPC migration at the MEP. Here, we report that adenosine signaling through spinal cord neuronal A2a ARs functions to regulate OPC migration at MEP TZs during development, and that this regulation is dependent on neuronal activity.

Results

Identification of molecules that induce ectopic OPC migration through the MEP TZ

Glial cells that establish a barrier to OPC migration across the MEP TZ have been identified in mice and fish (Coulpier et al., 2010; Frob et al., 2012; Smith et al., 2014). In zebrafish, MEP glia positioned along motor root axons prevent OPCs from migrating out of the spinal cord (Smith et al., 2014). During development, ventral OPCs within the spinal cord extend membrane processes through the MEP TZ and contact MEP glia (Figure 4-2A). When this occurs, the OPC is immediately repelled and retracts its process. When MEP glia are absent, OPCs freely migrate through the MEP TZ and onto peripheral motor nerves (Morris et al., 2017; Smith et al., 2014). However, the signals restricting OPC migration at the MEP are unknown. Therefore, to identify molecular mechanisms regulating OPC migration at the MEP TZ, we conducted an unbiased screen of pharmacologically active compounds to identify signaling cascades involved in OPC segregation to the CNS.

To conduct our screen, we treated *olig2:dsred* embryos, which express DsRed in motor neurons and OPCs, at 24 hours post fertilization (hpf) with compounds from the Library of Pharmacologically Active Compounds (LOPAC$^{®1280}$). In a primary screen, one or two embryos per well of a 96 well plate were treated with either 10 μM of a compound from the library, 1% DMSO as a negative control, or 4 μM AG1478 as a positive control (Figure 4-2B). The positive control AG1478 inhibits Erbb3 signaling and phenocopies

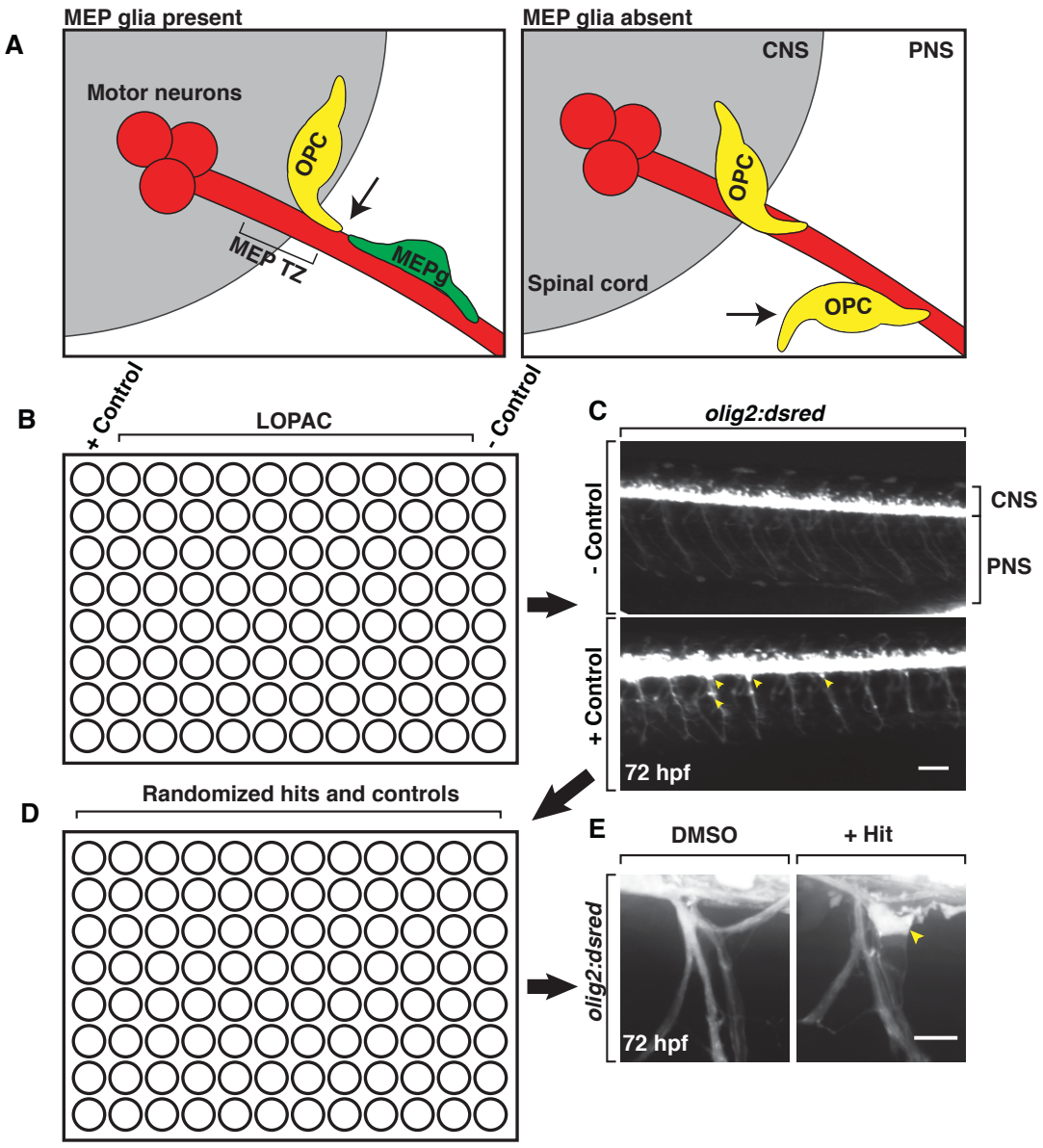

Figure 4-2 A small molecule screen identifies compounds that disrupt OPC migration at the MEP TZ. (A) Schematic of a transverse view of the MEP TZ. MEP glia (MEPg) prevent OPC exit from the spinal cord (gray). OPC processes (yellow, arrow) contact MEP glia (green) but are repelled. Without MEP glia, OPCs migrate onto peripheral nerves. (B) Schematic showing setup of primary small molecule screen. One or two embryos per well were treated with a single compound from the LOPAC library. AG1478 was the positive (+) control and 1% DMSO was the negative (-) control for each plate. (C) Low magnification images showing lateral views of negative (top) and positive (bottom) controls at 3 dpf. (D) Positive hits were repeated in triplicate and randomized with positive and negative controls in a blind secondary screen. (E) Images of 3 dpf *olig2:dsred* larvae control and validated hits showing ectopic OPC (arrowhead) on the peripheral nerve. Arrowheads mark peripheral OPCs. Scale bar, (C) 100 μM, (E) 20 μM.

the *erbb3b* mutation (Lyons et al., 2005). Previously, we demonstrated that *erbb3b* mutants have peripherally-migrated OPCs because they lack MEP glia (Morris et al., 2017; Smith et al., 2014). A pilot experiment confirmed that treatment with 4 μM AG1478 from 24 hpf to 3 days post fertilization (dpf) caused robust peripheral OPC migration, whereas 1% DMSO did not (Figure 4-2C). For the rest of our screen, we analyzed larvae at 3 dpf for the presence of *olig2*$^{+}$ cell bodies in the periphery (Figure 4-2C). Any compound resulting in at least one peripheral *olig2*$^{+}$ cell per larva was considered a positive "hit". 197 hits were found in our primary screen, with 910 compounds having no peripherally-migrated *olig2*$^{+}$ cells, and the remaining 173 compounds resulted in death of the embryo. All hits from the primary screen were retested in a secondary screen using the same protocol but with the following modifications: 1) each compound was tested in triplicate, 2) all compounds, including 12 positive and 12 negative controls, were randomized across the plate, and 3) we were blinded to which wells contained experimental compounds or controls until after analysis (Figure 4-2D). Any compound resulting in at least one peripheral *olig2*$^{+}$ cell in 3/3 or 2/2 (if one sample died) larvae was considered a validated hit (Figure 4-2E). This screening protocol resulted in 11 total validated hits, and 10 out of those 11 compounds resulted in multiple peripheral OPCs per larva. Table 4-1 describes all of the validated compounds. One of the 11 compounds was removed from the final list in Table 4-1 because an independent stock from the supplier did not reproduce the same ectopic OPC migration phenotype observed in the screen. Intriguingly, from this screen, we discovered multiple compounds involved in neurotransmission and/or modulation of neuronal activity (Table

Table 4-1. Validated hits from screen using LOPAC®[1280]. Gray shaded chemicals are predicted to affect neuronal activity.

Drug name	Description
CGS-15943	Highly potent, non selective adenosine receptor antagonist
1-Phenyl-3-(thiazolyl)-2-thiourea	Dopamine β-hydroxylase inhibitor
Acetylthiocholine chloride	Nicotinic acetylcholine receptor agonist
Brefeldin A from *Penicillium brefeldianum*	Causes collapse of Golgi apparatus, blocking exocytosis
N-Phenylanthranilic acid	Cl- channel blocker
Salmeterol xinafoate	Selective β2 adrenergic receptor agonist
I-OMe-Tyrphostin AG 538	Insulin growth factor I (IGF-1) receptor inhibitor
L-Canavanine sulfate	Selective inhibitor of inducible nitric oxide synthase (iNOS)
Clofibrate	Peroxisome proliferator-activated receptor-α (PPARα) agonist
Wortmannin from *Penicillium funiculosum*	Selective phosphatidylinositol 3-kinase (PI3-K) inhibitor

4-1). For the remainder of this manuscript, we will focus on one signaling cascade identified in this screen.

A2a ARs mediate OPC migration at the MEP TZ

One compound we identified, CGS-15943, is a highly potent, non-selective AR antagonist (Ongini et al., 1999). Adenosine is a well known modulator of neuronal activity and can either increase or decrease neuronal firing by binding to different ARs (Sebastiao and Ribeiro, 2015). Because adenosine can modulate neuronal activity, and purinergic signaling has been implicated in OL differentiation and migration (Dennis et al., 2012; Stevens et al., 2002) we focused our experiments on this cascade.

We first confirmed that CGS-15943 caused peripheral OPC migration through the MEP TZ by performing *in vivo*, time-lapse imaging. In order to distinguish OPCs from motor neurons, we used embryos expressing *olig2:dsred* and *sox10:eos*, where *sox10* regulatory elements drive expression of Eos in central and peripheral glia. Therefore, OPCs are Eos^{+} and $DsRed^{+}$ (yellow). We treated these embryos with 10 μM of CGS-15943 from 24 hpf to 3 dpf and imaged 3 larvae (10 nerves total) from 55 hpf to 3 dpf. In these time-lapse movies, we observed *sox10*$^{+}$*/olig2*$^{+}$ cells with highly dynamic membrane processes at the MEP TZ (Figure 4-3A). Because of the morphology, behavior and co-expression of *olig2* and *sox10,* we confirmed that they were OPCs. In 9 out of 10 nerves (90%) imaged, we observed OPCs extend highly dynamic membrane processes through the MEP TZ. On 6 out of 10 nerves (60%), OPC cell bodies

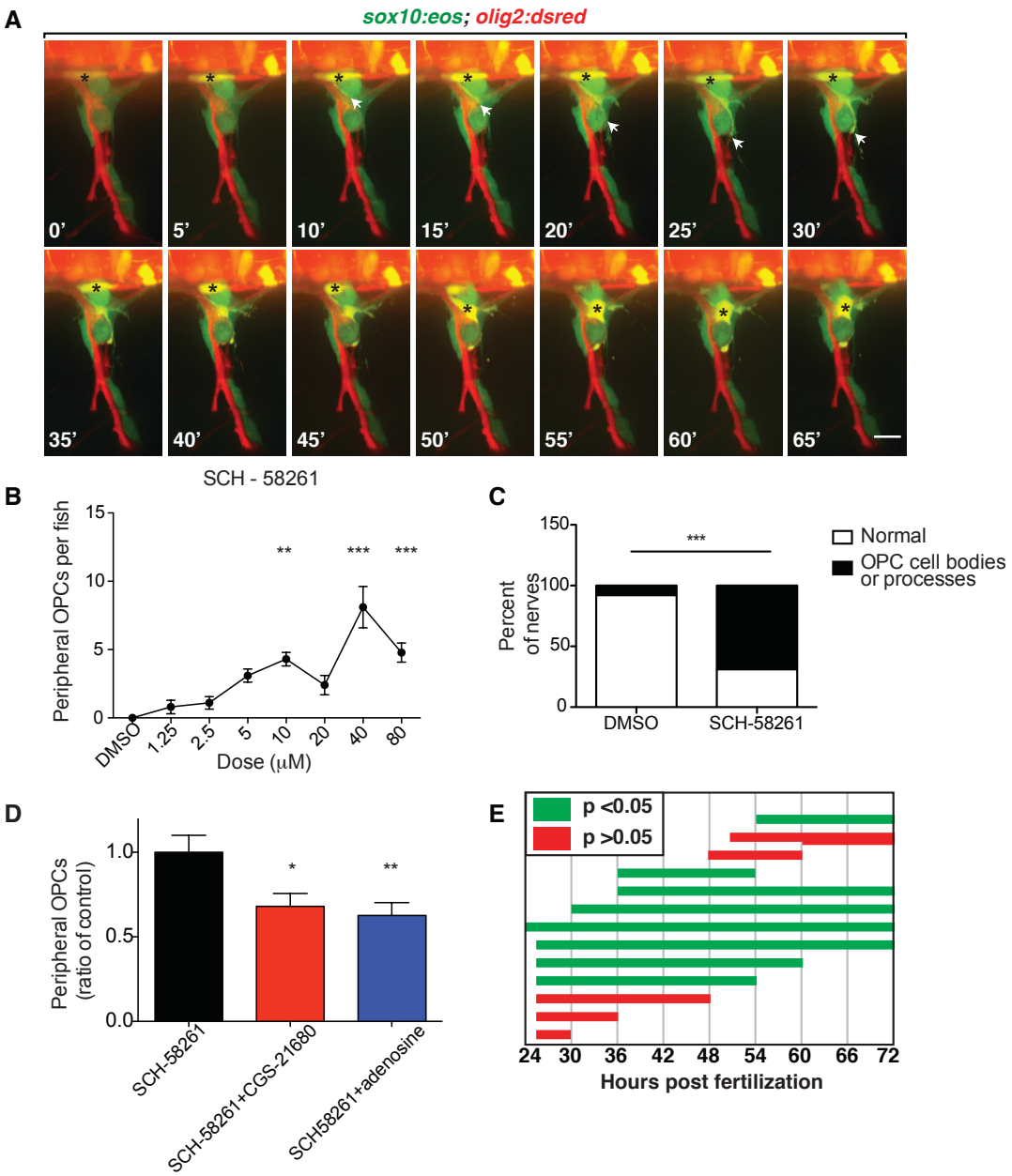

Figure 4-3 AR antagonists cause OPC migration through the MEP TZ. (A) Frames captured from a 15 hour time-lapse movie of a *sox10:eos;olig2:dsred* larvae treated with CGS-15943 from 24 hpf to 3 dpf and imaged from 57 to 72 hpf. 0' is 58 hpf. Black asterisk marks OPC cell body. Arrowhead marks OPC leading process. (B) Dose response curve of the number of peripheral OPCs for fish treated from 24 hpf to 3 dpf with SCH-58261. Mean ± SEM, n = 9-10 larvae per dose. (C) Percent of nerves at 3 dpf which have ectopic OPC processes and/or cell bodies. n = 60 (DMSO) n = 98 (SCH-58261). (D) Mean ± SEM of peripheral OPCs in *olig2:dsred* larvae treated with 10 μM SCH-58261 alone or in combination with 2.5 μM CGS-21680 or 5 μM adenosine from 36 hpf to 3 dpf. n= 29-30 fish per treatment. (E) Peripheral OPC counts for larvae treated with 10 μM SCH-58261 during distinct developmental periods. Green bars indicate mean peripheral OPC counts significantly above DMSO control ($p < 0.05$), and red bars indicate mean peripheral OPC counts not significantly different than DMSO ($p > 0.05$) n = 9-12 larvae per condition. * $p < 0.05$, ** $p < 0.01$ compared to DMSO. Scale bar, 20 μM.

squeezed through this opening and migrated onto peripheral spinal motor nerves during imaging (Figure 4-3A). This migration most often occurred between 60 and 72 hpf, although we sometimes observed OPCs already present on the nerve before 60 hpf (3 out of 10 nerves (30%)). Interestingly, we never observed any *olig2*$^{+}$*/sox10*$^{-}$ motor neurons in the periphery in these time-lapse movies (0 out of 10 nerves (0%)), indicating that adenosine signaling is necessary for restricting OPCs to the spinal cord, but not motor neurons. This is consistent with evidence from our lab and others demonstrating that distinct mechanisms regulate segregation of glia and neurons at the MEP TZ (Fröb et al., 2012; Kucenas et al., 2009).

We next sought to determine which AR subtype was required for preventing peripheral OPC migration. To do this, we treated embryos expressing *olig2:dsred* from 24 hpf to 3 dpf with varying concentrations of selective antagonists for each of the 4 AR subtypes: A1 (8-cyclopentyltheophylline (CPT), n = 9-10 embryos per dose), A2a (SCH-58261, n = 10 embryos per dose), A2b (MRS-1754, n = 10 embryos per dose), and A3 (MRS-1191, n = 10 embryos per dose), as well as the general AR antagonist, CGS-15943 (n = 5-10 embryos per dose) (Jiang et al., 1996; Ongini et al., 1999; Searl and Silinsky, 2012; Wei et al., 2013). We analyzed drug-treated larvae at 3 dpf using the same methods described for the original chemical screen, and quantified the number of peripheral *olig2*$^{+}$ OPCs. As expected, CGS-15943 caused significant peripheral OPC migration (Figure 4-4A, $p < 0.01$). This confirmed the qualitative results from our screen and time-lapse data that AR antagonism results in peripherally-migrated OPCs. The selective

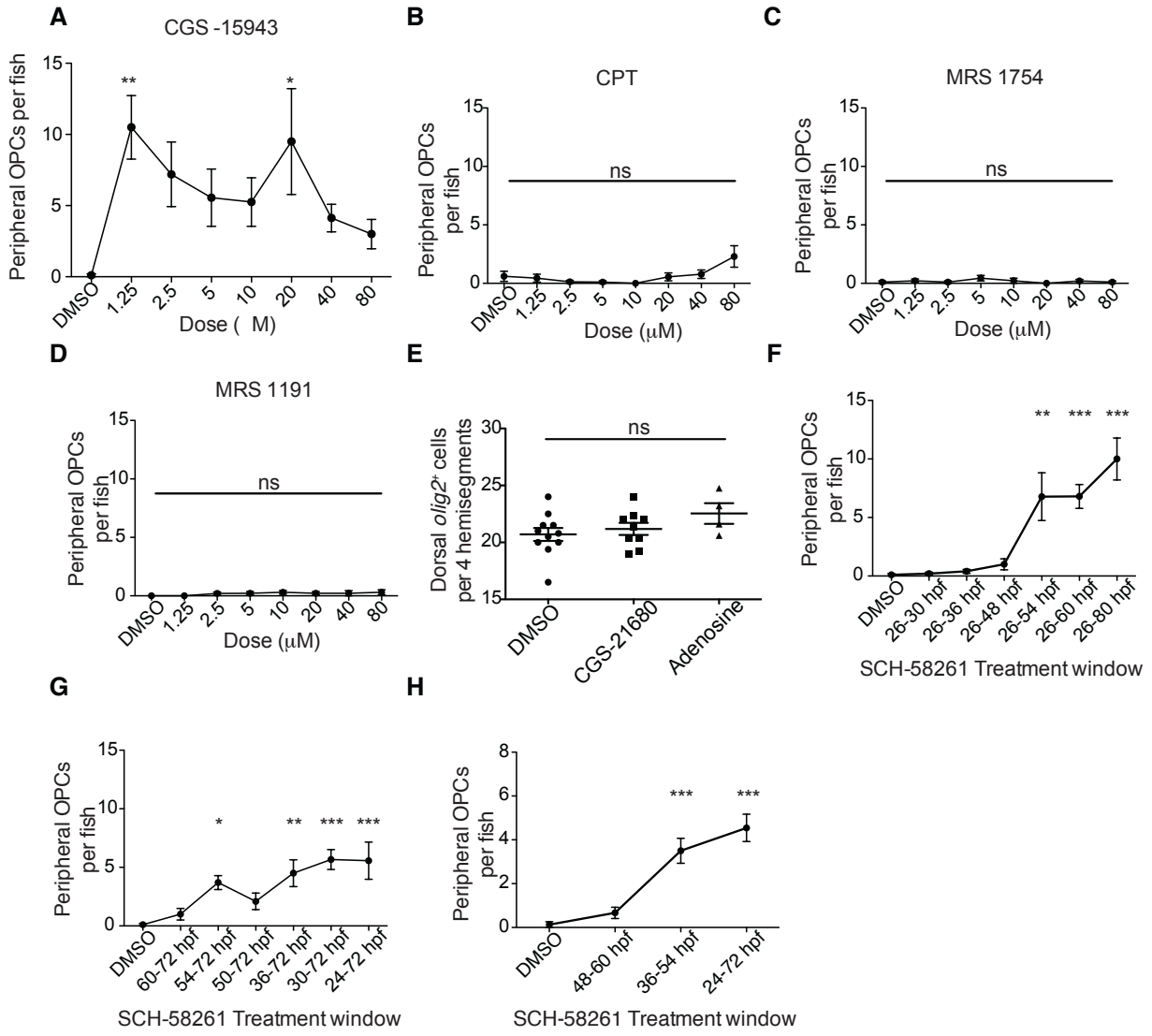

Figure 4-4 A2a AR specifically mediates OPC migration at the MEP TZ. (A-D) Dose responses for the general AR antagonist CGS-15943 and antagonists selective for A1 (CPT), A2b (MRS 1754), and A3 (MRS 1191). (E) Mean ± SEM dorsal *olig2*$^+$ cells at 3 dpf in *olig2:dsred* larvae treated with DMSO (n = 11), CGS-21680 (n = 9), or adenosine (n = 4), p = 0.23. (F-H) Numbers of peripheral OPCs in larvae treated with 10 μM SCH-58261 during various developmental stages. All data presented are mean ± SEM. * $p < 0.05$, ** $p < 0.01$, *** $p < 0.001$ compared to DMSO, n = 9-12 fish per condition.

A2a AR antagonist, SCH-58261, also resulted in significant numbers of peripheral *olig2*$^{+}$ OPC cell bodies and membrane processes (Figure 4-3B&C, $p < 0.01$ for 10 μM SCH-58261 compared to DMSO), whereas we did not observe peripheral OPCs following treatment with selective antagonists for any of the other AR subtypes (Figure 4-4B-D). From these data, we conclude that only A2a ARs are involved in regulating OPC migration at MEP TZs. Therefore, we performed all subsequent experiments using SCH-58261 at 10 μM, as this was the lowest dose that caused ectopic OPC migration into the periphery.

We sought to further confirm the selectivity of SCH-58261 activity to A2a ARs with competitive binding experiments. If SCH-58261 selectively antagonizes the A2a AR, we hypothesized that co-administering an A2a agonist would rescue the peripheral migration phenotype caused by SCH-58261. To test this, we treated 24 hpf *olig2:dsred* embryos with 10 μM SCH-58261 combined with 5 μM adenosine or 2.5 μM of the A2a selective agonist CGS-21680 and quantified the number of peripheral OPCs at 3 dpf (Jarvis and Williams, 1989). Both adenosine and CGS-21680 significantly decreased the number of peripheral OPCs when co-administered with SCH-58261 (Figure 4-3D, $p < 0.05$ CGS-21680; $p < 0.01$ adenosine compared to SCH-58261 alone, $n = 29$-30 larvae). These results support the conclusion that SCH-58261 selectively antagonizes A2a ARs to induce ectopic OPC migration, and this effect can be mitigated with A2a AR agonists. To confirm that adenosine or CGS-21680 treatment alone did not interfere with normal OPC development or migration within the spinal cord, we imaged

olig2:dsred zebrafish larvae at 3 dpf following treatment with adenosine, CGS-21680, or DMSO from 24 hpf to 3 dpf and quantified dorsal spinal cord *olig2*$^{+}$ OPCs in a 4-somite region and did not observe any differences among treatments (Figure 4-4E, $p = 0.23$; adenosine, n = 4 larvae; CGS-21680, n = 9 larvae; DMSO, n = 11 larvae).

In our initial screen, our treatment protocol spanned from 24 hpf to 3 dpf, encompassing OPC specification, proliferation, and migration (Kirby et al., 2006; Kucenas et al., 2008; Park et al., 2002). We sought to narrow the treatment window to see if A2a AR signaling was sufficient while OPCs were actively migrating. To do this, we treated *olig2:dsred* embryos with 10 μM SCH-58261 during various time windows and quantified the number of peripheral OPCs at 3 dpf. We found that exposure to SCH-58261 beginning later than 54 hpf or ending earlier than 54 hpf did not result in any peripheral OPC migration (Figure 4-3E and Figure 4-4F-H, n = 7-12 larvae). At this stage, OPCs are migrating throughout the spinal cord and we previously observed OPCs extending membrane processes into the periphery and contacting MEP glia at this developmental stage (Kirby et al., 2006; Smith et al., 2014). We conclude from these experiments that adenosine signaling is necessary when OPCs begin migrating, but not during their specification, to prevent them from migrating into the PNS. In subsequent experiments, we began treatments at 36 hpf since earlier treatment did not significantly increase the number of ectopic OPCs in the periphery.

A2a AR antagonists do not disrupt spinal motor nerve development

Previously, we demonstrated that loss of MEP glia results in OPC migration into the periphery (Morris et al., 2017; Smith et al., 2014). We therefore sought to determine whether antagonizing the A2a AR lead to ectopic OPC migration simply by perturbing MEP glial development. MEP glia can be identified by the co-expression of *sox10:eos* and *olig2:dsred* as well as expression of *wnt inhibitory factor 1 (wif1)* (Smith et al., 2014). To determine if MEP glia were present in larvae treated with the A2a AR antagonist, we quantified the percentage of motor nerves with *sox10*$^{+}$*/olig2*$^{+}$ MEP glia at the MEP TZ and observed no differences among larvae treated from 36 hpf to 3 dpf with 1.25 μM CGS-15943 (n = 6 larvae), 10 μM SCH-58261 (n = 9 larvae) or DMSO (n = 5 larvae) (Figure 4-5A&B p = 0.14, 10 nerves analyzed per larvae). We also observed *wif1*$^{+}$ MEP glia in larvae treated with 1.25 μM CGS-15943 (Figure 4-6A). From these data, we conclude that A2a AR antagonism does not affect MEP glial development.

To determine whether glial migration in general was disrupted at the MEP TZ in larvae treated with the A2a AR antagonist, we assayed the migration of perineurial glia (PG). These cells originate in the ventral spinal cord, exit the CNS via the MEP TZ, and migrate along motor nerves to form the perineurium, a component of the blood-nerve-barrier (Kucenas et al., 2008). If the A2a AR antagonist nonselectively disrupted cell migration at the MEP TZ, we would expect to see altered migration of PGs. We measured extension of PG from the spinal cord along the motor nerve in 55 hpf *nkx2.2a:megfp;olig2:dsred* larvae treated from 36 to 55 hpf with 1.25 μm CGS-15943, where *nkx2.2a* regulatory sequences drive membrane-tethered GFP in PG. In these

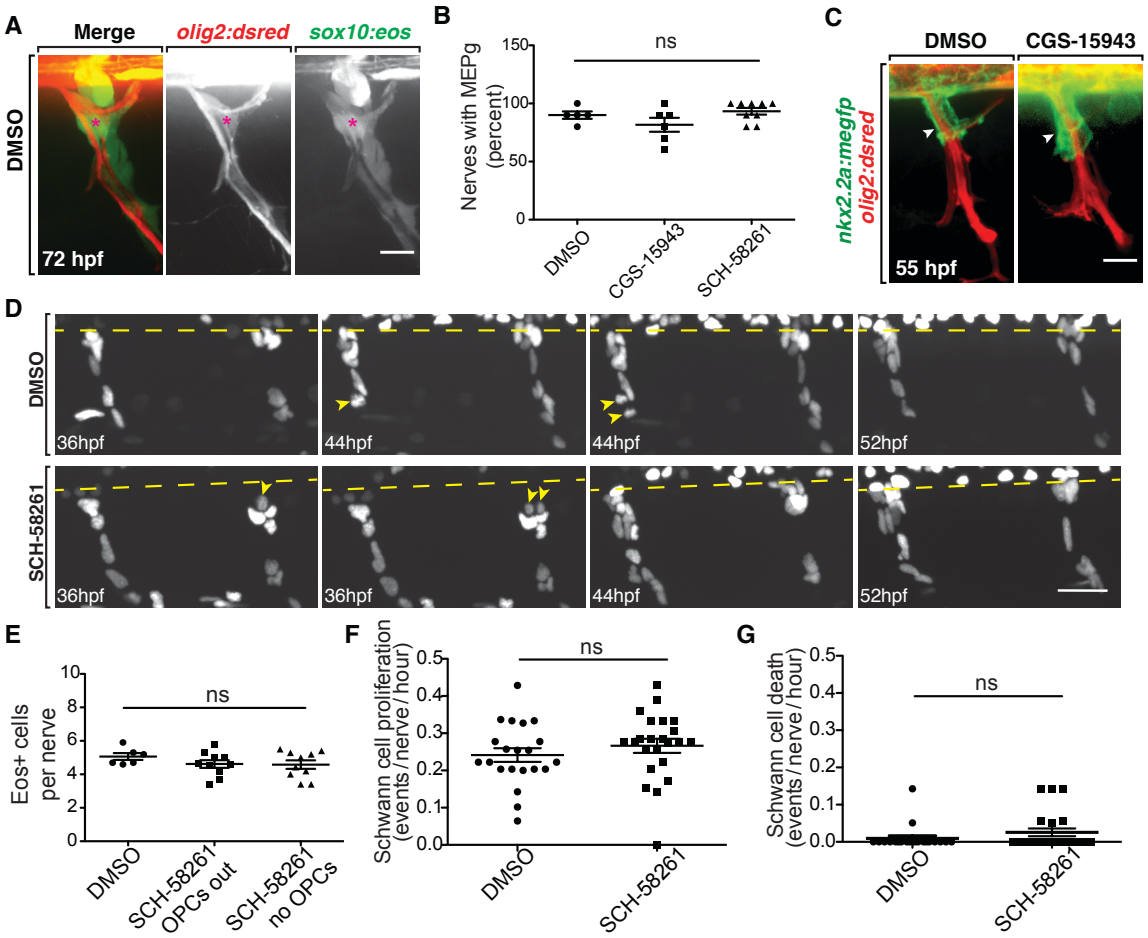

Figure 4-5 A2a AR antagonism does not affect spinal motor nerve development. (A) Motor nerve in a 3 dpf *olig2:dsred;sox10:eos* larvae treated with SCH-58261 from 36 hpf to 3 dpf. Magenta asterisks mark *sox10*$^{+}$*/olig2*$^{+}$ MEP glia with normal morphology at the MEP. (B) Mean ± SEM of the percent of nerves per larva at 3 dpf with *sox10*$^{+}$*/olig2*$^{+}$ MEP glia after treatment from 36 hpf to 3 dpf with DMSO (n = 5), CGS-15943 (n = 6), or SCH-58261 (n = 9). 10 nerves were quantified per larva. p = 0.14 (C) 55 hpf *nkx2.2a:megfp;olig2:dsred* larvae treated with DMSO or CGS-15943 from 36 to 55 hpf showing PG extension on the nerve. (D)Frames captured from a 20 hour time-lapse video starting at 36 hpf using *sox10:nls-eos* embryos treated with DMSO or SCH-58261. Transgene labels Schwann cell nuclei along the nerves and OPC nuclei within the spinal cord (dashed line). Schwann cells can be seen dividing (arrowheads) along the nerves of both treatments. (E) Quantification of Eos^{+} cells per nerve at 3 dpf in DMSO and SCH-58261-treated larvae. Mean ± SEM for n = 6 fish (DMSO) n = 10 fish (SCH-58261). 10 nerves per fish. p = 0.39. (F) Quantification of Schwann cell proliferation during these time-lapses. Mean ± SEM for n = 6 fish, 21 nerves (DMSO); 6 fish, 23 nerves (SCH-58261). p = 0.35. (G) Quantification of Schwann cell death during these time-lapses cell death Mean ± SEM for n = 6 fish, 21 nerves (DMSO); 6 fish, 23 nerves (SCH-58261). p = 0.20 Scale bars, 20 μM.

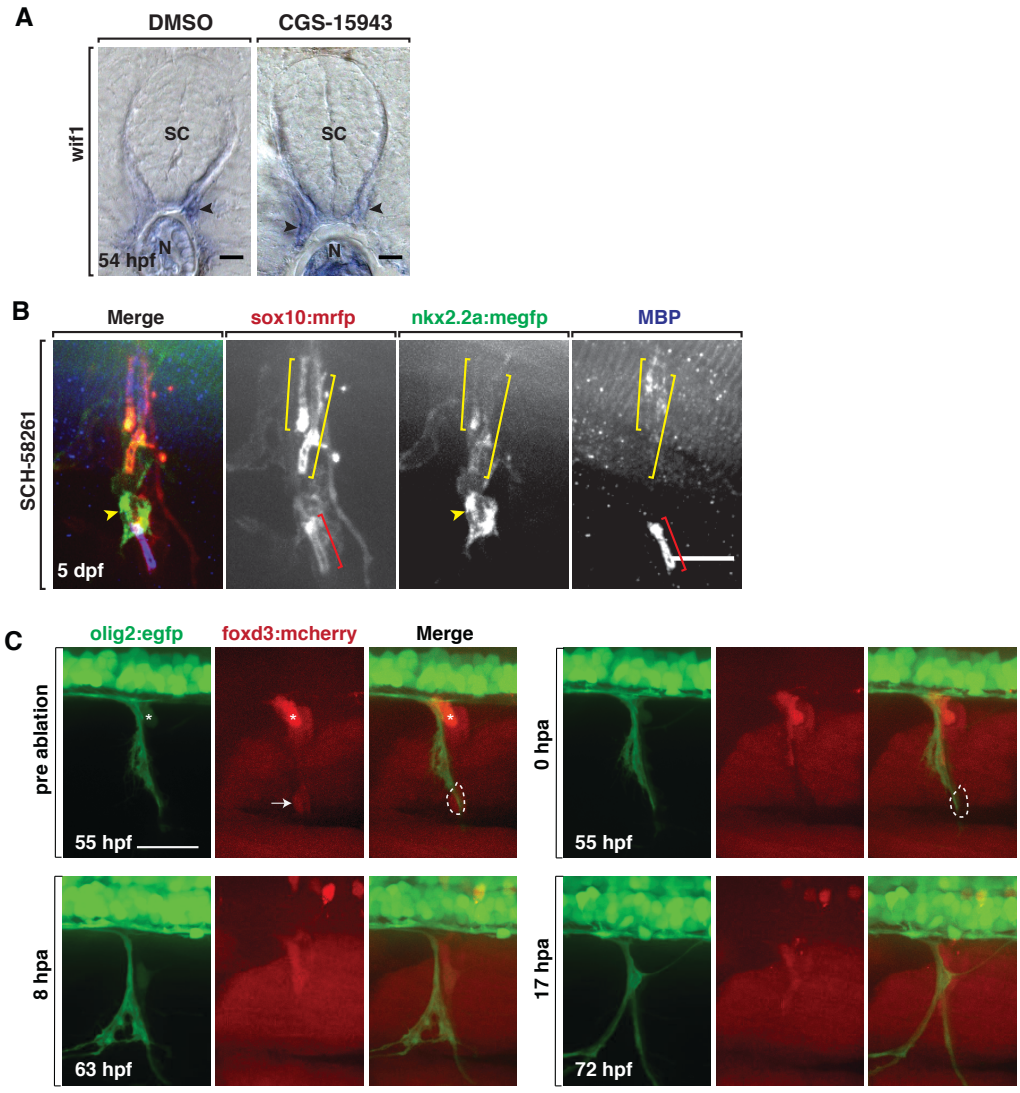

Figure 4-6 Drug treated larvae have *wif1*$^{+}$ MEP glia and healthy Schwann cells. (A) *In situ* hybridization for *wif1* in 54 hpf larvae treated 36 to 54 hpf with DMSO or 1.25 µM CGS-15943. Arrowheads mark MEP glia. SC, spinal cord; N, notochord. (B) Image of a 5 dpf larva treated from 30 hpf to 3 dpf with SCH-58261. Arrowhead marks a *nkx*$^{+}$*/sox10*$^{+}$ oligodendrocyte on the nerve, which is myelinating proximal segments of the nerve with *nkx*$^{+}$*/sox10*$^{+}$*/MBP*$^{+}$ myelin (yellow brackets). A differentiated Schwann cell also myelinates a nerve segment with a *nkx*$^{-}$*/sox10*$^{+}$*/MBP*$^{+}$ myelin sheath (red bracket). (C) Frames captured from a 17 hour time-lapse video starting at 55 hpf using a *olig2:egfp;foxd3:mcherry* embryo. Motor nerve *foxd3*$^{+}$*/olig2*$^{-}$ Schwann cells (arrow and dashed line), but not *foxd3*$^{+}$*/olig2*$^{+}$ MEP glia (asterisk), were ablated at 55 hpf. At 0 hour post ablation (hpa), MEP glia (asterisk), but not SCs, can be seen. At 8 and 17 hpa (63hpf and 72hpf respectively), MEP glial cells have divided and can be seen along the motor nerve root. No *olig2*$^{+}$*/foxd3*$^{-}$ oligodendrocyte lineage cells can be seen in the periphery at any time point. (n = 10 nerves in 10 fish.) Scale bar, (A) 20 µm, (B&C) 50 µm.

studies, we found no difference in PG extension between DMSO-treated and CGS-15943-treated larvae, indicating that A2a AR signaling is specifically required to regulate OPC migration and does not generally affect glial migration at the MEP TZ (Figure 4-5C, $p = 0.28$; DMSO 22.27 ± 0.88 μm (mean ± SEM) n = 6 larvae, 10 nerves analyzed per larva; CGS-15943 24.94 ± 1.75 μm (mean ± SEM) n = 10 larvae, 10 nerves analyzed per larva). Finally, we assessed Schwann cell (SC) development and health along motor nerve roots. Using 3 dpf *sox10:eos* larvae, where *sox10* drives expression of Eos in SCs and MEP glia in the PNS, we quantified the number of Eos^+ cells between the MEP TZ and horizontal myoseptum on 10 nerves per larva, for n=6 larvae per treatment. In this experiment, we observed that the number of Eos^+ cells per nerve was not significantly different between animals treated from 36 hpf to 3 dpf with DMSO or SCH-58261 ($p = 0.08$), and saw no difference in the number of Eos^+ glia along the nerve root when we compared counts between nerves populated with ectopic OPCs and those without (Figure 4-5E). We also performed time-lapse imaging to observe SC precursor migration and proliferation during A2a AR antagonism. Precursor migration was normal in these movies, and we did not observe any differences in proliferation rates between SCH-58261 treated and DMSO treated animals (Figure 4-5D&F). We also did not observe a difference in apoptosis between SCH-58261 treated animals and controls, and we observed differentiated Schwann cells myelinating spinal motor nerve axons with MBP^+ myelin membrane at 5 dpf (Figure 4-5G and Figure 4-6B). From these experiments, we conclude that the A2a AR antagonist, SCH-58261, does not cause peripheral OPC migration by nonselectively stimulating glial migration or by perturbing

peripheral glial development. Furthermore, Schwann cells do not appear to have any role in affecting OPC migration. Using *olig2:egfp;foxd3* larvae, where *foxd3* regulatory sequences drive expression of GFP in all peripheral glia, we were able to selectively label MEP glia *foxd3*$^{+}$*/olig2*$^{+}$ and Schwann cells *foxd3*$^{+}$*/olig2*$^{-}$*.* Then, using a pulsed nitrogen dye laser, we specifically ablated Schwann cells (*foxd3*$^{+}$*/olig2*$^{-}$ cells) along spinal motor nerves but not MEP glia (*foxd3*$^{+}$*/olig2*$^{+}$ cells) at 55 hpf. We then performed *in vivo,* time-lapse imaging through 3 dpf to determine if any *foxd3*$^{-}$*/olig*$^{+}$ OPCs migrated into the periphery in these experiments. In these studies, we never observed any OPCs migrate into the PNS (n = 10 nerves, 10 fish) (Figure 4-6C). Because we observed no effect of SCH-58261 treatment on spinal motor nerve development, and because direct Schwann cell ablation did not result in any ectopic OPC migration, we conclude that antagonizing A2a ARs specifically affects OPC migration.

The A2ab AR regulates OPC migration at MEP TZs

Zebrafish have two orthologous A2a ARs, A2aa and A2ab, which are encoded by *adora2aa* and *adora2ab*, respectively (Boehmler et al., 2009). We used Clustal Omega to compare the zebrafish A2aa, A2ab, and human A2A AR protein sequences (Goujon et al., 2010; Sievers et al., 2011). Zebrafish A2aa and A2ab ARs have 55% and 52% identical amino acids to human A2A AR (Figure 4-7). However, most of this variability is in the C-terminal cytoplasmic tail, which mediates interactions with other proteins and not ligand binding (Keuerleber et al., 2010). The ligand binding domains of zebrafish A2aa and A2ab ARs are 72% (21/29) conserved with human A2A AR, and A2aa and

Figure 4-7 A2a AR protein sequence homology. Clustal Omega sequence alignment for human A2a (top), zebrafish A2ab (middle), and zebrafish A2aa (bottom).

A2ab ARs have 76% (22/29) conserved amino acids with each other in this domain, so they likely have similar ligand affinities (Figure 4-7). However, *adora2aa* and *adora2ab* have distinct expression patterns, so we hypothesized that they may have unique functions in nervous system development (Boehmler et al., 2009).

To determine if A2aa and/or A2ab ARs were required to prevent peripheral OPC migration, we used a combination of genetic mutants and knock-down strategies. We created germline mutations in *adora2aa* using transcription activator-like effector nuclease (TALEN) targeted mutagenesis (Boch et al., 2009; Moscou and Bogdanove, 2009). *adora2aa*^{ct845} is a 7 base pair (bp) deletion within exon 3, causing a frameshift and an early stop codon, and this results in a severely truncated protein sequence (Figure 4-8A). The mutated A2aa AR protein lacks transmembrane domains 6 and 7, which contain conserved ligand binding residues (de Lera Ruiz et al., 2014). It also lacks the entire C-terminal cytoplasmic tail, which mediates interaction with G proteins and protects the receptor from ubiquitination and degradation (Keuerleber et al., 2010). For these reasons, we hypothesize that *adora2aa*^{ct845} is a presumptive null. Similar to *A2a*$^{-/-}$ mice, *adora2aa*$^{-/-}$ zebrafish mutants are homozygous viable, produce viable offspring and do not show any morphological defects compared to WT siblings at all stages investigated (Figure 4-8B-F; survival and hatching n = 50; heart rate n = 20; startle mutants n = 25, WT n = 34) (Chen et al., 1999).

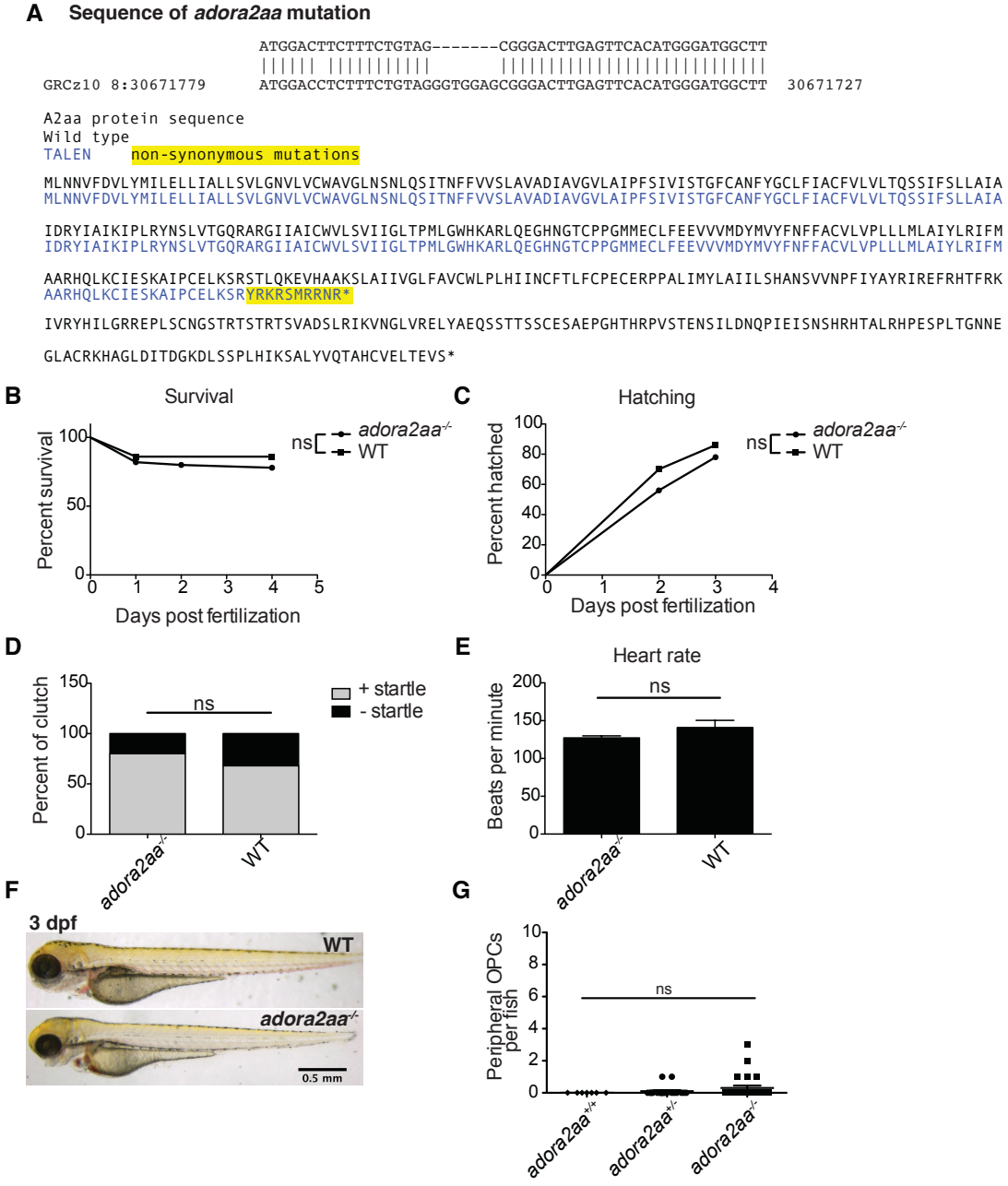

Figure 4-8 Characterization of *adora2aa* mutant larvae. (A) DNA sequence (top) and predicted protein sequence of *adora2aa*^{ct845} compared to WT. (B) Survival of *adora2aa*$^{-/-}$ larvae compared to WT. Data presented as percent of total fertilized eggs and analyzed by survival analysis; p = 0.30, n = 50 fish. (C) Percent of fish successfully hatched out of the chorion by 2 and 3 dpf. Analyzed by survival analysis, p = 0.18, n = 50 fish. (D) Percentage of larvae with positive (+) and negative (-) startle responses at 3 dpf. Analyzed by Chi-squared test, p = 0.38, n = 25 (*adora2aa*$^{-/-}$) n = 34 (WT). (E) Heart rate in WT and *adora2aa* mutant larvae at 50 hpf. Analyzed by unpaired t-test, p = 0.18, n = 20 (*adora2aa*$^{-/-}$) n = 21 (WT). (F) Brightfield images of 3 dpf WT and (D) Brightfield images of 3 dpf WT and *adora2aa*$^{-/-}$ larvae. (G) Mean ± SEM of peripheral OPCs per larvae for heterozygous *adora2aa*$^{+/-}$ and homozygous *adora2aa*$^{-/-}$ larvae at 3 dpf. p = 0.24, n = 20 (*adora2aa*$^{+/-}$) n = 26 (*adora2aa*$^{-/-}$). Scale bar, 0.5 mm.

To determine if *adora2aa* mediated OPC restriction from the PNS, we quantified the number of peripheral OPCs at 3 dpf in *olig2:dsred* larvae with *adora2aa* mutations (Figure 4-8G). At this stage (n = 7 *adora2aa*$^{+/+}$, n = 20 *adora2aa*$^{+/-}$, n = 26 *adora2aa*$^{-/-}$), we did not observe significant numbers of peripheral OPCs in *adora2aa*$^{-/-}$ mutants ($p = 0.69$). Based on this result, we concluded that A2aa ARs were likely not involved in regulating OPC migration and that the effect of the A2a AR antagonist on ectopic OPC migration may be working through A2ab ARs.

We tested this hypothesis by treating *olig2:dsred*;*adora2aa*$^{-/-}$ mutants, which still have functional A2ab ARs, with the A2a AR antagonist, SCH-58261, at 36 hpf. At 72 hpf, we did not observe peripherally-migrated OPCs in WT or *adora2aa*$^{-/-}$ mutants treated with DMSO (Figure 4-9A, n = 12). However, when WT or *adora2aa* mutants were treated with SCH-58261 from 36 to 72 hpf, we observed peripheral OPCs in both genotypes (Figure 4-9A, n = 12). Two-way ANOVA analysis showed a significant effect of drug treatment ($p < 0.0001$), but not for genotype ($p = 0.53$) or the interaction between treatment and genotype ($p = 0.93$). In other words, both WT and *adora2aa* mutant larvae have the same number of peripherally-migrated OPCs when treated with the A2a AR antagonist. These results are consistent with the hypothesis that A2ab, and not A2aa, is primarily responsible for affecting OPC migration.

To further confirm the roles of the two orthologous receptors, we used morpholino oligonucleotides (MO) to selectively knock down expression of *adora2aa* and *adora2ab*.

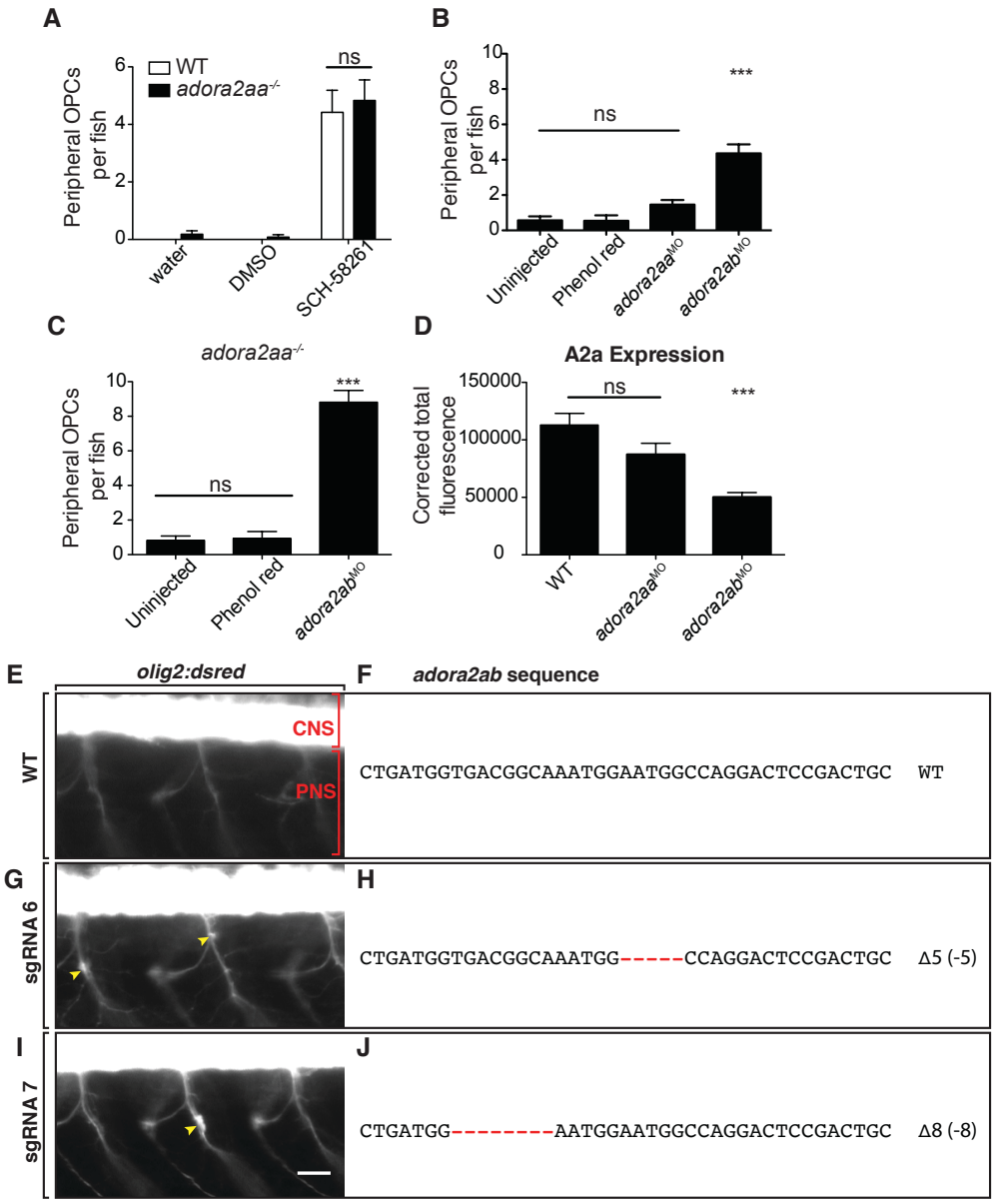

Figure 4-9 A2ab ARs mediate OPC migration at the MEP TZ. (A) Mean ± SEM of peripheral OPCs per fish for *olig2:dsred;adora2aa*$^{-/-}$ and WT larvae treated with water, DMSO or 10 µM SCH-58261 from 36 to 72 hpf. n = 12 fish, $p < 0.0001$ for Treatment, $p = 0.53$ for Genotype, $p = 0.93$ for Interaction of Treatment and Genotype. (B) Mean ± SEM of peripheral OPCs at 3 dpf in WT *olig2:dsred* embryos injected with vehicle, 1ng/nl *adora2aa*^{MO} or 1ng/nl *adora2ab*^{MO}. n = 42 (WT), 11 (phenol red), 65 (*adora2aa*^{MO}), 42 (*adora2ab*^{MO}), *** $p < 0.0001$ *adora2ab*^{MO} compared to WT. (C) Mean ± SEM of peripheral OPCs at 3 dpf in *olig2:dsred;adora2aa*$^{-/-}$ larvae injected with *adora2ab*^{MO}. n = 44 (uninjected), n = 30 (phenol red), n = 84 (*adora2ab*^{MO}), *** $p < 0.0001$ compared to uninjected. (D) Quantification of A2a antibody at the nerve root of WT, *adora2aa*^{MO}, or *adora2ab*^{MO} injected larvae. Mean ± SEM *** $p < 0.0001$ compared to WT, n = 20 nerves (WT), 59 nerves (*adora2aa*^{MO}), 80 nerves (*adora2ab*^{MO}). (E,G,I) Lateral views of 3 dpf *olig2:dsred* WT or CRISPR F0 injected larvae. Arrowheads mark peripheral OPCs in F0 larvae. (F,H,J) *adora2ab* sequences from individual WT or F0 larvae. Red dashes indicate deletions compared to WT sequence. Frameshift mutations shown in H and J were identified in the F0 larvae shown in G and I, respectively. Scale bar, 25 µm.

A translation blocking *adora2aa*^{MO} has been previously described (Haas et al., 2013). To create the translation blocking *adora2ab*^{MO}, we used the Oligo Design service at Gene Tools (https://oligodesign.gene-tools.com/request/). In preliminary experiments, we injected *olig2:dsred* embryos at the 1 to 2 cell stage with 2 to 3 nl of *adora2ab*^{MO} solution at various concentrations and observed that 1 ng/nl *adora2ab*^{MO} (n = 19) resulted in peripherally-migrated OPCs compared to control (n = 5) at 72 hpf (Figure 4-10A, $p < 0.01$). Larvae injected with 1 ng/nl *adora2aaMO* or *adora2ab MO* had normal gross morphology compared to WT (Figure 4-10C), so we used 1 ng/nl of *adora2ab*^{MO} for future experiments. We then performed experiments to test whether *adora2ab* is required to prevent peripheral OPC migration. When we quantified peripherally-migrated OPCs in MO-injected animals, *adora2ab*^{MO} morphants (n=42), but not *adora2aa*^{MO} morphants (n=65), had significantly more peripheral OPCs at 3 dpf compared to uninjected (n=42) or phenol red-injected (n=11) embryos ($p < 0.0001$) (Figure 4-9B). This result is consistent with our finding that *adora2aa*$^{-/-}$ mutants do not have peripherally-migrated OPCs (Figure 4-9A). We next injected *adora2ab*^{MO} into *adora2aa*$^{-/-}$ mutants expressing *olig2:dsred* and quantified the number of peripheral *olig2*$^{+}$ OPCs at 3 dpf. We observed peripheral OPCs only in mutants injected with *adora2ab*^{MO} (n = 84) and not in uninjected (n = 44) or phenol red-injected (n = 30) mutants (Figure 4-9C, $p < 0.0001$). We conclude from these experiments that A2ab ARs are required to regulate OPC migration at the MEP TZ.

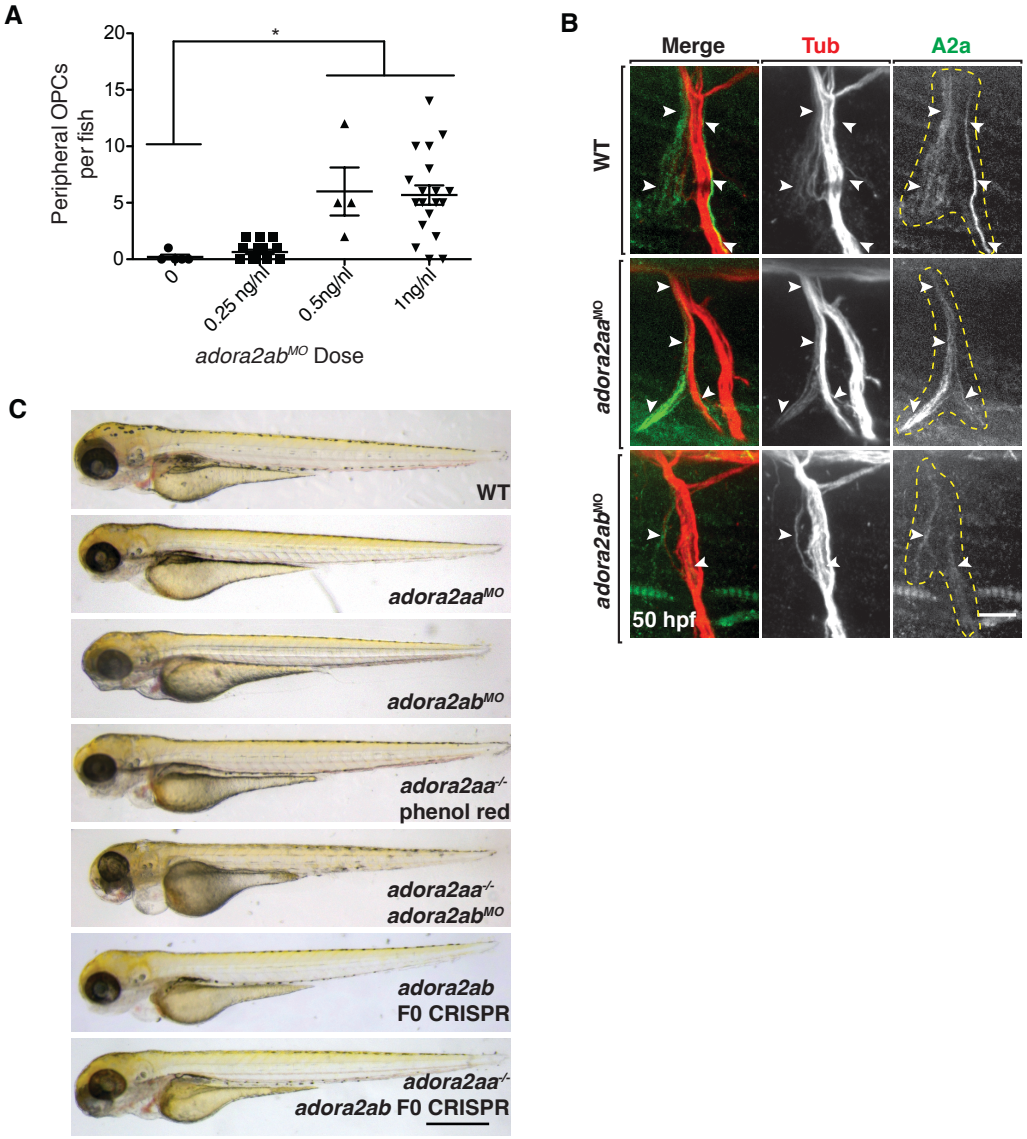

Figure 4-10 Validation of *adora2ab^{MO}*. (A) Dose response for *adora2ab^{MO}*. Data are mean ± SEM peripheral OPCs per larva at 3 dpf. n = 4 to 19 larvae per dose, * $p < 0.01$. (B) Images of peripheral nerves in WT larvae or larvae injected with *adora2aa^{MO}* or *adora2ab^{MO}* labeled with A2a antibody. Arrowheads mark motor and sensory axons. Yellow outlines show example ROIs used for quantification. (C) Brightfield images of 3 dpf WT or *adora2aa$^{-/-}$* injected with MO or sgRNA. Scale bars, (B) 20 µM, (C) 0.5 mm.

We validated that *adora2ab*^{MO} effectively knocked down A2ab AR protein expression, by injecting *olig2:dsred* embryos with 1 ng/nl *adora2aa*^{MO} or *adora2ab*^{MO} and performed antibody labeling with an A2a antibody that has previously been used to detect expression in the zebrafish pancreas (Andersson et al., 2012). We observed A2a antibody labeling in the spinal cord and along peripheral nerves at 50 hpf (Figure 4-10B), which is consistent with previously described expression of *adora2ab* mRNA in the spinal cord (Boehmler et al., 2009). Embryos injected with 1 ng/nl *adora2ab*^{MO} (n = 80) had significantly reduced A2ab AR expression along motor nerve roots at 50 hpf compared to WT (n = 20 nerves) and *adora2aa*^{MO} injected embryos (n = 59 nerves) ($p < 0.0001$) (Figure 4-9D and Figure 4-10B).

To provide further support for the specific requirement of *adora2ab* to restrict OPC migration, we generated mutations in the *adora2ab* gene using CRISPR/Cas9. We designed 2 sgRNAs targeting *adora2ab* exon 2, just downstream of the translation start site, and injected the sgRNA along with Cas9 protein into *olig2:egfp* or *olig2:dsred* embryos at the 1 cell stage (Figure 4-11A). We confirmed that each sgRNA produced frameshift mutations in *adora2ab* by TOPO cloning and sequencing individual DNA clones from F0 injected embryos (Figure 4-11B). Embryos injected with Cas9 and a previously published sgRNA targeting *tyr* or *slc45a2*, which both affect pigment formation and are not expected to affect OPC migration, were used as controls (Irion et al., 2014; Jao et al., 2013). We then quantified the number of larvae with peripherally-migrated *olig2*$^{+}$ OPCs at 3 dpf (Table 4-2). After analysis, DNA from individual embryos

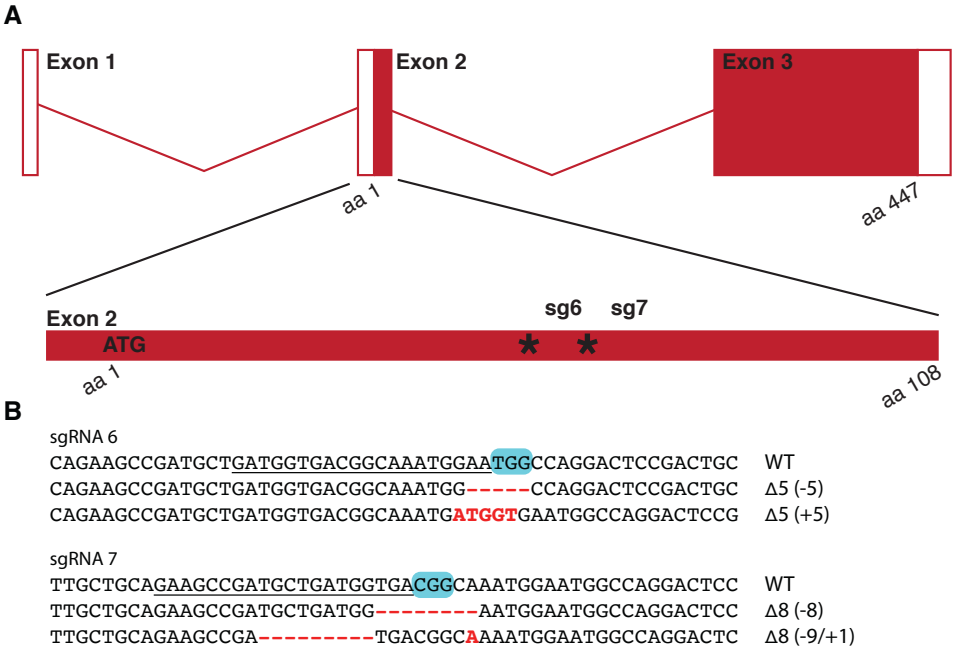

Figure 4-11 *Adora2ab* CRISPR-induced indels. (A) Schematic of *adora2ab* gene and regions targeted by sgRNA 6 and sgRNA 7. (B) WT sequences and example frameshift mutations caused by sgRNA + Cas9 injections. Underlined sequence is the sgRNA target, and blue highlighted region is the protospacer adjacent motif (PAM). Red letters or dashes indicate insertions or deletions, respectively.

Table 4-2. F0 CRISPR injection data. For number of larvae with peripheral OPCs, percent of total injected larvae is given. Each larvae with peripheral OPCs was sequenced to detect mutations in *adora2ab*, and the percentage of the number with peripheral OPC phenotype is given. For *slc45a2* and *tyr* sgRNA, 12 larvae were randomly selected for *adora2ab* sequencing, and the percentage of these samples with mutations in *adora2ab* is given.

	Total number injected	**Number with ectopic OPCs (%)**	**Number with ectopic OPCs and mutation (%)**	**Number with ectopic OPCs but no mutation (%)**
adora2ab sgRNA 6	73	18 (24.7%)	18 (100%)	0 (0%)
adora2ab sgRNA 7	82	23 (28.0%)	22 (95.7%)	1 (4.3%)
adora2aa$^{-/-}$ *adora2ab* sgRNA	14	5 (35.7%)	5 (100%)	0 (0%)
control sgRNA	28	1 (3.6%)	**Number with *adora2ab* mutation**	
			0 (0%)	

was sequenced to identify CRISPR-induced indels in *adora2ab*. Figures 4-9E, 4-9G, and 4-9I show representative WT and F0 larvae injected with sgRNA6 or sgRNA7. *Olig2*$^{+}$ OPCs can be seen in the periphery of F0 larvae, and the *adora2ab* sequences shown in 4-9F, 4-9H, and 4-9J correspond to the individual larvae in 4-9E, G and I. For gRNA 6, 24.7% (18/73) of injected larvae had peripheral *olig2*$^{+}$ OPCs. Of the larvae with peripheral OPCs, 100% (18/18) had frameshift mutations in *adora2ab*. For gRNA 7, 28% (23/82) of injected larvae had peripheral OPCs, and of the larvae with this phenotype, 95.7% (22/23) had frameshift mutations in *adora2ab* (Table 4-2).

We used previously published sgRNAs targeting *tyr or slc45a2* as a separate control to test the possibility that CRISPR injections non-selectively result in peripheral OPC migration. Out of 28 *olig2:dsred* larvae injected with either *tyr* or *slc45a2* sgRNA, 26 (96.3%) had the expected pigmentation phenotype, whereas only 1 (3.6%), had peripheral *olig2*$^{+}$ OPCs. Additionally, injections of *tyr* or *slc45a2* sgRNa did not result in any mutations in *adora2ab*. This suggests that the effect of *adora2ab* CRISPR injections on peripheral OPC migration is the result of selective targeting of *adora2ab*.

Finally, we injected *adora2ab* sgRNA into *adora2aa*$^{-/-}$ embryos to determine if perturbation of *adora2ab* resulted in peripheral OPC migration. At 72 hpf, we observed peripheral OPCs in 5/14 (35.7%) *adora2aa* mutants. Of the larvae with peripheral OPCs, 100% (5/5) had mutations in *adora2ab* (Table 4-2). These results support our

previous MO data and confirm that A2ab ARs are specifically required to prevent peripheral OPC migration.

Neuronal activity influences peripheral OPC migration

Adenosine signaling through A2a ARs is a well known neuromodulatory pathway that generally acts to increase neurotransmitter release (Ciruela et al., 2006; Golder et al., 2008; Rebola et al., 2008). To determine whether adenosine signaling through A2a ARs regulates peripheral OPC migration directly as a repulsive cue to OPCs, or indirectly by modifying neuronal activity, we assessed the expression of the A2a AR during developmental stages when we observed ectopic OPC migration across the MEP TZ

In these studies, we observed A2a antibody expression at 60 and 72 hpf on peripheral motor and sensory axons, as well as on some neuronal cell bodies and axons in the spinal cord, including *olig2*$^{+}$ motor neurons (Figure 4-12A and Figure 4-13A). As another method to detect expression, we used *in situ* hybridization to observe *adora2ab* mRNA expression. Consistent with our results using the A2a antibody, we observed *adora2ab* expression in spinal cord neurons, some of which were located in the ventral spinal cord where motor neurons reside (Figure 4-12B). We did not detect any A2a AR or *adora2ab* expression on OPCs or any other glial cells at these stages, which is consistent with published RNAseq data sets that do not show *adora2a* expression in mouse OPCs (data not shown) (Zhang et al., 2014). When we used fluorescently-tagged SCH-58261 (SCH-red), we observed SCH-red binding to *olig2*$^{+}$ spinal cord motor neurons at 25 hpf

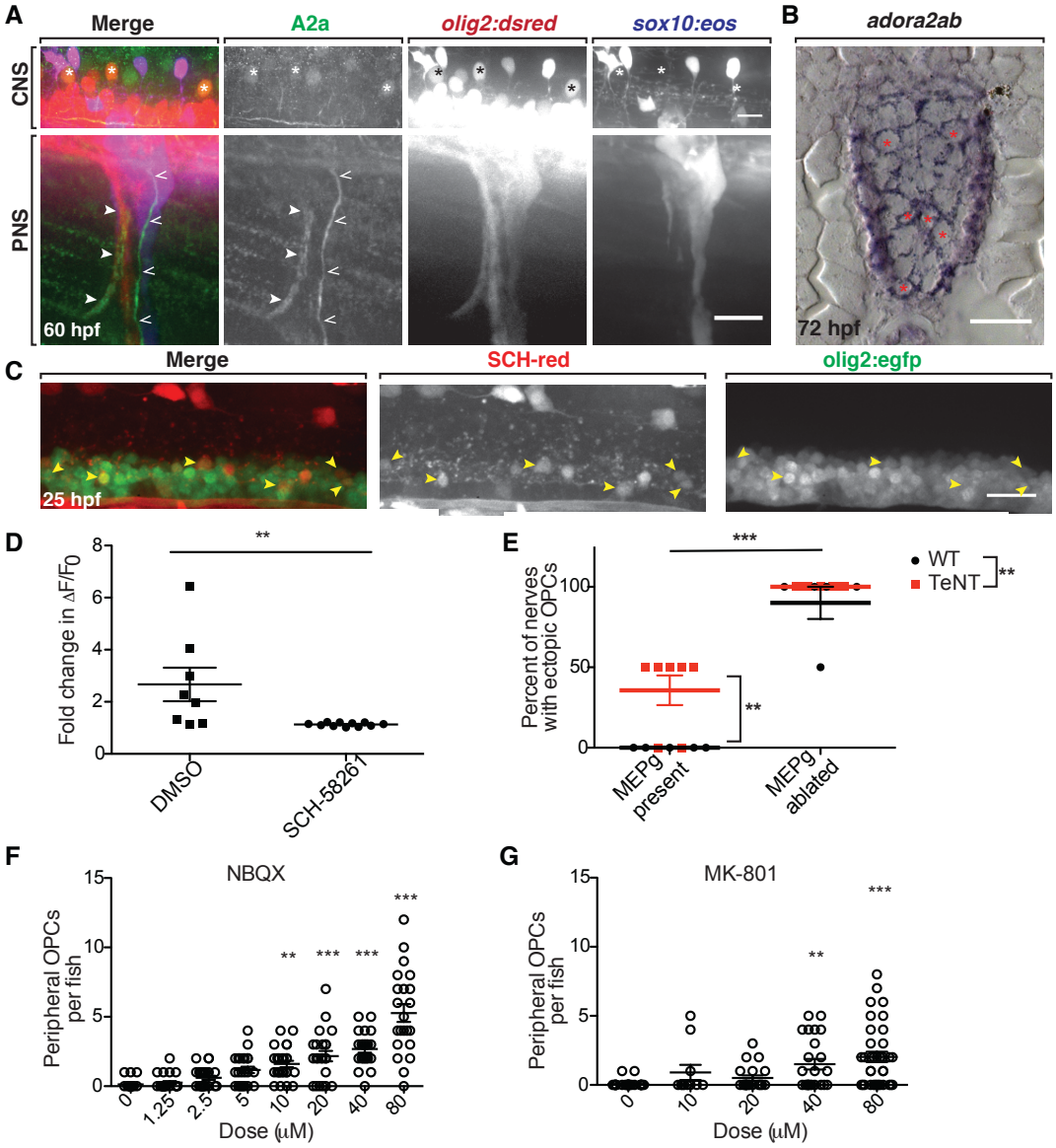

Figure 4-12 Modulation of neuronal activity affects OPC migration. (A) Lateral views of 60 hpf WT *olig2:dsred;sox10:eos* larvae stained with A2a AR antibody. Upper panels show spinal cord (CNS) with A2a expression in a subset of *olig2*$^{+}$ motor neurons (asterisks) and axons. Lower panels (PNS) show peripheral spinal nerves with A2a expression in motor (closed arrowheads) and sensory (open arrowheads) axons. (B) *adora2ab* mRNA expression at 72 hpf in the spinal cord of a WT larva. (C) 25 hpf *olig2:egfp* embryo labeled with SCH-red fluorescent antagonist. Arrowheads mark spinal cord *olig2*$^{+}$ motor neurons. (D) Mean ± SEM of the fold change in $\Delta F/F_0$ over time per individual firing events for larvae treated with DMSO (n = 8 neurons from 8 larvae) and larvae treated with SCH-58261 (n = 11 neurons from 10 larvae. p = 0.01. (E) Mean ± SEM of the percent of nerves with peripheral OPC cell bodies and/or processes at 3 dpf following TeNT mRNA injections and/or MEP glial ablation. n = 5 larvae (uninjected), n = 7 larvae (TeNT). ** p = 0.004 for TeNT vs WT, p < 0.0001 for MEPg ablated vs MEPg present. (F) Mean ± SEM peripheral OPCs per larvae at 3 dpf after treatment with NBQX from 36 hpf to 3 dpf. n = 22-25 larvae per dose. * p < 0.05 ** p < 0.001 compared to DMSO. (G) Mean ± SEM peripheral OPCs per larvae at 3 dpf after treatment with MK-801 from 36 hpf to 3 dpf. n = 11-36 larvae per dose. * p < 0.05, ** p < 0.001 compared to 0 μM. Scale bars, 20 μM.

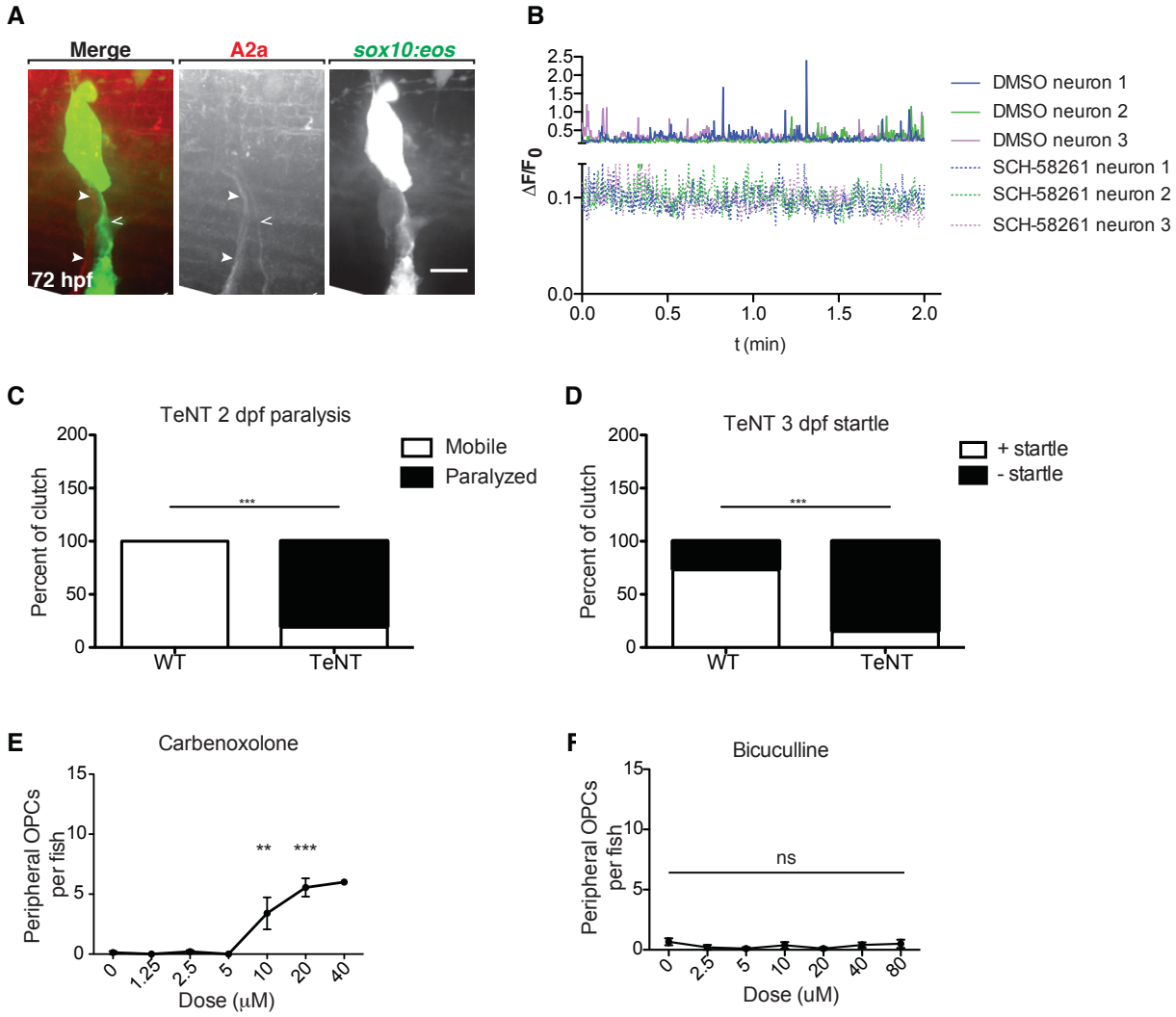

Figure 4-13 Modulation of neuronal activity affects OPC migration. (A) A2a antibody expression in motor axons (solid arrowheads) and sensory axons (open arrowheads) in a 72 hpf *sox10:eos* larva. (B) Example traces for calcium responses in individual GcAMP-expressing neurons in larvae treated with DMSO or SCH-58261. (C) Percentage of embryos that were mobile or paralyzed during dechorionation with forceps at 2 dpf. Analyzed by Chi-squared test; $p < 0.0001$, n = 54 (WT), n = 57 (TeNT). (D) Percentage of fish with positive and negative startle responses at 3 dpf. Analyzed by Fisher's exact test; $p < 0.0001$, n = 52 (WT), n = 53 (TeNT). (E) Mean ± SEM peripheral OPCs per larvae at 3 dpf after treatment with carbenoxolone from 36 hpf to 3 dpf. n = 8 (0 μM), n = 9 (1.25 μM), n = 10 (2.5 μM), n = 9 (5 μM), n = 5 (10 μM), n = 9 (20 μM) and n = 1 (40 μM. 40 μM dose was excluded from statistical analysis). * indicates $p < 0.05$ **, indicates $p < 0.001$ compared to 0 μM. (F) Mean ± SEM peripheral OPCs per larvae at 3 dpf after treatment with bicuculline from 36 hpf to 3 dpf. n = 8-12 larvae per dose. p = 0.58. Scale bar, 20 μM.

(Figure 4-12C). This expression pattern matches the previously published expression of *adora2ab* mRNA in spinal cord neurons, and further supports the selectivity of SCH-58261 for zebrafish A2a ARs on neurons (Boehmler et al., 2009). Our expression data is consistent with observations of A2a expression in the mammalian spinal cord dorsal and ventral horn (Patel et al., 2001; Witts et al., 2015). Because A2a ARs are expressed by neurons in the spinal cord and motor nerve root axons and not OPCs, we hypothesized that adenosine signaling must affect OPC migration by altering neuronal activity. Because adenosine is a well-known modulator of neuronal activity, we decided to test whether neuronal activity itself could regulate OPC migration during development.

Extracellular adenosine can increase or decrease activity in many kinds of neurons by binding to A1 or A2a receptors, respectively. Generally, adenosine binding to A2a ARs on neurons increases firing and in the spinal cord, A2a ARs increase motor neuron firing (Golder et al., 2008; Patel et al., 2001; Sebastiao and Ribeiro, 2015). Therefore, we hypothesized that inhibiting A2a ARs decreased neuronal activity, which resulted in peripheral OPC migration. To test this hypothesis, we first tested whether inhibiting A2ab decreased neuronal activity. Using the calcium indicator GCaMP5 to detect neuronal firing, we drove expression of *UAS:GCaMP* in spinal cord neurons using *neurod:gal4*. We then quantified calcium transients as a measure of neuronal activity in 48 hpf larvae treated with SCH-58261 or DMSO. We measured the change in fluorescence intensity over time, and quantified fluorescence spikes compared to

baseline. Treatment with the A2ab antagonist SCH-58261 significantly reduced neuronal firing compared to control, such that $\Delta F/F_0$ values rarely rose above baseline (Figure 4-12D and Figure 4-13B). We conclude from this experiment that, consistent with the effects of A2a antagonists in other species, antagonizing A2ab receptors with SCH-58261 decreases neuronal activity in zebrafish.

We next tested whether other methods of inhibiting neuronal activity would result in peripheral OPC migration. To do this, we inhibited all synaptic vesicle release using tetanus toxin light chain (TeNT) (Yu et al., 2004). Previous studies demonstrate that injections of TeNT mRNA effectively inhibits synaptic vesicle release and results in significant paralysis of zebrafish larvae at 3 and 4 dpf (Fontenas et al., 2016; Mensch et al., 2015). When we injected *olig2:dsred* embryos at the 1 to 2-cell stage with 1 to 2 nl of 175 ng/μl TeNT mRNA, we confirmed that neuronal activity was indeed inhibited as larvae were paralyzed at 2 (n = 54) and 3 dpf (n = 52) (Figure 4-13C&D; 2 dpf $p < 0.0001$; 3 dpf $p < 0.0001$). Consistent with our hypothesis, silencing neurons using TeNT resulted in significant numbers of OPC cell bodies and/or OPC processes in the periphery (Figure 4-12E n = 5 larvae (uninjected), n = 7 larvae (TeNT). ** p = 0.004 for TeNT vs WT).

Because zebrafish have a combination of electrically and chemically coupled neurons at the developmental stages we were assaying, we also tested the effect of inhibiting activity of electrically coupled neurons with carbenoxolone, a gap junction blocker. We

treated *olig2:dsred* embryos from 30 hpf to 3 dpf and quantified peripheral OPCs at 3 dpf. Consistent with our hypothesis, blocking gap junctions also resulted in significant numbers of peripherally-migrated OPCs (Figure 4-13E, $p < 0.001$ for 10 μM carbenoxolone and $p < 0.0001$ for 20 μM carbenoxolone n = 5 to 10 larvae per dose) (Saint-Amant and Drapeau, 2001). We conclude from these experiments adenosine signaling through A2a receptors regulates neuronal activity, and that decreased neuronal firing results in aberrant OPC migration through the spinal cord MEP TZ.

OPCs express many neurotransmitter receptors, and recent work demonstrates a role for neuronal activity in OL myelination (Bergles et al., 2000; Etxeberria et al., 2016; Gibson et al., 2014; Stevens et al., 2002). Specifically, activity-dependent vesicular release from neurons can influence OPC differentiation and/or myelination (Bergles et al., 2000; 2010; Hines et al., 2015; Koudelka et al., 2016; Mensch et al., 2015). Therefore, we hypothesized that neuronal activity might act to regulate OPC migration at the MEP by releasing neurotransmitters that influence OPCs. In support of this, studies demonstrate that OPCs express functional neurotransmitter receptors that become activated in response to neuronal firing (Bergles et al., 2000; Lin and Bergles, 2004b). Therefore, we sought to identify the neuronal signal that might regulate OPC migration at the MEP by inhibiting neurotransmitter receptors. To do this, we treated *olig2:dsred* larvae from 36 hpf to 3 dpf with neurotransmitter receptor antagonists and quantified the number of peripherally migrated OPCs at 3 dpf. The selective AMPAR antagonist, NBQX, resulted in significant numbers of peripherally-migrated OPCs

compared to control (Figure 4-12F). Similarly, treatment with the NMDAR antagonist, MK-801, also resulted in peripheral OPC migration (Figure 4-12G). We additionally tested the selective $GABA_A$ receptor antagonist, bicuculline, and did not observe any peripherally migrated OPCs (Figure 4-13F). These results support our hypothesis that neuronal activity regulates OPC migration at the MEP, and also suggest that the effect on OPCs may be selectively mediated by glutamate receptors. However, we cannot rule out the possibility that neuronal NMDA and/or AMPA receptors may also be involved.

Peripherally-migrated OPCs rescue myelin deficits in peripheral myelin mutants

Our data demonstrates that A2ab AR inhibition results in OPC migration onto peripheral spinal motor nerves without otherwise disturbing overall nerve development. This led us to hypothesize that OPCs could be pharmacologically recruited onto peripheral nerves in order to myelinate them. Previous studies from the lab demonstrate that peripheral OPCs are capable of initiating myelination of peripheral nerves (Kucenas et al., 2009; Morris et al., 2017; Smith et al., 2014). However, in these studies, OPCs populated the nerve in the context of genetic mutations resulting in the death or absence of both SCs and MEP glia. Therefore, we wanted to determine if it was possible to recruit OPCs to myelinate peripheral motor nerves in a model more closely resembling human peripheral neuropathies, in which SCs are present, but fail to myelinate. To do this, we used zebrafish harboring a mutation in *g protein coupled receptor 126 (gpr126)*, a model of peripheral neuropathy in which SCs ensheath, but fail to myelinate, peripheral nerves

(Monk et al., 2009). OLs are present in normal numbers in these mutants, and central myelination is completely normal (Monk et al., 2009).

We first tested whether untreated *gpr126* mutant larvae had functional MEP glia. As we previously described, MEP glia along the spinal motor root can be identified by expression of the specific marker *wif1* at 72 hpf, or by fate mapping with photoconversion of the *sox10:eos* transgenic line (Smith et al., 2014). The nascent Eos protein exists in a green fluorescent state, but when exposed to UV light, it permanently shifts to a red fluorescent state. When we exposed whole embryos to UV light at 48 hpf, all neural crest-derived cells were photoconverted to red fluorescence. MEP glia, which are not neural crest-derived and begin expressing *sox10:eos* after 48 hpf, are not photoconverted and can be identified as green fluorescent cells on the nerve root by 54 hpf (Smith et al., 2014). Using both *wif1* and photoconverted *sox10:eos* as tools to visualize MEP glia, we found that these cells were present on spinal motor roots in *gpr126* mutant larvae at 72 hpf (Figure 4-14A&B). When we quantified peripheral OPC migration in *olig2:dsred;gpr126* larvae at 3 dpf, we did not observe any peripheral OPCs in mutants treated with DMSO (Figure 4-14C, n = 8). These data demonstrate that MEP glia are present and functioning properly and that the absence of myelin on peripheral nerves is not sufficient to elicit peripheral OPC migration.

Therefore, we tested whether treatment with the A2a AR antagonist would result in peripherally-migrated OPCs ensheathing peripheral spinal motor nerves in these

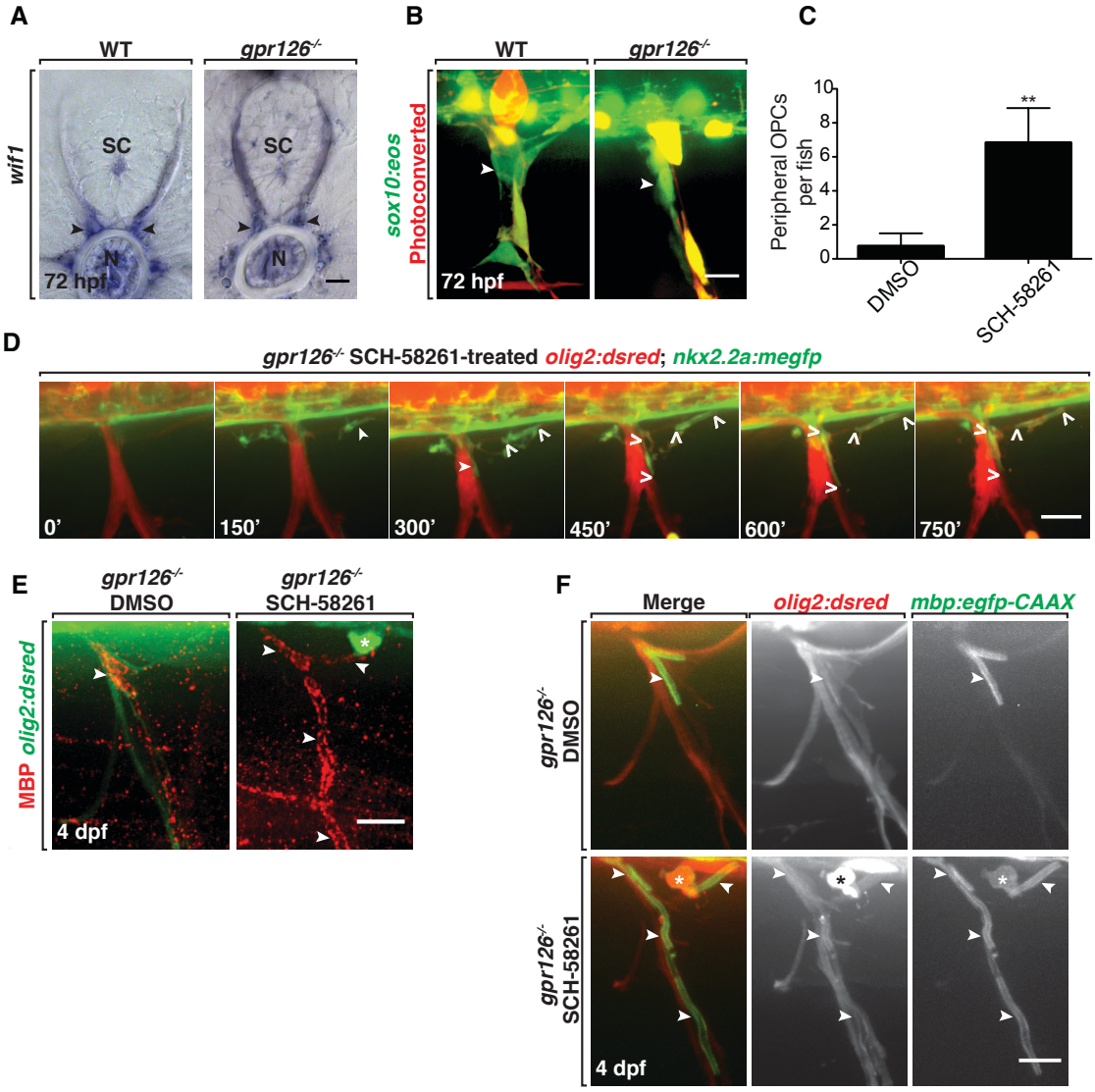

Figure 4-14 Peripheral OPCs myelinate spinal motor axons in *gpr126* mutant larvae. (A) *In situ* hybridization for *wif1* in WT and *gpr126*$^{-/-}$ larvae at 3 dpf shows MEP glia (arrowheads). SC, spinal cord; N, notochord. (B) Live images of photoconverted *sox10:eos* larvae at 3 dpf show unconverted (green) Eos^{+} MEP glia (arrowheads) in both WT and *gpr126*$^{-/-}$ larvae. (C) Mean ± SEM of peripheral OPCs in 3 dpf *gpr126*$^{-/-}$ larvae treated with DMSO or SCH-58261 from 36 hpf to 3 dpf. n = 8 (DMSO), n = 6 (SCH-58261). ** p = 0.009. (D) Frames from a 15 hour time-lapse movie of a *olig2:dsred;nkx2.2a:megfp;gpr126*$^{-/-}$ larva treated with SCH-58261 from 36 hpf to 3 dpf. 0' is 57 hpf. Arrowheads mark a *nkx2.2a*$^{+}$*/olig2*$^{+}$ OPC ensheathing motor axons. (E) Images of MBP antibody (arrowheads) on peripheral nerves of 4 dpf *olig2:dsred;gpr126*$^{-/-}$ larvae treated with DMSO or SCH-58261 from 36 hpf to 3 dpf. Asterisk marks peripheral OPC. (F) Live images of WT and *gpr126*$^{-/-}$ *olig2:dsred;mbp:egfp-CAAX* larvae treated with DMSO or SCH-58261 from 36 hpf to 3 dpf. Asterisk marks *olig2*$^{+}$ peripheral OPC with *mbp*$^{+}$ membrane sheaths (arrowheads) around peripheral motor axons. Scale bars, 20 μm.

mutants. When we treated *gpr126* mutant larvae with 10 μM of the A2a AR antagonist SCH-58261 from 36 hpf to 3 dpf, we observed a significant number of *olig2*$^{+}$ OPCs in the periphery compared to DMSO-treated controls (Figure 4-14C, $p = 0.009$, $n = 6$). We then performed *in vivo,* time-lapse imaging on *nkx2.2a:megfp;olig2:dsred;gpr126*$^{-/-}$ larvae in order to visualize whether these peripheral OPCs initiated myelination of peripheral nerves. The transgene *nkx2.2a:megfp* is expressed by pre-myelinating OPCs and enables clear visualization of membrane structures (Kucenas et al., 2008a). No other cells in the spinal cord or at the MEP TZ express both *nkx2.2a* and *olig2*, so use of these transgenes allowed us to unambiguously identify membrane sheaths coming from OPCs. We performed *in vivo,* time-lapse imaging on larvae treated with SCH-58261 from 36 hpf to 3 dpf and observed *nkx2.2a*$^{+}$*/olig2*$^{+}$ OPCs initiate ensheathment of peripheral spinal motor axons. Thin OPC membrane processes extended toward peripheral motor axons and formed membrane sheaths around them (Figure 4-14D). The timing of sheath initiation on peripheral axons coincided with sheath initiation within the spinal cord, and some peripheral sheaths stabilized and elongated during the course of the time-lapse (Figure 4-14D). This time-lapse data rules out the possibility that SCH-58261 treatment stimulates SCs to myelinate the nerve, since *nkx2.2a*$^{+}$ OPC processes can be clearly seen ensheathing nerve segments.

To examine whether these membrane sheaths were in fact myelin, we treated *gpr126* mutant larvae from 36 hpf to 3 dpf with SCH-58261 or DMSO, fixed them at 4 dpf, and labeled with an antibody specific to myelin basic protein (MBP) using

immunohistochemistry (Kucenas et al., 2009). In mutants treated with DMSO, we observed MBP only on a short segment of the proximal nerve root (Figure 4-14E), which is consistent with our previous data showing that differentiated MEP glia express MBP in this location (Smith et al., 2014). In mutants treated with the A2a AR antagonist, MBP labeling was present further distally along the nerve (Figure 4-14E). As further confirmation that peripheral OPCs myelinate spinal motor nerve roots following treatment with SCH-58261, we imaged *gpr126*$^{-/-}$ larvae expressing the transgenes *mbp:egfp* and *olig2:dsred* from 72 to 86 hpf (n = 3) (Figure 4-14F). In these time-lapses, we observed *olig2*$^{+}$ OPCs beginning to ensheath peripheral nerves with *mbp*$^{+}$ membrane tubes. Out of 12 nerves imaged, OPCs migrated out of the spinal cord onto 4 nerves, and an additional 3 nerves had OPCs already present at the beginning of the time-lapse. Multiple EGFP^{+} membrane tubes extended from single OPCs and ensheathed most of the nerve root on all 7 nerves with OPCs present. These long membrane tubes were consistent with the pattern of MBP antibody labeling on the nerves of SCH-58261-treated mutants (Figure 4-14E). Both the MBP antibody and *mbp:egfp* labeling were closely associated with an *olig2*$^{+}$ cell body, providing further evidence that peripherally-migrated OPCs and not SCs, initiate myelination in *gpr126* mutants treated with SCH-58261 (Figure 4-14E&F). From these experiments, we conclude that OPCs can be recruited onto peripheral motor nerves and initiate myelination, even in the presence of MEP glia and SCs.

Discussion

At MEP TZs, motor axons originating within the spinal cord cross through the glia limitans and transition into the PNS (Bonanomi and Pfaff, 2010). OPCs, in contrast, originate within the CNS but do not cross into the periphery, despite being highly migratory and extending membrane processes into the TZ (Fraher and Kaar, 1984; Smith et al., 2014). The mechanisms responsible for allowing axons and other glial populations to cross through the MEP TZ while preventing peripheral OPC migration are not fully understood, although work from our lab and others demonstrates that MEP glia in zebrafish and BC cells in mice are necessary to restrict OPC migration (Coulpier et al., 2010; Fröb et al., 2012; Smith et al., 2014). Using selective inhibitors for AR subtypes combined with genetic manipulation, we show that the A2ab AR is essential for preventing peripheral migration of OPCs, identifying adenosine signaling as a novel regulator of OPC migration during development. We also provide evidence that neuronal activity is involved in regulating OPC migration and is required to prevent OPCs from ectopically migrating into the PNS.

Adenosine and activity-dependent regulation of OPCs

Adenosine is a ubiquitous extracellular signaling ligand in the CNS and PNS (Abbracchio et al., 2009; Welsh and Kucenas, 2018). It can be released directly from cells, and can also be derived from hydrolysis of extracellular ATP, which is released from synaptic vesicles by most, if not all, neurons (Burnstock, 1972; Fields and Burnstock, 2006). In the spinal cord, adenosine modulates the activity of motor neurons

(Golder et al., 2008; Patel et al., 2001). In our studies, we demonstrate that motorneurons and interneurons within the spinal cord express A2ab receptors, and that inhibiting A2ab decreases neuronal activity (Figure 4-12A-D, Figure 4-13A&B). These results are consistent with data from many other model systems showing that neuronal A2a receptors act to promote activity of spinal cord motor neurons as well as other kinds of CNS neurons (Sebastiao and Ribeiro, 2015). Our experiments demonstrate that adenosine signaling via A2ab ARs is necessary to regulate OPC migration, and inhibition of A2ab with the selective antagonist SCH-58261 or genetic deletion results in ectopic migration of OPCs into the PNS.

Taken together, these experiments fit well with growing evidence from multiple labs that neuronal activity regulates OPC and OL behaviors, including migration, differentiation, and myelination (see Almeida and Lyons, 2017; Fields, 2015; Gallo et al., 2008 for recent reviews). Electrophysiological studies demonstrate that OPCs detect changes in neuronal activity or a variety of directly applied neurotransmitters (Bergles et al., 2010; Lin and Bergles, 2004a). Studies in mice and zebrafish demonstrate that increased neuronal activity promotes OPC differentiation and myelination, whereas decreased activity inhibits differentiation and leads to hypomyelination (Gibson et al., 2014; Hines et al., 2015; Makinodan et al., 2012; Mensch et al., 2015; Stevens et al., 2002). In addition, decreased neuronal activity results in altered OPC distribution and migration in mouse brains (Mangin et al., 2012; Tong et al., 2009). We hypothesize that because neuronal activity leads to OPC differentiation, decreased activity in our experiments

results in OPCs failing to differentiate, which causes them to maintain their highly migratory, exploratory behavior. Our findings that inhibiting neuronal firing with SCH-58261, an *adora2ab* mutation, TeNT, or carbenoxolone, result in ectopic OPC migration, are consistent with these studies and the hypothesis that neuronal activity regulates OPC migration and differentiation. We propose a model in which A2a AR regulation of neuronal activity is necessary to prevent peripheral migration of OPCs (Figure 4-15). The results presented here link two fields of study: neuromodulation by adenosine and activity-dependent regulation of OPCs. As further support for the importance of neuronal activity in regulating OPC migration, we identified 5 other compounds related to neuronal activity in our drug screen: 1-Phenyl-3-(2-thiazolyl)-2-thiourea and Brefeldin A, which interfere with the production and secretion of neurotransmitters; acetylthiocholine chloride and Salmetrol xinfoate, neurotransmitter receptor antagonists; and N-Phenylanthranilic acid, a chloride channel blocker which would disrupt membrane potentials. Further studies are needed to characterize the mechanisms driving ectopic OPC migration in zebrafish treated with these neuromodulators.

Because MEP glia are involved in repelling peripheral OPC migration, we considered the possibility that A2ab signaling could affect MEP glia differentiation. However, in our experiments, MEP glia have normal morphology and express both *wif1* and MBP, demonstrating normal differentiation. Therefore, our data supports the hypothesis that the effects of adenosine and neuronal activity directly affect OPCs and are a mechanism regulating OPC migration at the MEP TZ distinct from MEP glial restriction

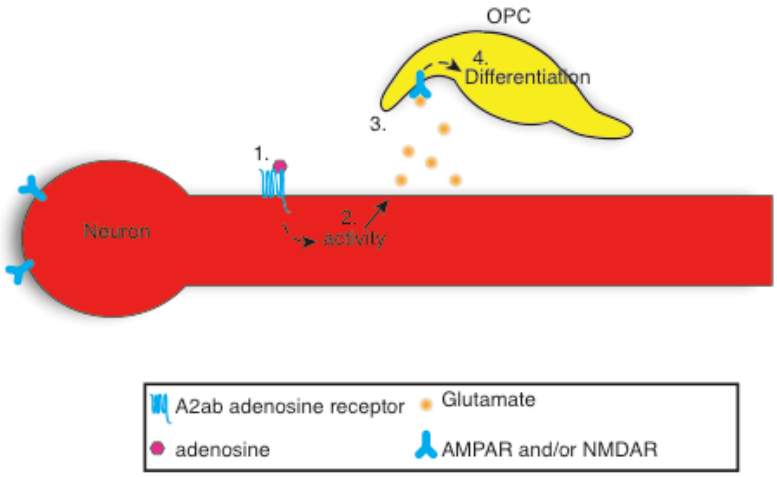

Figure 4-15 Model of OPC migration regulated by A2a AR neuromodulation. 1. Adenosine binds to A2ab AR on neurons, modulating neuronal activity. 2. Increased activity causes increased release of glutamate at axo-glial synapses, or via non-synaptic release into the extracellular space. 3. Neurotransmitters or other factors bind to receptors on OPCs. 4. Activation of the receptor(s) promotes OPC differentiation and decreased migration. Antagonism of the A2ab AR results in decreased neuronal activity and impaired differentiation of OPCs.

of OPCs. Although it was once thought that Schwann cells might repel OPCs from migrating into the PNS, our data demonstrate that Schwann cells play no role in repelling OPC migration through the MEP. In fact, selective ablation of Schwann cells from spinal motor nerve roots did not result in any peripheral OPC migration (Figure 4-6C). Furthermore, our experiments with *gpr126* mutants and previous studies using *trembler* mice demonstrate that OPCs do not migrate into the PNS even when Schwann cells fail to differentiate (Figure 4-14C) (Coulpier et al., 2010). In our current experiments, we also did not observe any effects of SCH-58261 on Schwann cell proliferation, migration, or differentiation (Figure 4-5D-F, Figure 4-6B). We also did not detect any effect on other measures of overall nerve health, including apoptosis, PG migration, and motor neuron/axon morphology (Figure 4-5C, G). Together, these data support our conclusion that A2ab and neuronal activity selectively affect OPC migration.

Glutamate and OPC migration

We have also sought to identify what signal is released by neurons to affect OPC repulsion at the MEP TZ. Glutamate is a likely candidate, as OPCs express receptors for this neurotransmitter (Lin and Bergles, 2004a). Synapses between OPCs and neurons have been observed using electron microscopy, and vesicular release of glutamate from neurons activates AMPA and/or NMDA receptors on OPCs (Bergles et al., 2000). We observed that AMPAR and NMDAR antagonists resulted in increased ectopic migration of OPCs through MEP TZs, suggesting that glutamate is important in regulating OPC migration. This is consistent with *in vitro* studies showing that glutamate

affects OPC migration (Gudz et al., 2006; Xiao et al., 2013). We also note the possibility that OPCs could respond to other factors released from neurons in an activity-dependent manner, such as ATP (Fields and Stevens, 2000). A recent study in zebrafish demonstrated that myelination can be modified by neuronal activity from certain classes of neurons, but is unresponsive to changes in activity of others (Koudelka et al., 2016). It would be interesting to know whether this is because of the particular neurotransmitters released by different neuronal populations, and if the same populations of neurons regulate OPC migration. In a review of synaptic communication between neurons and OPCs, Gallo et al. proposed that an OPC could detect relative differences in activity among populations of neurons, and this hypothesis has been supported experimentally (Etxeberria et al., 2016; Gallo et al., 2008; Hines et al., 2015). Since reports of ectopic peripheral OPC migration are incredibly rare in human tissues or animal models, it is likely that many overlapping mechanisms regulate spinal cord OPC migration. We previously demonstrated that MEP glia, peripheral glia positioned at the MEP TZ, repel migrating OPCs via contact-mediated repulsion (Smith et al., 2014). We believe that MEP glia and neuronal activity are two distinct mechanisms that regulate OPC migration. In support of this, ablating MEP glia while also inhibiting neuronal firing with TeNT results in even more peripherally-migrated of OPCs than TeNT alone (Figure 4-12E).

Potential for peripheral OPCs to myelinate peripheral nerves

Our findings also offer intriguing possibilities for the treatment of peripheral neuropathies. We and others have shown that OPCs are capable of myelinating peripheral axons (Coulpier et al., 2010; Kucenas et al., 2009; Morris et al., 2017; Smith et al., 2014). However, these previous studies were in the context of genetic mutations that result in the loss of all peripheral myelinating glia. In our model, SCs are present on nerves, but they fail to make myelin, which is a feature of some forms of Charcot-Marie-Tooth disease. Our data as well as previous studies in mice and zebrafish demonstrate no peripheral OPC migration in mutants with peripheral hypomyelination, and it is unclear whether OPCs would naturally migrate onto peripheral nerves in human neuropathy patients (Coulpier et al., 2010; Monk et al., 2009). Because of this, we are excited by the possibility of inducing OPCs to migrate onto peripheral nerves that lack myelin. Once in the periphery, OPCs are competent to initiate myelination without continued drug treatment. In combination with previous studies, this is strong evidence for the potential for OPCs to myelinate peripheral nerves in disease.

Chapter 5

Discussion and Future Directions

Summary

During spinal cord development, selective barriers are established at TZs where motor axons are permitted to grow out of the ventral spinal cord, and also at the dorsal spinal cord where peripheral sensory axons are guided in. However, even though axons traverse the boundary of the spinal cord at these specialized exit and entry zones, glial cell migration into and out of the spinal cord is restricted. Only two glial cell types that we know of are permitted to migrate out of the spinal cord during normal development. Other highly migratory central and peripheral glial progenitors frequently extend processes into spinal cord TZs, but they do not migrate through. The overall goal of my research has been to understand the mechanisms that establish and maintain segregation of CNS and PNS glial populations during development. In particular, I have focused on how glial interactions and intercellular signals restrict OPC migration and prevent ectopic migration of OPCs into the peripheral nervous system.

My work and that of others in the lab has led to the discovery of selective repulsive interactions between various populations of CNS and PNS glia. We have discovered a novel glial cell population, MEP glia, which is responsible for preventing peripheral OPC migration by repelling OPCs at the MEP (Smith et al., 2014). MEP glia are positioned on the peripheral side of the MEP. When they are ablated or fail to develop, OPCs freely migrate through the MEP and onto peripheral axons. The mechanism of repulsion

appears to be a direct, contact-mediated signal between MEP glia and OPCs, although the identity of that signal remains to be determined. Another mechanism operates independently of MEP glia to regulate OPC migration: neuronal activity. When we inhibited neuronal activity using various methods, we observed OPCs migrating through the MEP into the PNS in spite of the presence of MEP glia. These ectopically migrating OPCs are able to overcome the repulsion by MEP glia, and additional ablation of MEP glia results in even more ectopically migrated OPCs. The fact that MEP glia ablation and neuronal activity manipulations have additive effects on ectopic OPC migration suggests that these two mechanisms operate independently. I believe this is because MEP glia produce a direct repulsive effect on OPC migration, whereas manipulations of neuronal activity are capable of dialing up or down the overall migratory activity of OPCs. My discovery that neuronal activity is important for restricting OPC migration at TZs may reflect a more general role for neuronal activity in regulating OPC migration during development. Another intriguing finding from my research and that of others in the lab is that different cell types require distinct mechanisms to regulate their migration across TZs. While MEP glia-mediated repulsion and neuronal activity-mediated effects on migration are two mechanisms affecting OPCs, neither mechanism has a role in restricting motor neurons to the spinal cord. Previous studies suggest that *nkx2.2a*-expressing cells of the floor plate and/or perineurial glia at the motor root are important for restricting motor neuron cell body migration (Clark et al., 2014; Kucenas et al., 2008). My manipulations of adenosine signaling and neuronal firing also did not have any effect on perineurial glia or Schwann cell migration. We were surprised to find that

repulsion between PNS and CNS cells is not necessarily bi-directional. That is, MEP glia repel OPCs, but OPCs do not repel MEP glia. We initially hypothesized that bi-directional repulsion would be an efficient mechanism for establishing CNS-PNS boundaries. However, even without OPCs, neither MEP glia nor Schwann cells migrate into the spinal cord (Appendix II) (Smith et al., 2016). Rather, an entirely different glial population, CNS radial glia, is responsible for preventing MEP glia from migrating back into the spinal cord (Smith et al., 2016).

Chemical screens using zebrafish

As part of my research, I developed a chemical screening protocol to identify candidate signals involved in regulating OPC migration at the MEP. In addition to adenosine signaling, I identified 9 other compounds that resulted in ectopic peripheral OPC migration. Six of these I would expect to also have an effect on neuronal activity, so they may function in a similar way as the adenosine antagonist to regulate OPC migration. Further experiments are needed to test how these remaining compounds effect OPC migration. A first step would be to simply perform dose-response experiments to find the most effective dose of each drug and also to confirm that independent stocks of each compound reliably result in the same phenotype as the screen. A second important experiment would be to test whether each compound affects MEP glia development, since this was not assessed as part of the screen. Some compounds may affect OPC migration by perturbing MEP glia, while others, like the adenosine antagonist, could result in ectopic OPC migration independent of MEP glia. Either result would inform new

insights into the mechanisms maintaining TZ boundaries, since we know so little about any signals that are involved in OPC repulsion at the MEP.

Zebrafish are an advantageous model system to use in drug discovery screens for a number of reasons. First, since embryonic and early larval zebrafish absorb chemicals through the skin, drugs can be easily applied by bath application to the normal rearing water. Second, because of their small size, embryonic and early larval zebrafish can be reared individually in wells of 96 well plates. In this way, protocols for treatment and analysis can be set up similar to cell culture systems and even automated if robotic pipetting and plate reading technologies are available. For the robust, “all or nothing” phenotype of scoring the presence or absence of OPCs in the PNS, plates could be rapidly scored by eye using an inverted epifluorescence microscope for a semi-high throughput approach. Although not typically quite as high throughput as *in vitro* approaches, screens using zebrafish have the advantage of being able to assess whole tissue effects in a living, vertebrate organism. They can thus be applied to basic biology questions in a more physiologically relevant way, and also adapted to translational research by testing potential therapeutics on disease models. In fact, another student in the lab has adapted the screening protocol I developed to investigate signals involved in regulating OPC spacing and contact-mediated repulsion in the spinal cord.

Screens using zebrafish do also come with their limitations. One such limitation is that, the pharmacokinetics of receptor binding and affinities have not been established for

many compounds. Because of the close homology between many zebrafish genes and their mammalian homologs, similar kinetics can often be inferred, but there is no guarantee. Unlike working with cell culture, applying drug treatments to a whole embryo or larvae involves factors such as the breakdown and the removal of the drug from the body, tissue distribution and absorbtion, and potential differences between applied concentrations and the concentration of drug actually available to bind to receptors. For these reasons, it is expected that a screen will result in many “misses” of compounds that blocks or activates a relevant biological process, but was simply at the wrong dose or didn’t distribute well in the tissue. I would not recommend using a result of “no effect” for a certain drug in a screen as strong evidence for the target gene or protein truly having no effect on whatever is being studied. Because of the limitations of being able to optimize appropriate dosing, it is recommended to optimize and validate all other aspects of the screening protocol. The phenotype being analyzed should ideally have very low variability, or alternately be able to be robustly quantified. Dissolving compounds in a low percentage of DMSO (final concentration 0.5-1%) can also help with tissue distribution. Performing screens at time points later than 48 hpf, after embryos have hatched from their chorions, can slightly speed up throughput. However, even for screens performed before hatching, pronase can be used to quickly dechorionate embryos.

Boundary mechanism homology between species

As described in Chapter 3, MEP glia share many characteristics with mammalian BCCs. Both cell types, positioned at the ventral TZ, are required to prevent peripheral migration of OPCs. They also share expression of a number of genes, including *sox10* and *wif1*, both of which are important for MEP glia function. One notable difference is that BCCs express *krox20* whereas MEP glia do not. *Krox20* appears to be important for the ability of BCCs to repel OPCs, since peripheral OPCs are observed in mouse mutants without *krox20* function. Initially, the neural crest origin of BCCs led to difficulties in making inferences about homology between MEP glia and BCCs. However, more recent fate mapping studies have revealed heterogeneity among mouse BCCs, and that not all BCCs express *krox20*. It has even been suggested that a subpopulation of spinal cord-derived ventral BCCs may exist, similar to MEP glia (Radomska and Topilko, 2017). It would be informative to directly test this possibility with lineage tracing studies using markers for spinal cord progenitor populations, such as *olig2*. The fact that the origins of both zebrafish and mouse perineurial glia are from *nkx2.2*-expressing cells in the ventral spinal cord lends support to the idea that a subpopulation of mouse BCCs could derive from the ventral spinal cord (Clark et al., 2014). One advantage to studying MEP glia in zebrafish is that they can be labeled with fluorescent transgenes and easily identified. Future studies aimed at further elucidating signals involved in MEP glia differentiation and function will help us understand more about TZ boundary formation and, because of the similarities already identified between mammalian BCCs and zebrafish MEP glia, may lead to discoveries of conserved mechanisms across species. Continuing efforts in

the lab are working to create more selective transgenic markers for MEP glia. Currently, MEP glia can be fluorescently labeled using transgenes driven by *sox10, olig2,* or *foxd3*. However, each of these transgenes are also expressed in OPCs and/or Schwann cells. *wif1* expression can be used to selectively label MEP glia using *in situ* hybridization. Therefore, we are attempting to create a fluorescent transgene driven by *wif1* expression in order to study MEP glia in more detail. We are also using CRISPR Cas9 technology to create targeted mutations in *wif1* to test the role of this gene in MEP glia specification, differentiation, and function. The requirement for *wif1* may be another conserved boundary mechanism between mammals and fish, since MO knockdown of *wif1* leads to peripheral migration of OPCs in zebrafish, and preliminary experiments using *wif1* mouse mutants also shows OPCs located in the PNS (Figure 3-6 and Laura Fontenas, unpublished data). Another priority in learning more about these newly identified cells is identifying additional markers. Others in the lab are testing candidates from an RNAseq database.

Germline *adora2ab* mutants

In Chapter 4, I described experiments using MO knockdown of *adora2ab* and also CRISPR-based mutagenesis to test the requirement for *adora2ab* in restricting peripheral OPC migration. The results of both MO and CRISPR methods were consistent with the effect of blocking A2a receptors with a selective antagonist: knocking down *adora2ab* resulted in peripheral OPC migration. The experiments described above were performed using the F0 CRISPR injected generation of larvae. We performed

sequencing and identified targeted mutations in *adora2ab* in 91.7% and 86.7% of F0 larvae injected with *adora2ab* sgRNA 6 and 7, respectively, suggesting highly efficient mutagenesis. However, somatic mutations in the F0 generation are mosaic, so that not every cell harbors homozygous mutations. Additionally, mosaicism in the indels themselves can produce silent mutations in some cells, so that the F0 generation may not have as robust a phenotype as true homozygous mutants. Therefore, we wanted to analyze homozygous germline mutations to enable us to perform more robust quantitative measurements of the OPC migration phenotype as well as to establish a stably inherited line for future studies. By outcrossing founders and raising their progeny to adulthood, we have now identified F1 zebrafish who are heterozygous for mutations in *adora2ab*. We have identified multiple different alleles of with indels near the CRISPR target site which are frameshift mutations resulting in early stop codons. We have performed preliminary experiments analyzing peripheral OPC migration in F2 larvae with homozygous or compound heterozygous (mutations on both chromosomes but 2 different alleles). Surprisingly, germline mutant larvae in the F2 generation do not phenocopy our results with F0 injections or morpholino. We have observed peripheral OPC migration in some heterozygous larvae, but not homozygous mutants. It is possible that genetic compensation from other genes has occurred in raising founders and F1 generation adult zebrafish. There is evidence for differential gene expression compensating for the loss of a mutated gene in zebrafish (Rossi et al., 2015). This compensation occurs (and may even be selected for) in the process of raising founders and future generations to adulthood, whereas it is not seen in genetic knockdown

studies using morpholinos or F0 CRISPR analysis. This phenomenon may result in discrepancies between phenotypes observed between morpholino, F0, and F2 based studies. In ongoing work in the lab, we are testing the possibility that the closely related *adora2aa* could compensate for the loss of *adora2ab*. Although neither mutations in *adora2aa* alone nor MO knockdown resulted in significant peripheral OPC migration, it is possible that loss of *adora2ab* initiates compensatory expression of *adora2aa*. We are testing this possibility by quantifying levels of *adora2aa* transcript in *adora2ab*$^{-/-}$ larvae compared to WT. We will also test functional compensation by *adora2aa* by analyzing peripheral OPC migration in *adora2aa-/-;adora2ab-/-* double mutant larvae. If *adora2aa* does compensate for the loss of *adora2ab*, we would expect to see significant numbers of peripherally-migrated OPCs when both genes are knocked out. Recently, a new ortholog, *adora2c*, has been identified in zebrafish (Wakisaka et al., 2017). The A2c receptor is expressed by sensory neurons in the olfactory epithelium, and its activation by adenosine increases firing of these neurons (Wakisaka et al., 2017). Since A2c, like A2ab, increases neuronal firing, it is also a candidate to compensate for the loss of *adora2ab*. We have recent evidence that *adora2c* is expressed in spinal cord neurons, also supporting the evidence that it can compensate for knockout of *adora2ab* (Laura Fontenas, unpublished data). We plan to compare *adora2c* expression in spinal cord neurons in WT and *adora2ab* mutants and create *adora2c* mutants using CRISPR in order to address the possibility that this gene could compensate for *adora2ab*.

Neuronal activity regulates OPC behaviors

In Chapter 4, I describe my discovery that decreasing neuronal activity either with an A2a adenosine receptor antagonist or TeNT results in ectopically migrated peripheral OPCs. Growing evidence indicates that changes in neuronal activity can affect OPC differentiation and myelin production (see Almeida and Lyons, 2017; Fields, 2015; Gallo et al., 2008 for reviews). However, there is less direct evidence for neuronal activity influencing OPC migration (Gudz et al., 2006; Xiao et al., 2013). This is also the first report of adenosine signaling regulating OPC migration by modulating neuronal activity. The connection between adenosine, neuronal activity, and OPC migration was an unexpected discovery, since I initially hypothesized that adenosine was acting as a direct chemotactic signal to OPCs. In hindsight, this signaling mechanism is not so surprising, given the decades-old knowledge that adenosine modulates activity of many kinds of neurons, including spinal cord motor, sensory, and interneuron populations, and the more recent evidence that OPCs respond to changes in neuronal activity with changes in proliferation, migration, differentiation, and myelin production (Almeida and Lyons, 2017; Cunha, 2001).

The effects of A2a adenosine receptors on neurons are quite clear: activation decreases neuronal firing (Golder et al., 2008; Quarta et al., 2004; Rebola et al., 2008). The effects of neuronal activity on OPCs are a bit more difficult to resolve. How OPCs respond to neuronal activity may depend not only on whether activity is increased or decreased, but also on the frequency of neuronal firing or the type of neuron (Nagy et al., 2017). *In vitro*

cell culture studies can tightly control firing of a single population of neurons and analyze the effects of these manipulations on OPCs. However, *in vivo*, OPCs are likely to detect and integrate information about activity levels of multiple kinds of neurons at once. In fact, evidence for this hypothesis comes from the study by Hines et al. in which synaptic activity of single spinal cord neurons *in vivo* results in a bias or preference of OPCs to myelinate other nearby neurons (Hines et al., 2015). When the activity of all neurons was suppressed, no effect on myelination was observed (Hines et al., 2015). For this reason, although *in vitro* studies of neuron-OPC interactions are attractive because of their simplicity and control, an experimental set up with only one neuronal population may be too artificial to reveal any real effects on OPC behaviors. Unfortunately, since CNS circuits are complex, and manipulations of one neuron in a circuit can have unpredictable effects on the overall circuit activity, *in vivo* manipulations of neuronal activity can also have complex and unpredictable results on OPC behaviors. One example of seemingly conflicting results is in comparing the study by Gibson et al. in Michelle Monje's lab with that of Etxeberria et al. in Jonah Chan's lab. In one study, projection neurons within the premotor cortex were optogenetically stimulated, and quantification of OPC proliferation and differentiation was performed in the region surrounding the stimulated neurons, as well as at the descending axonal projections through the corpus callosum (Gibson et al., 2014). In the other study, visually-evoked action potentials were blocked by suturing one eye shut, and differentiation and proliferation of OPCs was quantified in the optic tract of the deprived eye compared to the control eye (Etxeberria et al., 2016). Optogenetic stimulation of premotor cortical

projection neurons resulted in increased OPC proliferation and differentiation (Gibson et al., 2014). Surprisingly, decreased evoked firing of optic tract neurons caused by sensory deprivation also resulted in increased differentiation of OPCs, but no change in proliferation (Etxeberria et al., 2016). The disparate results from the two studies are probably equally valid and illustrate that the effects of neuronal activity on OPCs are more complex than simply turning a switch on or off. As discussed by Etxeberria et al., silencing evoked firing of a population of neurons such as retinal ganglion neurons still allows spontaneous firing and could have unpredictable effects on nearby interneurons and overall circuit activity (Etxeberria et al., 2016). The same is true of optogenetic manipulations of projection neurons in the premotor cortex: even though firing of these neurons was directly stimulated at a given frequency, the effects on surrounding neuronal activity are unknown. Since OPC processes simultaneously contact multiple neurons, they could be detecting activity levels not only of the neurons being directly manipulated in these experiments, but also other nearby neuronal populations. Differences in the neurotransmitters being released could also be a factor in differing responses to OPCs. In my research, decreasing the activity of a subset of spinal cord neurons (those expressing A2ab receptors) resulted in ectopic OPC migration. Globally decreasing neuronal firing with TeNT resulted in the same qualitative effect on OPC migration, but to a much lesser degree. Like the result obtained by Hines et al., this may be another example in which changes in activity of a subset of neurons but not others have a greater effect on OPCs than a universal decrease in activity. Another key factor may be the particular kind of neuron being affected. Receptors for multiple different

neurotransmitters have been identified on OPCs, but it is not known whether different neurotransmitters exert different effects. In my experiments, glutamate antagonists (both AMPA and, to a lesser extend, NMDA) resulted in significant peripheral OPC migration. However, the $GABA_A$ antagonist bicuculline did not result in any peripheral OPC migration. Unfortunately, we were unable to specifically test the effects of glutamate on OPCs, since the antagonists inhibit receptors expressed by OPCs as well as by neurons. The effect of neuronal activity on migration and other OPC behaviors is a promising area for future studies. Because calcium signaling, proliferation, migration, and initiation of myelin sheaths can be visualized in real time in live zebrafish larvae, there is great potential for future studies to answer some of the open questions of how neurons and OPCs interact in intact tissues (Czopka et al., 2013; Kirby et al., 2006; Mensch et al., 2015).

Some of my preliminary data suggests that adenosine signaling and neuronal activity affects overall OPC development within the spinal cord, not just migration at the MEP. As an initial step in characterizing the effects of adenosine signaling on OPC development, I quantified the number of OPCs within the spinal cord of zebrafish larvae treated with the nonselective adenosine receptor antagonist CGS-15943. I also quantified distribution within the spinal cord as an indication of migration. Treatment with CGS-15943 resulted in slightly increased numbers of spinal cord OPCs compared to DMSO-treated controls, and more OPCs were located in the dorsal half of the spinal cord (Figure 5-1). This suggests that adenosine signaling affects the migration of OPCs

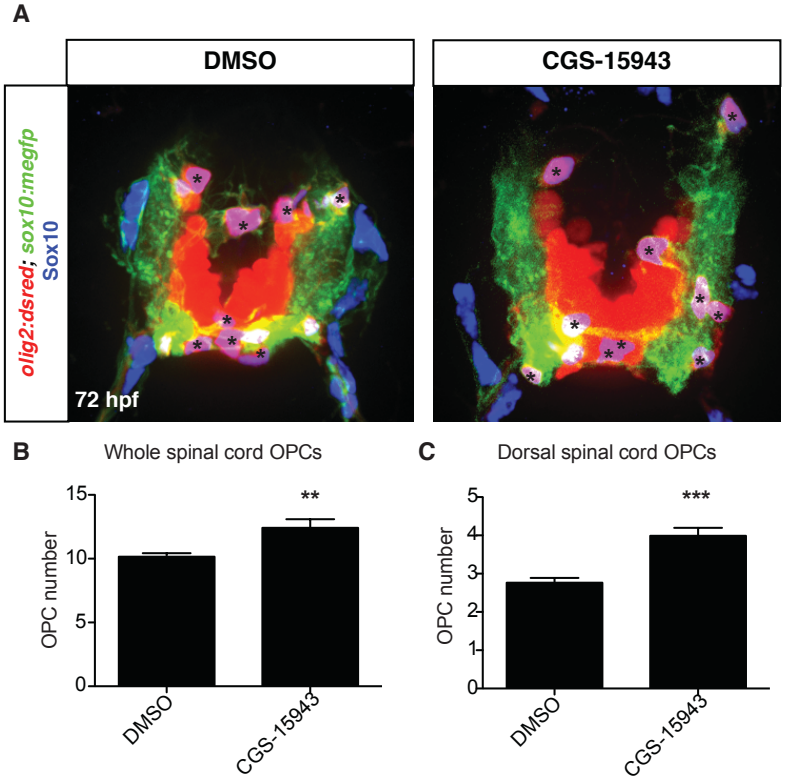

Figure 5-1 Adenosine signaling affects spinal cord OPC numbers and distribution. (A) Cross sections of spinal cords from 72 hpf larvae expressing *olig2:dsred* and *sox10:megfp*. Larvae were treated from 24 to 72 hpf with 1% DMSO or 1.25 μM CGS-15943, fixed at 72 hpf, and stained with anti-Sox10 antibody. OPCs (asterisks) co-express *olig2:dsred*, *sox10:megfp*, and Sox10. (B, C) Quantification of total OPCs per section (B) and OPCs in the dorsal half of spinal cord sections (C). 10 sections per larvae starting from the mid-trunk (yolk extension) for n = 11 larvae were quantified. $p = 0.0041$ (whole spinal cord) $p < 0.0001$ (dorsal spinal cord) analyzed by unpaired student's t test.

from the ventral spinal cord to the dorsal spinal cord and may also affect proliferation. In the future, it will be informative to perform time-lapse imaging in order to quantify migration rates and/or distances, as well as proliferation and even the frequency or number of contacts between OPCs and nearby axons. It is possible to selectively increase or decrease the activity of certain populations of neurons using neuronal subtype-specific promoters driving optogenetic channels or inhibitors like TeNT (Hines et al., 2015; Koudelka et al., 2016; Portugues et al., 2013). The response of OPCs to changes in activity of different kinds of neurons in relation to others can be quantified to give a better picture of how relative changes in activity levels, or manipulations of certain kinds of neurons, affects OPC development.

I am particularly interested in the question of how neuronal release of glutamate impacts OPC migration and differentiation. In my research, inhibiting ionotropic glutamate signaling resulted in ectopic OPC migration. Is this due to a direct result of neuronal glutamate binding to receptors expressed by OPCs? Multiple studies have demonstrated that mouse OPCs express glutamate receptors (Bergles et al., 2000; De Biase et al., 2010). Ongoing work in the lab is assessing whether zebrafish OPCs express AMPA receptors using *in situ* hybridization. We also plan to test the effects of knocking out the genes encoding AMPA receptor subunits. Unfortunately, we are unable to selectively knockout glutamate receptors on OPCs as a direct test of the role of glutamate on OPC behaviors. One potential way to get around this limitation would be to selectively silence glutamatergic spinal cord neurons using selective promoters driving

TeNT expression. An undergraduate student who has worked closely with me studying the effects of adenosine and neuronal activity on OPCs, Melanie Piller, is interested in doing further testing of how glutamate regulates OPC development. By performing time-lapse imaging during the phase of active OPC proliferation and migration in the spinal cord before the onset of myelination, she is analyzing the effects of the AMPA antagonist NBQX on OPC proliferation and migration, and myelin initiation. She has preliminary results indicating that OPC migration is increased by AMPA antagonist treatment (Melanie Piller, unpublished data). This work could even be expanded to test the effects of increasing or decreasing activity of different populations of neurons on OPC behaviors. Optogenetic stimulation using promoters for certain neuronal populations can be used to precisely regulate neuronal firing, and levels of activity can even be measured using gcAMP or SypHy, a reporter of synaptic vesicle release (Koudelka et al., 2016; Muto et al., 2011). Robust measurements of many OPC behaviors can then be made using time-lapse imaging, including process interactions with stimulated axons, migration speed/distances, proliferation rate, and initiation/stabilization of myelin sheaths. Recent studies have expressed TeNT in different neuronal populations and demonstrated different effects on myelination depending on the type of neuron (Hines et al., 2015; Koudelka et al., 2016). This same approach could be applied to analyzing OPC migration, and it would be very informative to more precisely control firing rates with optogenetics and compare the effect of differential firing rates on OPC behaviors.

How do transition zones form?

Thanks to TEM studies, the structure of the mammalian transition zone is known in detail (Fraher, 1978, 1992, 1997; Fraher and Kaar, 1984; Fraher et al., 2007). At the MEP and DREZ, axons crossing through the TZ are surrounded by a meshwork of glial processes, mostly astrocytes and/or radial glia. Around the time of axon growth into and out of the spinal cord, there is a relatively loose network of glial processes, with available space for axons to grow through. When motor axons first cross through the MEP, they navigate through gaps between immature radial glia endfeet. As development progresses, the glial processes become more tightly associated with axons, more processes fill the area, and a thick meshwork of glial processes and axons is formed. In fact, the glia limitans is thickened at mature TZs relative to the rest of the spinal cord (Fraher et al., 2007). In zebrafish as well, radial glia endfeet do not form a complete barrier around the neural tube until 48 hpf, well after motor axons have extended into the PNS (Smith et al., 2016). In mice and zebrafish, motor axons emerge through the MEP before OPCs have been specified or any peripheral glia have reached the site of the nerve root (Fraher et al., 2007; Lewis and Eisen, 2003; McGraw et al., 2008). After motor axon exit, OPC and peripheral glial processes extend along axons and contact each other at the TZ (Fraher et al., 2007; Smith et al., 2014). In contrast to cell interactions at the MEP, neural crest-derived BCCs form clusters at locations of the presumptive DREZ before sensory axons grow into the spinal cord (Fraher et al., 2007). It has been hypothesized that BCCs may play a role in forming the DREZ, since they are found at presumptive DREZ locations before axons grow through. An alternate

possibility is that an unidentified signal at a pre-formed DREZ attracts BCC clusters, and that BCCs subsequently secrete signals to guide axons to the DREZ. In contrast, it is unlikely that peripheral glia play any role in guiding motor axons through the MEP, since the first motor axons emerge through the MEP before any neural crest cells or other peripheral glia are present (Fraher et al., 2007).

As informative as descriptions of TZ structure have been in showing what cell types are present at developing TZs and when, they cannot test the question of how TZs form during development. In particular, what regulates the location of the TZ? Studies using zebrafish have begun to provide answers to these questions. MEPs are regularly spaced along the anterior-posterior axis of the spinal cord midway between each segmental border. The secreted axon guidance molecule *semaphorin3ab* (*sema3ab*) expressed at the posterior of each spinal cord segment is necessary for establishing this regular pattern by signaling to *plexina3*/*neuropilin1a* (*plxna3*/*nrp1a*) co-receptors expressed by motor axons (Palaisa and Granato, 2007). MO knockdown of *sema3ab* or its co-receptors *plxna3* or *nrp1a* results in motor axon exit through additional, ectopic exit points (Feldner et al., 2005, 2007; Sato-Maeda et al., 2008). Additionally, *plxna3* homozygous mutant embryos (also called *sidetracked*) also have this phenotype of additional, ectopic motor exit points (Palaisa and Granato, 2007). Furthermore, the ventral neuroepithelium appears to play an important role in determining proper exit locations in both zebrafish and mice. In zebrafish with MO knockdown of *nkx2.2a* and in mice with a conditional deletion in *Nkx2.2*, motor axons exit the spinal cord in irregular

positions (Clark et al., 2014; Kucenas et al., 2008). Since *nkx2.2a* is expressed in spinal cord cells of the p3 domain as well as perineurial glia present along the motor roots, it is not clear whether perineurial glia or their precursors within the ventral spinal cord are necessary for proper MEP positioning. Unpublished data from another graduate student in the lab suggests that *nkx2.2a*-expressing cells of the lateral floor plate may actively determine the location of the MEP, since these cells create actin-based protrusions concentrated at the future site of motor axon exit, shortly before any motor axons have emerged from the spinal cord (Yunlu Zhu, unpublished data). Environmental cues also regulate the dorsal-ventral position of the MEP. A combination of Slit/Robo repulsion and Netrin/Dcc attraction fine-tunes this position. Mice with mutations in *Slit1;Slit2*, expressed in the ventral spinal cord, or its receptors *Robo1;Robo2*, expressed by motor neurons, have ventrally-shifted MEPs (Kim et al., 2017). Conversely, mice with mutations in *Netrin1*, expressing in the ventral and lateral spinal cord, or its receptor *Dcc*, expressed by motor neurons, had dorsally-shifted MEPs (Kim et al., 2017). In each case, the MEP had a larger diameter than WT controls. This suggests that a balance of secreted attractive and repulsive axon guidance molecules is necessary for tight regulation of MEP location. Another axon guidance receptor expressed by motor neurons, *cxcr4*, is also important in guiding motor axons to the MEP, since mutations in either *cxcr4* or its ligand *cxcl12* result in misrouted axons within the spinal cord, some of which fail to exit the spinal cord entirely and others exit at ectopic, more dorsal locations (Lieberam et al., 2005).

Studies using zebrafish have shown that once primary motor neurons pioneer axon trajectories through the MEP, later secondary motor axons follow (Lewis and Eisen, 2003). Are other signals required for assembly of other peripheral nerve components: MEP glia and Schwann cells? The DRG, which forms after initial motor axon exit, is positioned near the motor nerve, and sensory neurons from the DRG send axons into the spinal cord at the DREZ, which is positioned at approximately the same level along the A-P axis as the MEP. How is the location of the DRG and DREZ so closely coordinated with the location of the MEP? In mice, BCCs cluster at the location of the presumptive DREZ before sensory axons enter the spinal cord. They are hypothesized to play a role in guiding sensory axons to the DREZ, since they form a permissive substrate for DRG axon growth *in vitro*, and mutations disrupting Semaphorin/Plexin signaling between BCCs and axons result in DREZs with irregular shapes (Golding and Cohen, 1997; Mauti et al., 2007). However, the fact that DRGs and DREZs were located at generally the correct segmental location in these mutants suggests that additional mechanisms determine proper positioning. In Appendix I, I describe evidence that the position of the MEP orchestrates motor nerve assembly and DRG/DREZ positioning. I used *plxna3* mutants, which have additional, ectopic MEPs, to test whether glial components assembled on ectopic motor axons, or whether PNS glia were restricted to their regular, midsegmental locations and would ignore ectopically positioned nerves. The segmental migration of NCCs has been previously described, and positional cues in the somatic mesoderm are involved in regulating this migration (Honjo and Eisen, 2005). However, time-lapse imaging has revealed that a subset of NCCs migrate

directly to the MEP shortly after initial axon exit, pause at this location, and eventually form the DRG (Honjo et al., 2008; McGraw et al., 2008; Prendergast et al., 2012). Since blocking *erbb3* signaling disrupts this NCC migration and DRG formation, it is possible that *neuregulin* expressed by motor axons guides migrating NCCs to the MEP, and that the presence of motor axons determines DRG location (Honjo et al., 2008). My experiments using *plxna3* mutants support this model, since DRGs form at locations of ectopic motor nerves, in addition to correctly positioned DRGs at adjacent nerves. The ectopic DRGs even send central axonal projections into the spinal cord, where they join the dorsal longitudinal fasciculus, suggesting that the presence of motor axons is sufficient to recruit migrating NCC and initiate DRG development. The presence of central and peripheral axonal projections and the downregulation of *sox10* expression from the ectopic DRG neurons in *plxna3* mutants suggest that sensory neurons have differentiated. However, in the future, it would be interesting to test specific markers of DRG differentiation, like *neurogenin*. It would also be interesting to test whether other peripheral glial elements, such as Schwann cells and perineurial glia, are recruited to ectopic motor axons. Since NCC migrate to ectopic motor axons to form DRGs, I would predict that they would also differentiate into Schwann cells. It would also be useful to assess ectopic DRG formation in a different genetic mutant that also has extraneous motor exit points, in order to be sure that the positioning of ectopic DRGs is due to ectopic motor axons, not aberrant Semaphorin/Plexin signaling. I tested whether another peripheral glial cell type, MEP glia, form at ectopic motor nerves. MEP glia are identifiable at every ectopic motor nerve that I imaged in *plxna3* mutants, in addition to

the MEP glia present along nerves at their normal midsegmental positions. Not only are MEP glia present at ectopic nerves, but they are also functional, because I never observed any peripheral OPC migration in *plxna3* mutant larvae. These results suggest that motor axon exit from the spinal cord is also sufficient to recruit MEP glia to migrate out of the spinal cord and associate with the axon. This recruitment may also involve axonal expression of *neuregulin*, similar to the recruitment of NCCs, since MEP glia are missing from the nerve in zebrafish *erbb3* mutant larvae, which lack the receptor for *neuregulin* (Figure 3-1) (Smith et al., 2014). As an alternative way to test this hypothesis, a post doc in the lab, Dr. Laura Fontenas, is examining MEP glia migration in zebrafish overexpressing *neuregulin1*, to see if axonal *neuregulin* is an attractive cue for MEP glia migration. She is also developing tools to selectively ablate motor neurons early in development, to test whether the presence of motor axons is required for MEP glia to exit the spinal cord. This could also be a good model for testing the requirement for motor axons to regulate the position of DRG formation, by testing whether DRGs are missing or irregularly positioned at spinal cord segments with ablated motor neurons.

Another outstanding question regarding MEP formation is: what confines motor neuron cell bodies to the spinal cord? After specification in the ventricular zone, newly born motor neurons migrate away from the ventricle to reach their places in the ventral gray matter (Kim et al., 2017). What prevents motor neuron cell bodies from continuing to migrate along their axons and exit the spinal cord? In mice and chicks, neural crest-derived BCCs positioned at the MEP prevent this migration. When BCCs are surgically

removed or genetically ablated using conditional expression of diphtheria toxin, motor neuron cell bodies are seen ectopically positioned along peripheral motor axons (Vermeren et al., 2003). The ability of BCCs to prevent ectopic motor neuron migration depends on Semaphorin signaling, as *Sema6a* knockdown in chick embryos or homozygous mutation in mouse embryos led to ectopic peripheral motor neurons (Bron et al., 2007; Mauti et al., 2007). In zebrafish, the mechanism for preventing peripheral OPC migration is also likely to involve Semaphorin signaling, since ectopic peripheral motor neuron cell bodies have been identified in zebrafish following MO knockdown of *nrp1a*. However, *plxna3*$^{-/-}$ larvae do not have any peripheral motor neuron cell bodies, so this receptor is not required to repel motor neuron migration (Appendix I). Intriguingly, unlike in mice and chick embryos, neural crest-derived cells do not play any role in regulating motor neuron migration in zebrafish. It seems unlikely that zebrafish even have neural crest-derived boundary cap cells. Other than expression of *wif1* and *sox10* by CNS-derived MEP glia, I did not observe expression of any previously identified BCC markers at the zebrafish dorsal or ventral motor roots (Appendix I). As an alternate method to test whether zebrafish neural crest-derived cells are important for gating motor neuron migration, I used *mob*$^{-/-}$*;mos*$^{-/-}$ mutant embryos, in which no neural crest cells are specified (Arduini et al., 2009). I tested whether any motor neuron cell bodies were present in the periphery in zebrafish without any neural crest-derived cells by labeling with an Islet1/2 antibody at 36 hpf and 72 hpf. I did not observe a single ectopic motor neuron cell body at either age (Appendix I). Taken together, these results suggest that zebrafish do not have neural crest derived BCCs, and that other mechanisms are

responsible for preventing ectopic motor neuron migration. One likely mechanism involves *nkx2.2a*-expressing cells. I have already described two studies in which knockdown or deletion of *nkx2.2a* in zebrafish or *Nkx2.2* in mice resulted in irregularly positioned motor exit points (Clark et al., 2014; Kucenas et al., 2008). In these same studies, ectopic motor neuron cell bodies were observed along the peripheral motor nerves (Clark et al., 2014; Kucenas et al., 2008). These results are in contrast to experiments showing that neural crest-derived BCCs are needed to prevent peripheral motor neuron migration, highlighting some of the remaining questions regarding whether multiple mechanisms exist for gating motor neurons, or whether previous manipulations to BCCs could have unexpected effects on perineurial glia, or vice versa. Since the formation of the MEP is an important early event in organizing much of peripheral nerve development, future studies examining how the MEP is formed and regulated could have significant implications for understanding many areas of neurobiology.

Conclusions

My research has discovered new mechanisms regulating cell migration at TZ boundaries during nervous system development. From an evolutionary perspective, some of these mechanisms are conserved between fish and rodents. Since multiple mechanisms exist for restricting the migration of different cell types, this suggests a tight control of TZ formation and maintenance. Neuronal activity modulation through adenosine is a novel regulator of OPC migration at TZs, and may be an important mechanism for fine-tuning and targeting OPC migration throughout the CNS. This work

demonstrates the importance and specificity of cellular interactions in regulating how cell migration establishes nervous system patterning.

Appendix I Ectopic transition zones and ectopic motor neuron migration

In zebrafish, Semaphorin-Plexin signaling guides motor axons to the correct exit points along the spinal cord anterior-posterior axis. Mutations in *plxna3* cause motor axons to exit the spinal cord in additional, ectopic locations (Palaisa and Granato, 2007). I used *plxna3*$^{-/-}$ zebrafish to test two questions: 1) is Plxna3 signaling involved in regulating OPC migration at the MEP and 2) does the presence of ectopic motor axons initiate the formation of other peripheral nerve components? I first tested whether MEP glia are present on peripheral nerves in *plxna3* mutants. I identified *wif1*$^{+}$ MEP glia along spinal motor roots in *plxna3*$^{-/-}$ embryos at 54 hpf, a stage consistent with when MEP glia express *wif1* in WT embryos (Appendix I-1A). I also used photoconversion to identify *sox10:eos*-expressing MEP glia in 72 hpf *plxna3*$^{-/-}$ larvae. In larvae expressing the photoconvertible protein Eos driven by *sox10*, Eos is initially expressed as a green fluorescent protein. Upon exposure to UV light, any green Eos protein present in the tissue is permanently converted to red. Any progeny of the photoconverted cells inherit red Eos protein, whereas Eos that is newly synthesized after UV exposure is green. When we expose *sox10:eos* embryos to UV light at 48 hpf, all neural-crest derived cells are converted to red fluorescence. MEP glia, which are not neural-crest derived and initiate *sox10* expression after 48 hpf, are green (Smith et al., 2014). I analyzed WT and *plxna3*$^{-/-}$ larvae at 72 hpf for the presence of green Eos^{+} MEP glia at the motor root. I did not observe any differences in MEP glia between WT and *plxna3* mutants (Appendix I-1B&C n = 2 WT, n = 4 *plxna3*$^{-/-}$, 14-20 nerves analyzed per larva). In these images, I

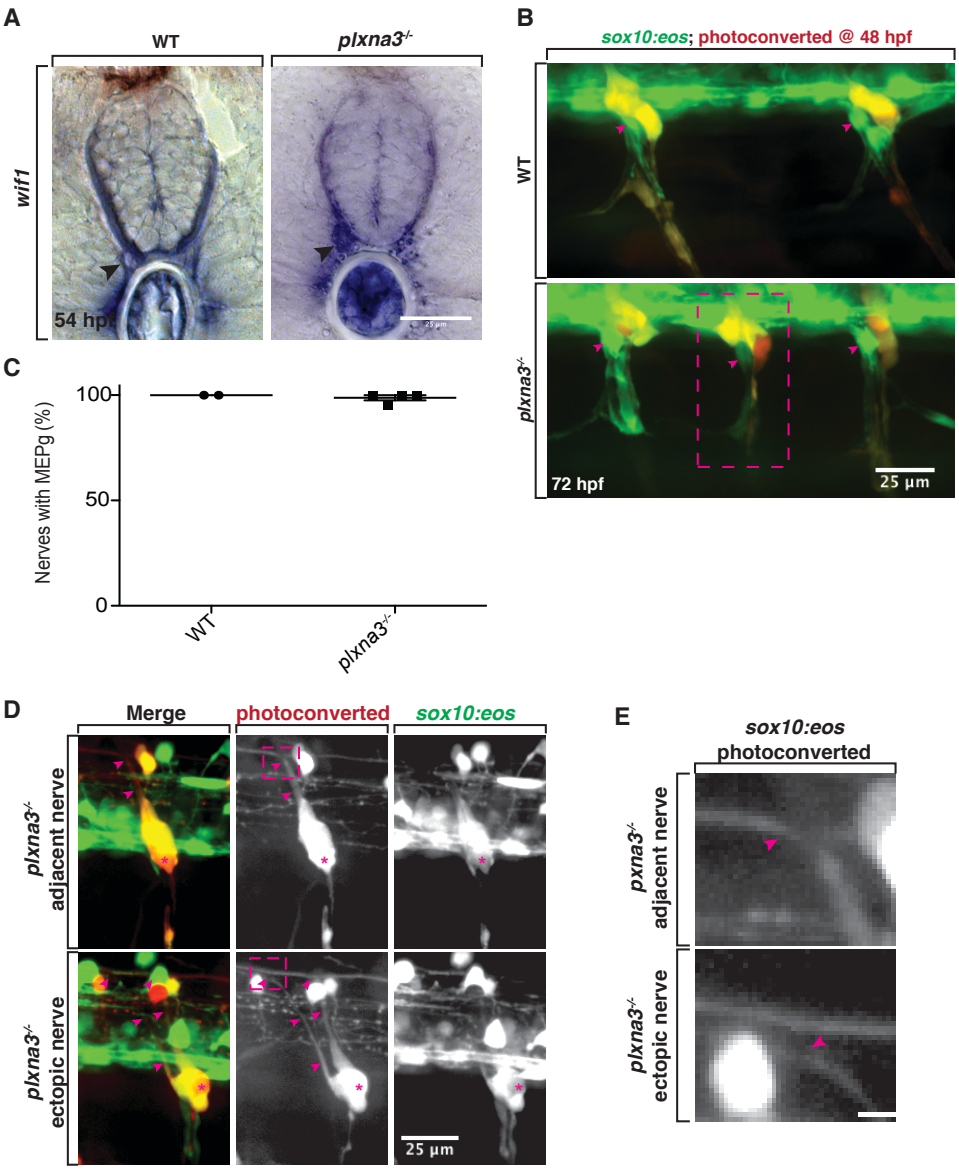

Appendix 1-1 MEP glia, DRGs, and DREZ form at sites of ectopic motor axon exit. (A) *In situ* hybridization for *wif1* showing expression in MEP glia of WT and *plxna3*$^{-/-}$ embryos at 54 hpf. Arrowheads mark MEP glia (B) WT and *plxna3*$^{-/-}$ larvae expressing *sox10:eos* were photoconverted at 48 hpf to identify MEP glia (green, unconverted cells) Arrowheads mark MEP glia. Boxed nerve is an ectopic motor nerve with MEP glia in a *plxna3* mutant larva. (C) Quantification of *eos*$^{+}$ MEP glia in WT and *plxna3*$^{-/-}$ larvae at 72 hpf. Ectopic nerves were included in *plxna3* quantification. (D) Images of adjacent nerves of *plxna3*$^{-/-}$ larvae expressing *sox10:eos* and photoconverted at 48 hpf. Top row is a nerve at the correct, midsegmental level, and bottom row is an additional, ectopic nerve that has formed within the same segment. Asterisks mark photoconverted DRG neurons which have downregulated *sox10* expression, and arrowheads mark central axonal projections from DRG neurons into the dorsal spinal cord. (E) Close up views of the boxed regions in (D), showing where the sensory axonal projection meets the dorsolateral fasciculus inside the spinal cord (arrowheads). Scale bars, 25 µm in A, B, D, 10 µm in E.

also did not observe any peripherally-migrated OPCs. Altogether, my findings that *plxna3*$^{-/-}$ larvae have *wif1*$^{+}$, *sox10*$^{+}$ MEP glia and do not have any peripheral OPC migration suggests that *plxna3* is not involved in positioning of MEP glia or in repelling OPCs from migrating into the PNS. Intriguingly, I observed MEP glia present at ectopic motor axons in *plxna3*$^{-/-}$ larvae (Appendix I-1B). This observation led me to hypothesize that motor axons themselves may initiate signaling to assemble other cellular components of peripheral nerves, regardless of their position. To investigate this possibility more closely, I quantified MEP glia specifically at ectopic motor roots in 72 hpf *plxna3*$^{-/-}$ larvae. MEP glia were present on 9 out of 10 (90%) of ectopic nerves (n = 4 larvae), suggesting that the presence of peripheral motor axons is sufficient to recruit MEP glia to the motor root.

It has previously been described that positional cues within the somatic mesoderm pattern early neural crest migration into streams along the somites (Honjo and Eisen, 2005). However, axonal *neuregulin* guides some migrating neural crest cells to pause and cluster adjacent to the MEP, where the will form the DRG (Honjo et al., 2008). In zebrafish *erbb3*$^{-/-}$ embryos, neural crest cells lack the receptor to detect axonal *neuregulin*, and they migrate past the MEP, never forming DRGs (Honjo et al., 2008). This led me to ask whether ectopic motor axons would recruit migrating neural crest cells to form ectopic DRGs. I imaged *plxna3*$^{-/-}$ larvae expressing *sox10:eos* at 72 hpf to test whether DRGs formed at locations of ectopic motor axon exit. I photoconverted embryos at 48 hpf in order to distinguish neural crest-derived DRGs from MEP glia.

Another benefit of photoconversion is that it can be used to identify differentiated DRG neurons among satellite glia or precursors. Because differentiated DRG neurons downregulate *sox10* expression and only have photoconverted Eos protein, they appear red, whereas satellite glia, which continue to express *sox10*, appear yellow because of the combination of photoconverted red and newly synthesized green Eos. I identified DRGs associated with all ectopic motor nerves in 72 hpf *plxna3*$^{-/-}$ lavae (Appendix I-1D). The ectopic DRGs had differentiated sensory neurons surrounded by satellite glia, and, amazingly, the sensory neuron extended axonal projections centrally toward the spinal cord (Appendix I-1D). A closer examination of the central projections showed that they reached the spinal cord and joined the dorsolateral fasciculus, the correct axonal tract (Appendix I-1E). These results suggest that not only does the location of the MEP determine DRG location, but that MEP location also determines the site of the DREZ. It would be useful to test for more specific markers of sensory neuron differentiation, such as *neurogenin*, as well as perform time lapse imaging of central axon growth along with a transgene labeling radial glia endfeet in order to more precisely visualize the formation of the DREZ associated with ectopic DRGs. Another outstanding question is whether perineurial glia also exit the spinal cord at ectopic MEPs and ensheathe the ectopic motor nerve. It will also be important to repeat these experiments with a different mutant line with ectopic motor axon exit, in order to confirm that ectopic motor axons, not aberrant *plxna3* signaling, are responsible for the phenotypes observed.

I was also interested in the question of how motor neuron cell body migration is restricted during development. In mouse and chick embryos, a population of neural crest-derived BCCs are present at the MEP shortly after motor axon exit (Fraher et al., 2007; Golding and Cohen, 1997; Vermeren et al., 2003). BCCs are necessary to prevent motor neurons cell bodies from migrating out of the spinal cord along their axons, as embryos without ventral BCCs have motor neuron cell bodies ectopically located along peripheral spinal motor roots (Vermeren et al., 2003). Do zebrafish have a similar mechanism for preventing peripheral motor neuron migration? I first attempted to answer this question by looking for BCCs in zebrafish embryos. I performed *in situ* hybridization for zebrafish orthologs of BCC markers on 24 hpf zebrafish embryos, shortly after the first motor axons have emerged from the spinal cord and migrating neural crest cells have reached the MEP. I did not detect expression of any of these markers in cells at the MEP at this stage (Appendix I-2A). However, there was the possibility that if zebrafish have neural crest-derived BCCs, they may express different markers than those identified in other species. I therefore tested whether neural crest-derived cells were required to prevent ectopic motor neuron migration. I analyzed whether motor neurons migrated into the periphery in *mob*$^{-/-}$;*mos*$^{-/-}$ embryos, in which all neural crest specification is blocked (Arduini et al., 2009). At 36 hpf, *mob*$^{-/-}$*mos*$^{-/-}$ embryos did not have any Isl^{+} motor neurons present outside the spinal cord, identical to WT (Appendix I-2B, n = 2). I also did not observe any ectopic Isl^{+} motor neurons at 72 hpf (n = 8). Together, these results strongly argue against neural crest-derived BCCs as a mechanism for restricting peripheral motor neuron migration in zebrafish.

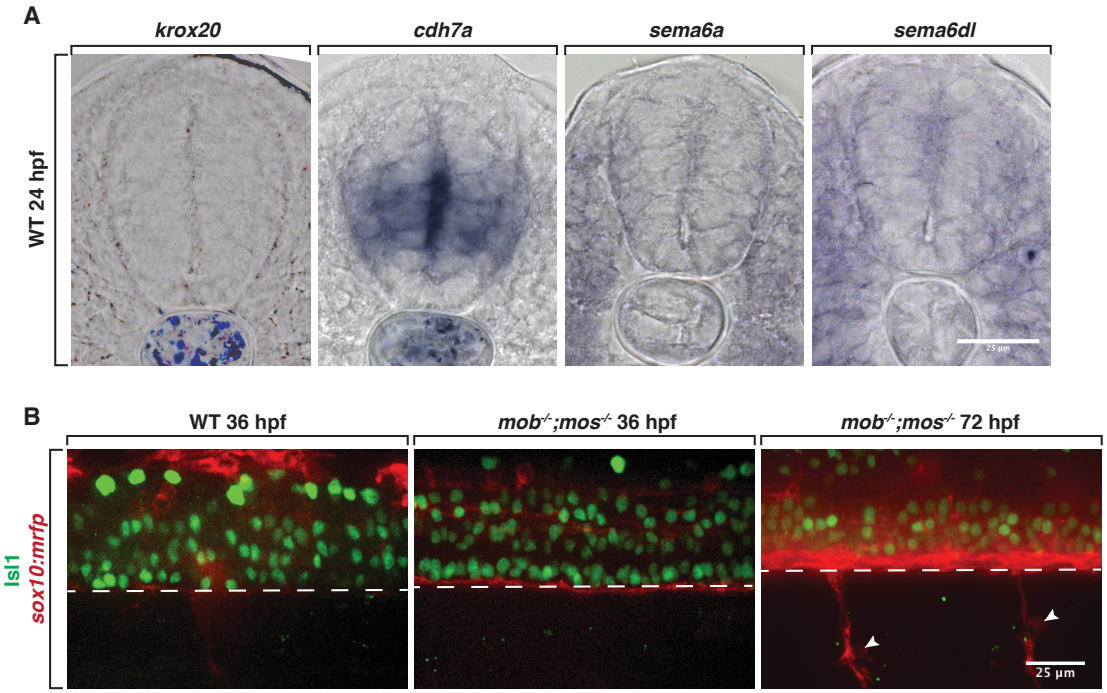

Appendix 1-2 No evidence for neural-crest derivatives restricting motor neuron migration in zebrafish. (A) *In situ* hybridization for zebrafish orthologs for mammalian and chick BCC markers in 24 hpf WT embryos. (B) Isl1/2 antibody labeling to identify any ectopically-migrated motor neurons in WT and *mob*$^{-/-}$;*mos*$^{-/-}$ embryos and larvae. Dashed line marks the ventral boundary of the spinal cord. Arrowheads mark *sox10+*/Isl^{-} OPCs that have migrated onto peripheral nerves in a 72 hpf *mob*$^{-/-}$;*mos*$^{-/-}$ larva. Scale bars, 25 μm

Appendix II Cell migration into the CNS

Most of my research has focused on mechanisms restricting migration of CNS cells out of the spinal cord. However, another question is how migratory PNS glia are prevented from entering the spinal cord. Since MEP glia repel OPCs from exiting the spinal cord, and OPCs and MEP glia derive from the same spinal cord progenitor domain, I initially hypothesized that OPCs might repel migration of PNS cells into the spinal cord. I tested this hypothesis by preventing OPC specification by treating zebrafish embryos beginning at 36 hpf with 100 ng/ml of the drug Trichostatin A (TSA). This HDAC inhibitor has been previously described to prevent OPC specification (Takada and Appel, 2010). I performed time lapse imaging beginning at 48 hpf on TSA-treated larvae expressing *sox10:eos*. During 24 hour time lapse movies, I did not observe any PNS glia migrate into the spinal cord in TSA-treated larvae (Appendix II, n = 6) (Smith et al., 2016). In contrast, ablation of radial glia using selective expression of nitroreductase with metronidazole treatment resulted in significant migration of *sox10+* peripheral glial cells into the spinal cord (Smith et al., 2016). This result is in agreement with experiments in mice showing that radial glia are important for preventing central migration of PNS glia (Zhu et al., 2015). These results suggest that, unlike MEP glia, OPCs do not play a role in gating TZ boundaries.

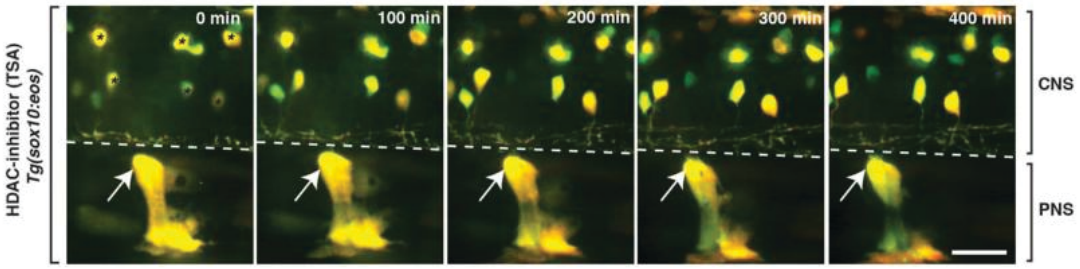

Appendix II OPCs do not restrict PNS glia migration. Images from a 24 hour time-lapse movie starting at 48 hpf of a *sox10:eos* embryo treated with TSA beginning at 36 hpf. Arrows denote PNS glia that do not migrate into the spinal cord. Asterisks indicate Eos^{+} neurons that are labeled by *sox10:eos*. Dashed lines denote the boundary of spinal cord. Scale bars, 25 μm. From Smith et al. Glia, 2016.

Appendix III

List of abbreviations

Abbreviations are listed in alphabetical order. For transgene abbreviations and mutant lines, refer to Table 2-1 on page 28

4-AP	4-aminopyridine
A1	adenosine receptor subtype
A2a	adenosine receptor subtype
A2b	adenosine receptor subtype
A3	adenosine receptor subtype
ADP	adenosine diphosphate
AMP	adenosine monophosphate
AR	adenosine receptor
ATP	adenosine triphosphate
BCC	boundary cap cell
bp	base pair
cAMP	cyclic AMP
CMR	contact-mediated repulsion
CNS	central nervous system
CPT	8-cyclopentyltheophylline
CRISPR	clustered regularly interspaced short palindromic repeats
dhh	*desert hedgehog*
DMSO	dimethyl sulfoxide
dpf	days post fertilization
DREZ	dorsal root entry zone
egr2	*early growth response 2*
enpp	*ectonucleotide pyrophosphatase/phosphodiesterase*
entpd	*ectonucleoside triphosphate diphosphohydrolase*
EPSC	exitatory post synaptic current
erbb2	*erb-b2 receptor tyrosine kinase 2*
erbb3	*erb-b2 receptor tyrosine kinase 3*
foxd3	*forkhead box D3*
gfap	*glial fibrillary acidic protein*
gpr126	*g protein coupled receptor 126*
hpf	hours post fertilization
Isl	Islet
LOPAC®^{1280}	Library of Pharmacologically Active Compounds®^{1280}
mbp	*myelin basic protein*
MEP	motor exit point
MO	*morpholino oligonucleotide*

mog	*myelin oligodendrocyte glycoprotein*
mpz	*myelin protein zero,* also called *P0*
nkx2.2	*NK2 homeobox 2*
NMJ	neuromuscular junction
nrg1	*neuregulin 1*
nrp1a	*neuropilin1a*
OL	differentiated oligodendrocyte
olig2	*oligodendrocyte transcription factor 2*
OPC	oligodendrocyte progenitor cell
P1	class of adenosine receptors
P2X	ionotropic ATP and/or ADP receptor
P2Y	metabotropic ATP and/or ADP receptor
PFA	paraformaldehyde
PG	*perineurial glia*
plp	*proteolipid protein*
plxna3	*plexina3*
pMN	spinal cord motor neuron and OPC progenitor domain
pmp22	*peripheral myelin protein 22*
PNS	peripheral nervous system
pou3f1	*POU class 3 homeobox 1*
PTU	phenylthiourea
PTZ	pentylenetetrazole
ROI	region of interest
s100	*S100 calcium binding protein*
SC	Schwann cell
SCH-red	fluorescently-tagged A2a antagonist SCH-58261
SCP	*Schwann cell precursor*
sema3ab	*semaphorin3ab*
sema6a	*semaphorin6a*
sema6d	*semaphorin6d*
shh	*sonic hedgehog*
slc45a2	*solute carrier family 45 member 2*
sox10	*SRY (sex determining region Y)-box 10*
TALEN	transcription activator-like effector nuclease
TEM	transmision electron microscopy
TeNT	*tetanus neurotoxin*
tfap2a	*transcription factor AP-2 alpha*
TSA	*Trichostatin A*
TTX	tetrodotoxin
tyr	*tyrosinase*
TZ	transition zone
UV	ultraviolet light
VAAC	volume activated anion channel

wif1	*WNT inhibitory factor 1*
WT	wild type

References

Abbracchio, M., Burnstock, G., Verkhratsky, A., and Zimmermann, H. (2009). Purinergic signalling in the nervous system: an overview. Trends in Neurosciences *32*, 19–29.

Abbracchio, M.P., Burnstock, G., Boeynaems, J.-M.M., Barnard, E.A., Boyer, J.L.L., Kennedy, C., Knight, G.E., Fumagalli, M., Gachet, C., Jacobson, K.A., et al. (2006). International Union of Pharmacology LVIII: update on the P2Y G protein-coupled nucleotide receptors: from molecular mechanisms and pathophysiology to therapy. Pharmacological Reviews *58*, 281–341.

Ackerman, S.D., Garcia, C., Piao, X., Gutmann, D.H., and Monk, K.R. (2015). The adhesion GPCR Gpr56 regulates oligodendrocyte development via interactions with Gα12/13 and RhoA. Nat Commun *6*, 6122.

Agresti, C., Meomartini, M.E., Amadio, S., Ambrosini, E., Serafini, B., Franchini, L., Volonté, C., Aloisi, F., and Visentin, S. (2005). Metabotropic P2 receptor activation regulates oligodendrocyte progenitor migration and development. Glia *50*, 132–144.

Almeida, R., and Lyons, D. (2016). Oligodendrocyte Development in the Absence of Their Target Axons In Vivo. PLoS ONE *11*, e0164432.

Almeida, R., and Lyons, D. (2017). On Myelinated Axon Plasticity and Neuronal Circuit Formation and Function. The Journal of Neuroscience *37*, 10023–10034.

Almeida, R.G., Czopka, T., Ffrench-Constant, C., and Lyons, D.A. (2011). Individual axons regulate the myelinating potential of single oligodendrocytes in vivo. Development

138, 4443–4450.

Andersson, O., Adams, B.A., Yoo, D., Ellis, G.C., Gut, P., Anderson, R.M., German, M.S., and Stainier, D.Y. (2012). Adenosine signaling promotes regeneration of pancreatic β cells in vivo. Cell Metab. *15*, 885–894.

Arduini, B.L., Bosse, K.M., and Henion, P.D. (2009). Genetic ablation of neural crest cell diversification. Development *136*, 1987–1994.

Arrigoni, E., Rainnie, D., McCarley, R., and Greene, R. (2001). Adenosine-mediated presynaptic modulation of glutamatergic transmission in the laterodorsal tegmentum. The Journal of Neuroscience *21*, 1076–1085.

Bannon, N., Zhang, P., Ilin, V., Chistiakova, M., and Volgushev, M. (2014). Modulation of synaptic transmission by adenosine in layer 2/3 of the rat visual cortex in vitro. Neuroscience *260*, 171–184.

Barrallo-Gimeno, A., Holzschuh, J., Driever, W., and Knapik, E.W. (2004). Neural crest survival and differentiation in zebrafish depends on mont blanc/tfap2a gene function. Development *131*, 1463–1477.

Barres, B.A., and Raff, M.C. (1993). Proliferation of oligodendrocyte precursor cells depends on electrical activity in axons. Nature *361*, 258–260.

Barres, B., Koroshetz, W., Swartz, K., Chun, L., and Corey, D. (1990). Ion channel expression by white matter glia: The O-2A glial progenitor cell. Neuron *4*, 507–524.

Berger, T. (1995). AMPA-type glutamate receptors in glial precursor cells of the rat corpus callosum: Ionic and pharmacological properties. Glia *14*, 101–114.

Bergles, D.E., and Richardson, W.D. (2015). Oligodendrocyte Development and Plasticity. Cold Spring Harb Perspect Biol *8*, a020453.

Bergles, D.E., Jabs, R., and Steinhäuser, C. (2010). Neuron-glia synapses in the brain. Brain Res Rev *63*, 130–137.

Bergles, D.E., Roberts, J.D., Somogyi, P., and Jahr, C.E. (2000). Glutamatergic synapses on oligodendrocyte precursor cells in the hippocampus. Nature *405*, 187–191.

De Biase, L.M., Nishiyama, A., and Bergles, D.E. (2010). Excitability and synaptic communication within the oligodendrocyte lineage. The Journal of Neuroscience *30*, 3600–3611.

Binari, L.A., Lewis, G.M., and Kucenas, S. (2013). Perineurial glia require Notch signaling during motor nerve development but not regeneration. The Journal of Neuroscience *33*, 4241–4252.

Birey, Kokkosis, and Aguirre (2017). Oligodendroglia-lineage cells in brain plasticity, homeostasis and psychiatric disorders. Curr Opin Neurobiol *47*, 93–103.

Boch, J., Scholze, H., Schornack, S., Landgraf, A., Hahn, S., Kay, S., Lahaye, T., Nickstadt, A., and Bonas, U. (2009). Breaking the code of DNA binding specificity of TAL-type III effectors. Science (New York, N.Y.) *326*, 1509–1512.

Boehmler, W., Petko, J., Woll, M., Frey, C., Thisse, B., Thisse, C., Canfield, V.A., and Levenson, R. (2009). Identification of zebrafish A2 adenosine receptors and expression in developing embryos. Gene Expression Patterns *9*, 144–151.

Bonanomi, D., and Pfaff, S.L. (2010). Motor Axon Pathfinding. Cold Spring Harbor Perspectives in Biology *2*, a001735.

Boué-Grabot, E., and Pankratov, Y. (2017). Modulation of Central Synapses by Astrocyte-Released ATP and Postsynaptic P2X Receptors. Neural Plasticity.

Bravo-Ambrosio, A., and Kaprielian, Z. (2011). Crossing the border: molecular control of motor axon exit. Int J Mol Sci *12*, 8539–8561.

Brinkmann, B.G., Agarwal, A., Sereda, M.W., Garratt, A.N., Müller, T., Wende, H., Stassart, R.M., Nawaz, S., Humml, C., Velanac, V., et al. (2008). Neuregulin-1/ErbB signaling serves distinct functions in myelination of the peripheral and central nervous system. Neuron *59*, 581–595.

Britsch, S., Goerich, D.E., Riethmacher, D., Peirano, R.I., Rossner, M., Nave, K.A., Birchmeier, C., and Wegner, M. (2001). The transcription factor Sox10 is a key regulator of peripheral glial development. Genes Dev. *15*, 66–78.

Bron, R., Vermeren, M., Kokot, N., Andrews, W., Little, G.E., Mitchell, K.J., and Cohen, J. (2007). Boundary cap cells constrain spinal motor neuron somal migration at motor exit points by a semaphorin-plexin mechanism. Neural Dev *2*, 21.

Burnstock, G. (1972). Purinergic nerves. Pharmacological Reviews *24*, 509–581.

Burnstock, G. (1999). Release of vasoactive substances from endothelial cells by shear stress and purinergic mechanosensory transduction. Journal of Anatomy *194*, 335–342.

Burnstock, G. (2013). Introduction to purinergic signalling in the brain. Advances in Experimental Medicine and Biology *986*.

Burnstock, G., and Knight, G.E. (2004). Cellular distribution and functions of P2 receptor subtypes in different systems. International Review of Cytology *240*, 31–304.

Carlsen, E., and Perrier, J. (2014). Purines released from astrocytes inhibit excitatory synaptic transmission in the ventral horn of the spinal cord. Frontiers in Neural Circuits *8*.

Carpenter, B., Nehmé, R., Warne, T., Leslie, A.G., and Tate, C.G. (2016). Structure of the adenosine A2A receptor bound to an engineered G protein. Nature *536*, 104–107.

Casano, A.M., Albert, M., and Peri, F. (2016). Developmental Apoptosis Mediates Entry and Positioning of Microglia in the Zebrafish Brain. Cell Reports *16*, 897–906.

Cheli, V., González, D., Spreuer, V., and Paez (2015). Voltage-gated Ca++ entry promotes oligodendrocyte progenitor cell maturation and myelination in vitro. Experimental Neurology *265*, 69–83.

Chen, J.-F., Lee, C., and Chern, Y. (2014). Adenosine Receptor Neurobiology: Overview. International Review of Neurobiology *119*, 1–49.

Chen, J.F., Huang, Z., Ma, J., Zhu, J., Moratalla, R., Standaert, D., Moskowitz, M.A., Fink, J.S., and Schwarzschild, M.A. (1999). A(2A) adenosine receptor deficiency

attenuates brain injury induced by transient focal ischemia in mice. The Journal of Neuroscience *19*, 9192–9200.

Ciruela, F., Casadó, V., Rodrigues, R.J., Luján, R., Burgueño, J., Canals, M., Borycz, J., Rebola, N., Goldberg, S.R., Mallol, J., et al. (2006). Presynaptic control of striatal glutamatergic neurotransmission by adenosine A1-A2A receptor heteromers. The Journal of Neuroscience *26*, 2080–2087.

Ciruela, F., Fernández-Dueñas, V., and Jacobson, K.A. (2015). Lighting up G protein-coupled purinergic receptors with engineered fluorescent ligands. Neuropharmacology *98*, 58–67.

Clark, J.K., O'keefe, A., Mastracci, T.L., Sussel, L., Matise, M.P., and Kucenas, S. (2014). Mammalian Nkx2.2+ perineurial glia are essential for motor nerve development. Developmental Dynamics *243*, 1116–1129.

Coppi, E., Cellai, L., Maraula, G., Pugliese, A.M., and Pedata, F. (2013). Adenosine A_2A receptors inhibit delayed rectifier potassium currents and cell differentiation in primary purified oligodendrocyte cultures. Neuropharmacology *73*, 301–310.

Coppi, E., Cellai, L., Maraula, G., Dettori, I., Melani, A., Pugliese, A.M., and Pedata, F. (2015). Role of adenosine in oligodendrocyte precursor maturation. Front Cell Neurosci *9*, 155.

Coulpier, F., Le Crom, S., Maro, G.S., Manent, J., Giovannini, M., Maciorowski, Z., Fischer, A., Gessler, M., Charnay, P., and Topilko, P. (2009). Novel features of

boundary cap cells revealed by the analysis of newly identified molecular markers. Glia *57*, 1450–1457.

Coulpier, F., Decker, L., Funalot, B., Vallat, J.-M., Garcia-Bragado, F., Charnay, P., and Topilko, P. (2010). CNS/PNS Boundary Transgression by Central Glia in the Absence of Schwann Cells or Krox20/Egr2 Function. The Journal of Neuroscience *30*, 5958–5967.

Cunha, R. (2001). Adenosine as a neuromodulator and as a homeostatic regulator in the nervous system: different roles, different sources and different receptors. Neurochemistry International *38*, 107–125.

Czopka, T., Ffrench-Constant, C., and Lyons, D.A. (2013). Individual oligodendrocytes have only a few hours in which to generate new myelin sheaths in vivo. Dev. Cell *25*, 599–609.

Davalos, D., Grutzendler, J., Yang, G., Kim, J.V., Zuo, Y., Jung, S., Littman, D.R., Dustin, M.L., and Gan, W.-B.B. (2005). ATP mediates rapid microglial response to local brain injury in vivo. Nature Neuroscience *8*, 752–758.

Dennis, J., Morgan, M., Graf, M., and Fuss, B. (2012). P2Y12 receptor expression is a critical determinant of functional responsiveness to ATX's MORFO domain. Purinergic Signalling *8*, 181–190.

Deuchars, S., Brooke, R., and Deuchars, J. (2001). Adenosine A1 receptors reduce release from excitatory but not inhibitory synaptic inputs onto lateral horn neurons. The Journal of Neuroscience *21*, 6308–6320.

Dias, R., Ribeiro, J., and Sebastião, A. (2012). Enhancement of AMPA currents and GluR1 membrane expression through PKA-coupled adenosine A2A receptors. Hippocampus *22*, 276–291.

Dunwiddie, T.V., and Masino, S.A. (2001). The role and regulation of adenosine in the central nervous system. Annual Review of Neuroscience *24*, 31–55.

Dutton, K.A., Pauliny, A., Lopes, S.S., Elworthy, S., Carney, T.J., Rauch, J., Geisler, R., Haffter, P., and Kelsh, R.N. (2001). Zebrafish colourless encodes sox10 and specifies non-ectomesenchymal neural crest fates. Development *128*, 4113–4125.

Edstrom, A., Edbladh, M., and Ekstrom, P. (1992). Adenosine inhibition of the regeneration in vitro of adult frog sciatic sensory axons. Brain Research *570*, 35–41.

Edwards, F.A., Gibb, A.J., and Colquhoun, D. (1992). ATP receptor-mediated synaptic currents in the central nervous system. Nature *359*, 144–147.

Elliott, M., Chekeni, F., Trampont, P., Lazarowski, Kadl, A., Walk, S., Park, D., Woodson, R., Ostankovich, M., Sharma, P., et al. (2009). Nucleotides released by apoptotic cells act as a find-me signal to promote phagocytic clearance. Nature *461*, 282–286.

Emery, B., and Lu, R.Q. (2015). Transcriptional and epigenetic regulation of oligodendrocyte development and myelination in the central nervous system. Cold Spring Harb Perspect Biol *7*, a020461.

Etxeberria, A., Hokanson, K.C., Dao, D.Q., Mayoral, S.R., Mei, F., Redmond, S.A., Ullian, E.M., and Chan, J.R. (2016). Dynamic Modulation of Myelination in Response to

Visual Stimuli Alters Optic Nerve Conduction Velocity. The Journal of Neuroscience *36*, 6937–6948.

Feldner, J., Becker, T., Goishi, K., Schweitzer, J., Lee, P., Schachner, M., Klagsbrun, M., and Becker, C.G. (2005). Neuropilin-1a is involved in trunk motor axon outgrowth in embryonic zebrafish. Developmental Dynamics *234*, 535–549.

Feldner, J., Reimer, M.M., Schweitzer, J., Wendik, B., Meyer, D., Becker, T., and Becker, C.G. (2007). PlexinA3 restricts spinal exit points and branching of trunk motor nerves in embryonic zebrafish. The Journal of Neuroscience *27*, 4978–4983.

Fields, R.D. (2015). A new mechanism of nervous system plasticity: activity-dependent myelination. Nature Reviews. Neuroscience *16*, 756–767.

Fields, D.R., and Burnstock, G. (2006). Purinergic signalling in neuron–glia interactions. Nature Reviews Neuroscience *7*, 423–436.

Fields, R., and Ni, Y. (2010). Nonsynaptic communication through ATP release from volume-activated anion channels in axons. Science Signaling *3*.

Fields, R.D., and Stevens, B. (2000). ATP: an extracellular signaling molecule between neurons and glia. Trends in Neurosciences *23*, 625–633.

Fontenas, L., and Kucenas, S. (2017). Livin' On The Edge: glia shape nervous system transition zones. Curr. Opin. Neurobiol. *47*, 44–51.

Fontenas, L., Santis, F., Donato, V., Degerny, C., Chambraud, B., Bene, F., and Tawk,

M. (2016). Neuronal Ndrg4 Is Essential for Nodes of Ranvier Organization in Zebrafish. PLOS Genetics *12*, e1006459.

Fraher, J.P. (1978). The maturation of the ventral root-spinal cord transitional zone. An ultrastructural study. J. Neurol. Sci. *36*, 427–449.

Fraher, J.P. (1992). The CNS-PNS transitional zone of the rat. Morphometric studies at cranial and spinal levels. Prog. Neurobiol. *38*, 261–316.

Fraher, J.P. (1997). Axon-glial relationships in early CNS-PNS transitional zone development: an ultrastructural study. Journal of Neurocytology *26*, 41–52.

Fraher, J.P., and Kaar, G.F. (1984). The transitional node of Ranvier at the junction of the central and peripheral nervous systems: an ultrastructural study of its development and mature form. J. Anat. *139 (Pt 2)*, 215–238.

Fraher, J.P., Dockery, P., O'Donoghue, O., Riedewald, B., and O'Leary, D. (2007). Initial motor axon outgrowth from the developing central nervous system. J. Anat. *211*, 600–611.

Fredholm, B., Arslan, G., Halldner, L., Kull, B., Schulte, G., and Wasserman, W. (2000). Structure and function of adenosine receptors and their genes. Naunyn-Schmiedeberg's Archives of Pharmacology 364–374.

Fröb, F., Bremer, M., Finzsch, M., Kichko, T., Reeh, P., Tamm, E., Charnay, P., and Wegner, M. (2012). Establishment of myelinating schwann cells and barrier integrity between central and peripheral nervous systems depend on Sox10. Glia *60*, 806–819.

Fu, H., Qi, Y., Tan, M., Cai, J., Takebayashi, H., Nakafuku, M., Richardson, W., and Qiu, M. (2002). Dual origin of spinal oligodendrocyte progenitors and evidence for the cooperative role of Olig2 and Nkx2.2 in the control of oligodendrocyte differentiation. Development *129*, 681–693.

Gagnon, J.A., Valen, E., Thyme, S.B., Huang, P., Akhmetova, L., Ahkmetova, L., Pauli, A., Montague, T.G., Zimmerman, S., Richter, C., et al. (2014). Efficient mutagenesis by Cas9 protein-mediated oligonucleotide insertion and large-scale assessment of single-guide RNAs. PloS One *9*, e98186.

Gallo, V., Zhou, J.M., McBain, C.J., Wright, P., Knutson, P.L., and Armstrong, R.C. (1996). Oligodendrocyte progenitor cell proliferation and lineage progression are regulated by glutamate receptor-mediated K+ channel block. The Journal of Neuroscience *16*, 2659–2670.

Gallo, V., Mangin, J.-M.M., Kukley, M., and Dietrich, D. (2008). Synapses on NG2-expressing progenitors in the brain: multiple functions? The Journal of Physiology *586*, 3767–3781.

Garratt, A.N., Britsch, S., and Birchmeier, C. (2000). Neuregulin, a factor with many functions in the life of a schwann cell. BioEssays *22*, 987–996.

Gibson, E., Purger, D., Mount, C., Goldstein, A., Lin, G., Wood, L., Inema, I., Miller, S., Bieri, G., Zuchero, J.B., et al. (2014). Neuronal Activity Promotes Oligodendrogenesis and Adaptive Myelination in the Mammalian Brain. Science *344*, 1252304.

Golder, F., Ranganathan, L., Satriotomo, I., Hoffman, M., Lovett-Barr, M., Watters, J., Baker-Herman, T., and Mitchell, G. (2008). Spinal Adenosine A2a Receptor Activation Elicits Long-Lasting Phrenic Motor Facilitation. Journal of Neuroscience *28*, 2033–2042.

Golding, J.P., and Cohen, J. (1997). Border controls at the mammalian spinal cord: late-surviving neural crest boundary cap cells at dorsal root entry sites may regulate sensory afferent ingrowth and entry zone morphogenesis. Mol. Cell. Neurosci. *9*, 381–396.

Goujon, M., McWilliam, H., Li, W., Valentin, F., Squizzato, S., Paren, J., and Lopez, R. (2010). A new bioinformatics analysis tools framework at EMBL–EBI. Nucleic Acids Research *38*, W695–W699.

Gudz, T.I., Komuro, H., and Macklin, W.B. (2006). Glutamate stimulates oligodendrocyte progenitor migration mediated via an alphav integrin/myelin proteolipid protein complex. The Journal of Neuroscience *26*, 2458–2466.

Gundlfinger, A., Bischofberger, J., Johenning, F., Torvinen, M., Schmitz, D., and Breustedt, J. (2007). Adenosine modulates transmission at the hippocampal mossy fibre synapse via direct inhibition of presynaptic calcium channels. The Journal of Physiology *582*, 263–277.

Haas, J., Frese, K.S., Park, Y.J., Keller, A., Vogel, B., Lindroth, A.M., Weichenhan, D., Franke, J., Fischer, S., Bauer, A., et al. (2013). Alterations in cardiac DNA methylation in human dilated cardiomyopathy. EMBO Mol Med *5*, 413–429.

Hargus, N., Bertram, E., and Patel, M. (2009). Adenosine A1 receptors presynaptically

modulate excitatory synaptic input onto subiculum neurons. Brian Research *1280*, 60–68.

Hawryluk, J., Ferrari, L., Keating, S., and Arrigoni, E. (2012). Adenosine inhibits glutamatergic input to basal forebrain cholinergic neurons. Journal of Neurophysiology *107*, 2769–2781.

Hewitt, J.E., Davies, K., Patton, B.L., Uncini, A., Wrabetz, L., and Feltri, L.M. (2009). A laminin-2, dystroglycan, utrophin axis is required for compartmentalization and elongation of myelin segments. Journal of Neuroscience *29*, 3908–3919.

Hines, J.H., Ravanelli, A.M., Schwindt, R., Scott, E.K., and Appel, B. (2015). Neuronal activity biases axon selection for myelination in vivo. Nature Neuroscience *18*, 683–689.

Hochgreb-Hägele, T., and Bronner, M.E. (2012). A novel FoxD3 gene trap line reveals neural crest precursor movement and a role for FoxD3 in their specification. Developmental Biology *374*, 1–11.

Holton, F.A., and Holton, P. (1954). The capillary dilator substances in dry powders of spinal roots; a possible role of adenosine triphosphate in chemical transmission from nerve endings. The Journal of Physiology *126*, 124–140.

Honjo, Y., and Eisen, J.S. (2005). Slow muscle regulates the pattern of trunk neural crest migration in zebrafish. Development *132*, 4461–4470.

Honjo, Y., Kniss, J., and Eisen, J.S. (2008). Neuregulin-mediated ErbB3 signaling is required for formation of zebrafish dorsal root ganglion neurons. Development

(Cambridge, England) *135*, 2615–2625.

Huang, P., Xiao, A., Zhou, M., Zhu, Z., Lin, S., and Zhang, B. (2011). Heritable gene targeting in zebrafish using customized TALENs. Nat. Biotechnol. *29*, 699–700.

Hughes, E., Kang, S., Fukaya, M., and Bergles, D. (2013). Oligodendrocyte progenitors balance growth with self-repulsion to achieve homeostasis in the adult brain. Naute Neuroscience *16*, 668–676.

Irion, U., Krauss, J., and Nüsslein-Volhard, C. (2014). Precise and efficient genome editing in zebrafish using the CRISPR/Cas9 system. Development *141*, 4827–4830.

Jao, L.-E.E., Wente, S.R., and Chen, W. (2013). Efficient multiplex biallelic zebrafish genome editing using a CRISPR nuclease system. Proc. Natl. Acad. Sci. U.S.A.

Jarvis, M., and Williams, M. (1989). Direct autoradiographic localization of adenosine A2 receptors in the rat brain using the A2-selective agonist,[3H] CGS 21680. Eur J Pharmacol *168*, 243–246.

Jessen, K.R. (2004). Glial cells. The International Journal of Biochemistry & Cell Biology *36*, 1861–1867.

Jessen, K.R., and Mirsky, R. (2002). Signals that determine Schwann cell identity. J. Anat. *200*, 367–376.

Jiang, J.L., van Rhee, A.M., Melman, N., Ji, X.D., and Jacobson, K.A. (1996). 6-phenyl-1,4-dihydropyridine derivatives as potent and selective A3 adenosine receptor

antagonists. J. Med. Chem. *39*, 4667–4675.

Keuerleber, S., Gsandtner, I., and Freissmuth, M. (2010). From cradle to twilight: The carboxyl terminus directs the fate of the A2A-adenosine receptor. Biochimica et Biophysica Acta (BBA) - Biomembranes *1808*.

Kim, H., Shin, J., Kim, S., Poling, J., Park, H.-C.C., and Appel, B. (2008). Notch-regulated oligodendrocyte specification from radial glia in the spinal cord of zebrafish embryos. Developmental Dynamics *237*, 2081–2089.

Kim, M., Fontelonga, T.M., Lee, C.H., Barnum, S.J., and Mastick, G.S. (2017). Motor axons are guided to exit points in the spinal cord by Slit and Netrin signals. Developmental Biology *432*, 178–191.

Kimmel, C.B., Ballard, W.W., Kimmel, S.R., Ullmann, B., and Schilling, T.F. (1995). Stages of embryonic development of the zebrafish. Developmental Dynamics *203*, 253–310.

Kirby, B., N, Latimer, A., Shin, J., Carney, T., Kelsh, R., and Appel, B. (2006). In vivo time-lapse imaging shows dynamic oligodendrocyte progenitor behavior during zebrafish development. Nat. Neurosci. *9*, 1506–1511.

Koudelka, S., Voas, M.G., Almeida, R.G., Baraban, M., Soetaert, J., Meyer, M.P., Talbot, W.S., and Lyons, D.A. (2016). Individual Neuronal Subtypes Exhibit Diversity in CNS Myelination Mediated by Synaptic Vesicle Release. Current Biology *26*, 1447–1455.

Kriegler, S., and Chiu, S.Y. (1993). Calcium signaling of glial cells along mammalian

axons. The Journal of Neuroscience *13*, 4229–4245.

Kucenas, S., Snell, H., and Appel, B. (2008a). nkx2.2a promotes specification and differentiation of a myelinating subset of oligodendrocyte lineage cells in zebrafish. Neuron Glia Biology *4*, 71–81.

Kucenas, S., Takada, N., Park, H.-C.C., Woodruff, E., Broadie, K., and Appel, B. (2008b). CNS-derived glia ensheath peripheral nerves and mediate motor root development. Nat. Neurosci. *11*, 143–151.

Kucenas, S., Wang, W., Knapik, E., and Appel, B. (2009). A selective glial barrier at motor axon exit points prevents oligodendrocyte migration from the spinal cord. Journal of Neuroscience *29*, 15187–15194.

Kukley, M., Capetillo-Zarate, E., and Dietrich, D. (2007). Vesicular glutamate release from axons in white matter. Nature Neuroscience *10*, 311–320.

Lee, S., Leach, M., Redmond, S., Chong, S., Mellon, S., Tuck, S., Feng, Z., Corey, J., and Chan, J. (2012). A culture system to study oligodendrocyte myelination processes using engineered nanofibers. Nature Methods *9*.

Lemus, H., Warrington, A., and Rodriguez, M. (2018). Multiple Sclerosis: Mechanisms of Disease and Strategies for Myelin and Axonal Repair. Neurol Clin *36*, 1–11.

De Lera Ruiz, M., Lim, Y.-H.H., and Zheng, J. (2014). Adenosine A2A receptor as a drug discovery target. Journal of Medicinal Chemistry *57*, 3623–3650.

Lewis, K.E., and Eisen, J.S. (2003). From cells to circuits: development of the zebrafish spinal cord. Prog. Neurobiol. *69*, 419–449.

Lieberam, I., Agalliu, D., Nagasawa, T., Ericson, J., and Jessell, T.M. (2005). A Cxcl12-CXCR4 chemokine signaling pathway defines the initial trajectory of mammalian motor axons. Neuron *47*, 667–679.

Lin, S.-C.C., and Bergles, D.E. (2004a). Synaptic signaling between neurons and glia. Glia *47*, 290–298.

Lin, S.C., and Bergles, D.E. (2004b). Synaptic signaling between GABAergic interneurons and oligodendrocyte precursor cells in the hippocampus. Nature Neuroscience *7*, 24–32.

Lin, S.-C.C., Huck, J.H., Roberts, J.D., Macklin, W.B., Somogyi, P., and Bergles, D.E. (2005). Climbing fiber innervation of NG2-expressing glia in the mammalian cerebellum. Neuron *46*, 773–785.

Lopes, L.V., Cunha, R.A., Kull, B., Fredholm, B.B., and Ribeiro, J.A. (2002). Adenosine A(2A) receptor facilitation of hippocampal synaptic transmission is dependent on tonic A(1) receptor inhibition. Neuroscience *112*, 319–329.

Lyons, D.A., Pogoda, H.-M.M., Voas, M.G., Woods, I.G., Diamond, B., Nix, R., Arana, N., Jacobs, J., and Talbot, W.S. (2005). erbb3 and erbb2 are essential for schwann cell migration and myelination in zebrafish. Current Biology *15*, 513–524.

Makinodan, M., Rosen, K., Ito, S., and Corfas, G. (2012). A critical period for social

experience–dependent oligodendrocyte maturation and myelination. Science *337*, 1357–1360.

Mangin, J., Kunze, A., Chittajallu, R., and Gallo, V. (2008). Satellite NG2 progenitor cells share common glutamatergic inputs with associated interneurons in the mouse dentate gyrus. The Journal of Neuroscience *28*, 7610–7623.

Mangin, J.-M.M., Li, P., Scafidi, J., and Gallo, V. (2012). Experience-dependent regulation of NG2 progenitors in the developing barrel cortex. Nature Neuroscience *15*, 1192–1194.

Mauti, O., Domanitskaya, E., Andermatt, I., Sadhu, R., and Stoeckli, E.T. (2007). Semaphorin6A acts as a gate keeper between the central and the peripheral nervous system. Neural Development *2*.

McGraw, H.F., Nechiporuk, A., and Raible, D.W. (2008). Zebrafish dorsal root ganglia neural precursor cells adopt a glial fate in the absence of neurogenin1. The Journal of Neuroscience *28*, 12558–12569.

McGraw, H.F., Snelson, C.D., Prendergast, A., Suli, A., and Raible, D.W. (2012). Postembryonic neuronal addition in zebrafish dorsal root ganglia is regulated by Notch signaling. Neural Dev *7*, 23.

Meijering, E., Dzyubachyk, O., and Smal, I. (2012). Methods for Cell and Particle Tracking. Methods Enzymol *504*, 183–200.

Melani, A., Corti, F., Cellai, L., Vannucchi, M., and Pedata, F. (2014). Low doses of the

selective adenosine A2A receptor agonist CGS21680 are protective in a rat model of transient cerebral ischemia. Brain Res *1551*, 59–72.

Mensch, S., Baraban, M., Almeida, R., Czopka, T., Ausborn, J., El Manira, A., and Lyons, D.A. (2015). Synaptic vesicle release regulates myelin sheath number of individual oligodendrocytes in vivo. Nat. Neurosci. *18*, 628–630.

Meyer, D., Yamaai, T., Garratt, A., Riethmacher-Sonnenberg, E., Kane, D., Theill, L.E., and Birchmeier, C. (1997). Isoform-specific expression and function of neuregulin. Development *124*, 3575–3586.

Miller, R. (2002). Regulation of oligodendrocyte development in the vertebrate CNS. Prog. Neurobiol. *67*, 451–467.

Milojević, T., Reiterer, V., Stefan, E., Korkhov, V., Dorostkar, M., Ducza, E., Ogris, E., Boehm, S., Freissmuth, M., and Nanoff, C. (2006). The Ubiquitin-Specific Protease Usp4 Regulates the Cell Surface Level of the A2a Receptor. Mol Pharmacol *69*, 1083–1094.

Monk, K.R., Naylor, S.G., Glenn, T.D., Mercurio, S., Perlin, J.R., Dominguez, C., Moens, C.B., and Talbot, W.S. (2009). A G protein-coupled receptor is essential for Schwann cells to initiate myelination. Science *325*, 1402–1405.

Monk, K.R., Oshima, K., Jörs, S., Heller, S., and Talbot, W.S. (2011). Gpr126 is essential for peripheral nerve development and myelination in mammals. Development *138*, 2673–2680.

Montero-Balaguer, M., Lang, M.R., Sachdev, S.W., Knappmeyer, C., Stewart, R.A., De La Guardia, A., Hatzopoulos, A.K., and Knapik, E.W. (2006). The mother superior mutation ablates foxd3 activity in neural crest progenitor cells and depletes neural crest derivatives in zebrafish. Developmental Dynamics *235*, 3199–3212.

Morris, A.D., Lewis, G.M., and Kucenas, S. (2017). Perineurial Glial Plasticity and the Role of TGF-β in the Development of the Blood-Nerve Barrier. Journal of Neuroscience *37*, 4790–4807.

Moscou, M.J., and Bogdanove, A.J. (2009). A simple cipher governs DNA recognition by TAL effectors. Science *326*, 1501.

Muto, A., Ohkura, M., Kotani, T., Higashijima, S., Nakai, J., and Kawakami, K. (2011). Genetic visualization with an improved GCaMP calcium indicator reveals spatiotemporal activation of the spinal motor neurons in zebrafish. Proceedings of the National Academy of Sciences *108*, 5425–5430.

Myers, P.Z., Eisen, J.S., and Westerfield, M. (1986). Development and axonal outgrowth of identified motoneurons in the zebrafish. The Journal of Neuroscience *6*, 2278–2289.

Nagy, B., Hovhannisyan, A., Barzan, R., Chen, T., and Kukley, M. (2017). Different patterns of neuronal activity trigger distinct responses of oligodendrocyte precursor cells in the corpus callosum. PLoS Biol *15*, e2001993.

Nakayama, T., Blitz, I.L., Fish, M.B., Odeleye, A.O., Manohar, S., Cho, K.W., and

Grainger, R.M. (2014). Cas9-Based Genome Editing in Xenopus tropicalis. Methods Enzymol *546*, 355.

Niederländer, C., and Lumsden, A. (1996). Late emigrating neural crest cells migrate specifically to the exit points of cranial branchiomotor nerves. Development *122*, 2367–2374.

Noma, S., Kiyohara, K., Hirokado, R., Yamashita, N., Migita, Y., Tanaka, M., Furukawa, S., Ogihara, H., Morinaga, Y., Igura, N., et al. (2017). Increase in hydrophobicity of Bacillus subtilis spores by heat, hydrostatic pressure, and pressurized carbon dioxide treatments. J. Biosci. Bioeng.

Okada, M., Nutt, D.J., Murakami, T., Zhu, G., Kamata, A., Kawata, Y., and Kaneko, S. (2001). Adenosine receptor subtypes modulate two major functional pathways for hippocampal serotonin release. The Journal of Neuroscience *21*, 628–640.

Ongini, E., Dionisotti, S., Gessi, S., and Irenius, E. (1999a). Comparison of CGS 15943, ZM 241385 and SCH 58261 as antagonists at human adenosine receptors. Naunyn Schmiedebergs Arch Pharmacol. *359*, 7–10.

Ongini, E., Dionisotti, S., Gessi, S., Irenius, E., and Fredholm, B.B. (1999b). Comparison of CGS 15943, ZM 241385 and SCH 58261 as antagonists at human adenosine receptors. Naunyn-Schmiedeberg's Archives of Pharmacology *359*, 7–10.

Othman, T., Yan, H., and Rivkees, S. (2003). Oligodendrocytes express functional A1 adenosine receptors that stimulate cellular migration. Glia *44*, 166–172.

Palaisa, K.A., and Granato, M. (2007). Analysis of zebrafish sidetracked mutants reveals a novel role for Plexin A3 in intraspinal motor axon guidance. Development *134*, 3251–3257.

Park, H.-C.C., Mehta, A., Richardson, J.S., and Appel, B. (2002). olig2 is required for zebrafish primary motor neuron and oligodendrocyte development. Dev. Biol. *248*, 356–368.

Park, H.-C.C., and Appel, B. (2003). Delta-Notch signaling regulates oligodendrocyte specification. Development *130*, 3747–3755.

Parker, R.J., and Auld, V.J. (2006). Roles of glia in the Drosophila nervous system. Semin. Cell Dev. Biol. *17*, 66–77.

Patel, M.K., Pinnock, R.D., and Lee, K. (2001). Adenosine exerts multiple effects in dorsal horn neurones of the adult rat spinal cord. Brain Research *920*, 19–26.

Perlin, J.R., Lush, M.E., Stephens, W.Z., Piotrowski, T., and Talbot, W.S. (2011). Neuronal Neuregulin 1 type III directs Schwann cell migration. Development *138*, 4639–4648.

Petersen, S.C., Luo, R., Liebscher, I., Giera, S., Jeong, S.-J.J., Mogha, A., Ghidinelli, M., Feltri, M.L., Schöneberg, T., Piao, X., et al. (2015). The adhesion GPCR GPR126 has distinct, domain-dependent functions in Schwann cell development mediated by interaction with laminin-211. Neuron *85*, 755–769.

Peterson, S., and Freeman, J. (2009). RNA isolation from embryonic zebrafish and

cDNA synthesis for gene expression analysis. J Vis Exp Jove.

Philips, T., and Rothstein, J.D. (2017). Oligodendroglia: metabolic supporters of neurons. The Journal of Clinical Investigation *127*, 3271–3280.

Piersen, C., True, C., and Wells, J. (1994). A carboxyl-terminally truncated mutant and nonglycosylated A2a adenosine receptors retain ligand binding. Mol Pharmacol *45*, 861–870.

Portugues, R., Severi, K., Wyart, C., and Ahrens, M. (2013). Optogenetics in a transparent animal: circuit function in the larval zebrafish. Current Opinion in Neurobiology *23*.

Prendergast, A., Linbo, T.H., Swarts, T., Ungos, J.M., McGraw, H.F., Krispin, S., Weinstein, B.M., and Raible, D.W. (2012). The metalloproteinase inhibitor Reck is essential for zebrafish DRG development. Development *139*, 1141–1152.

Qi, Y., Cai, J., Wu, Y., Wu, R., Lee, J., Fu, H., Rao, M., Sussel, L., Rubenstein, J., and Qiu, M. (2001). Control of oligodendrocyte differentiation by the Nkx2. 2 homeodomain transcription factor. Development *128*, 2723–2733.

Quarta, D., Ferré, S., Solinas, M., You, Z., Hockemeyer, J., Popoli, P., and Goldberg, S. (2004). Opposite modulatory roles for adenosine A1 and A2A receptors on glutamate and dopamine release in the shell of the nucleus accumbens. Effects of chronic caffeine exposure. J Neurochem *88*, 1151–1158.

Radomska, K.J., and Topilko, P. (2017). Boundary cap cells in development and

disease. Curr. Opin. Neurobiol. *47*, 209–215.

Raible, D.W., and Eisen, J.S. (1994). Restriction of neural crest cell fate in the trunk of the embryonic zebrafish. Development *120*, 495–503.

Raible, D.W., Wood, A., Hodsdon, W., Henion, P.D., Weston, J.A., and Eisen, J.S. (1992). Segregation and early dispersal of neural crest cells in the embryonic zebrafish. Developmental Dynamics *195*, 29–42.

Rau, A., Ariwodola, O., and Weiner, J. (2015). Postsynaptic Adenosine A2A Receptors Modulate Intrinsic Excitability of Pyramidal Cells in the Rat Basolateral Amygdala. Int J Neuropsychoph *18*, pyv017.

Ravanelli, A.M., and Appel, B. (2015). Motor neurons and oligodendrocytes arise from distinct cell lineages by progenitor recruitment. Genes Dev. *29*, 2504–2515.

Rebola, N., Lujan, R., Cunha, R.A., and Mulle, C. (2008). Adenosine A2A receptors are essential for long-term potentiation of NMDA-EPSCs at hippocampal mossy fiber synapses. Neuron *57*, 121–134.

Richardson, W., Smith, H., Sun, T., Pringle, N., Hall, A., and Woodruff, R. (2000). Oligodendrocyte lineage and the motor neuron connection. Glia *29*, 136–142.

Rombo, D., Dias, R., Duarte, S., Ribeiro, Lamsa, K., and Sebastiao, A. (2014). Adenosine A1 Receptor Suppresses Tonic GABAA Receptor Currents in Hippocampal Pyramidal Cells and in a Defined Subpopulation of Interneurons. Cerebral Cortex *26*, 1081–1095.

Rossi, A., Kontarakis, Z., Gerri, C., Nolte, H., Hölper, S., Krüger, M., and Stainier, D.Y. (2015). Genetic compensation induced by deleterious mutations but not gene knockdowns. Nature *524*, 230.

Rowitch, D.H. (2004). Glial specification in the vertebrate neural tube. Nat. Rev. Neurosci. *5*, 409–419.

Sabirov, R., and Okada, Y. (2005). ATP release via anion channels. Purin Signal *1*, 311–328.

Sato-Maeda, M., Obinata, M., and Shoji, W. (2008). Position fine-tuning of caudal primary motoneurons in the zebrafish spinal cord. Development *135*, 323–332.

Schnädelbach, O., Ozen , I., Blaschuk, O.W., Meyer, R.L., and Fawcett, J.W. (2001). N-cadherin is involved in axon-oligodendrocyte contact and myelination. Mol. Cell. Neurosci. *17*, 1084–1093.

Schulte, G., and Fredholm, B.B. (2003). Signalling from adenosine receptors to mitogen-activated protein kinases. Cellular Signalling *15*, 813–827.

Searl, T.J., and Silinsky, E.M. (2012). Evidence for constitutively-active adenosine receptors at mammalian motor nerve endings. Eur. J. Pharmacol. *685*, 38–41.

Sebastiao, A., and Ribeiro, J. (2015). Neuromodulation and metamodulation by adenosine: impact and subtleties upon synaptic plasticity regulation. Brain Research *1621*, 102–113.

Sepp, K.J., Schulte, J., and Auld, V.J. (2001). Peripheral glia direct axon guidance across the CNS/PNS transition zone. Dev. Biol. *238*, 47–63.

Shen, H., Coelho, J., Ohtsuka, N., Canas, P., Day, Y., Huang, Q., Rebola, N., Yu, L., Boison, D., Cunha, R., et al. (2008). A critical role of the adenosine A2A receptor in extrastriatal neurons in modulating psychomotor activity as revealed by opposite phenotypes of striatum and forebrain …. The Journal of Neuroscience *28*, 2970–2975.

Shin, J., Park, H.-C.C., Topczewska, J.M., Mawdsley, D.J., and Appel, B. (2003). Neural cell fate analysis in zebrafish using olig2 BAC transgenics. Methods in Cell Science *25*, 7–14.

Sievers, F., Wilm, A., Dineen, D., Gibson, T., Karplus, K., Li, W., Lopez, R., McWilliam, H., Remmert, M., Soding, J., et al. (2011). Fast, scalable generation of high-quality protein multiple sequence alignments using Clustal Omega. Mol Syst Biol *7*, 539.

Simons, M., and Nave, K. (2016). Oligodendrocytes: myelination and axonal support. Cold Spring Harb Perspect Biol *8*, a020479.

Smith, C., Johnson, K., Welsh, T., Barresi, M., and Kucenas, S. (2016). Radial glia inhibit peripheral glial infiltration into the spinal cord at motor exit point transition zones. Glia *64*, 1138–1153.

Smith, C.J., Morris, A.D., Welsh, T.G., and Kucenas, S. (2014). Contact-mediated inhibition between oligodendrocyte progenitor cells and motor exit point glia establishes the spinal cord transition zone. PLoS Biol. *12*, e1001961.

Smith, C.J., Wheeler, M.A., Marjoram, L., Bagnat, M., Deppmann, C.D., and Kucenas, S. (2017). TNFa/TNFR2 signaling is required for glial ensheathment at the dorsal root entry zone. PLoS Genet. *13*, e1006712.

Sowa, N., Taylor-Blake, B., and Zylka, M. (2010). Ecto-5′-nucleotidase (CD73) inhibits nociception by hydrolyzing AMP to adenosine in nociceptive circuits. The Journal of Neuroscience.

Stevens, B., and Fields, R.D. (2000). Response of Schwann cells to action potentials in development. Science *287*, 2267–2271.

Stevens, B., Porta, S., Haak, L., Gallo, V., and Fields, R. (2002). Adenosine A Neuron-Glial Transmitter Promoting Myelination in the CNS in Response to Action Potentials. Neuron *36*, 855–868.

Stone, T. (1985). Purines: pharmacology and physiological roles.

Stolt, C.C., Rehberg, S., Ader, M., Lommes, P., Riethmacher, D., Schachner, M., Bartsch, U., and Wegner, M. (2002). Terminal differentiation of myelin-forming oligodendrocytes depends on the transcription factor Sox10. Genes Dev. *16*, 165–170.

Stuhlmiller, T.J., and García-Castro, M.I. (2012). Current perspectives of the signaling pathways directing neural crest induction. Cellular and Molecular Life Sciences .

Takada, N., and Appel, B. (2010). Identification of genes expressed by zebrafish oligodendrocytes using a differential microarray screen. Dev. Dyn. *239*, 2041–2047.

Takada, N., Kucenas, S., and Appel, B. (2010). Sox10 is necessary for oligodendrocyte survival following axon wrapping. Glia *58*, 996–1006.

Tanaka, H., Maeda, R., Shoji, W., Wada, H., Masai, I., Shiraki, T., Kobayashi, M., Nakayama, R., and Okamoto, H. (2007). Novel mutations affecting axon guidance in zebrafish and a role for plexin signalling in the guidance of trigeminal and facial nerve axons. Development *134*, 3259–3269.

Tebano, M., Martire, A., Rebola, N., Pepponi, R., Domenici, M., Gro, M., Schwarzschild, M., Chen, J., Cunha, R., and Popoli, P. (2005). Adenosine A2A receptors and metabotropic glutamate 5 receptors are co-localized and functionally interact in the hippocampus: a possible key mechanism in …. Journal of Neurochemistry *95*, 1188–1200.

Tong, X., Li, X., Zhou, B., Shen, W., Zhang, Z., Xu, T., and Duan, S. (2009). Ca 2+ signaling evoked by activation of Na + channels and Na + /Ca 2+ exchangers is required for GABA-induced NG2 cell migration. The Journal of Cell Biology *186*, 113–128.

Trussell, L., and Jackson, M. (1985). Adenosine-activated potassium conductance in cultured striatal neurons. Proceedings of the National Academy of Sciences *82*, 4857–4861.

Vaglia, J.L., and Hall, B.K. (2000). Patterns of migration and regulation of trunk neural crest cells in zebrafish (Danio rerio). Int. J. Dev. Biol. *44*, 867–881.

Vermeren, M., Maro, G.S., Bron, R., McGonnell, I.M., Charnay, P., Topilko, P., and Cohen, J. (2003). Integrity of developing spinal motor columns is regulated by neural crest derivatives at motor exit points. Neuron *37*, 403–415.

Wake, H., Lee, P.R., and Fields, R.D. (2011). Control of local protein synthesis and initial events in myelination by action potentials. Science *333*, 1647–1651.

Wakisaka, N., Miyasaka, N., Koide, T., Masuda, M., Hiraki-Kajiyama, T., and Yoshihara, Y. (2017). An Adenosine Receptor for Olfaction in Fish. Current Biology.

Wall, M., and Dale, N. (2007). Auto-inhibition of rat parallel fibre–Purkinje cell synapses by activity-dependent adenosine release. The Journal of Physiology *581*, 553–565.

Wang, W.-D.D., Melville, D.B., Montero-Balaguer, M., Hatzopoulos, A.K., and Knapik, E.W. (2011). Tfap2a and Foxd3 regulate early steps in the development of the neural crest progenitor population. Dev. Biol. *360*, 173–185.

Wei, W., Du, C., Lv, J., Zhao, G., Li, Z., Wu, Z., Haskó, G., and Xie, X. (2013). Blocking A2B adenosine receptor alleviates pathogenesis of experimental autoimmune encephalomyelitis via inhibition of IL-6 production and Th17 differentiation. Journal of Immunology *190*, 138–146.

Welsh, T.G., and Kucenas, S. (2018). Purinergic signaling in oligodendrocyte development and function. Journal of Neurochemistry *145*, 6–18.

Williams, M., Francis, J., Ghai, G., Braunwalder, A., Psychoyos, S., Stone, G.A., and Cash, W.D. (1987). Biochemical characterization of the triazoloquinazoline, CGS 15943,

a novel, non-xanthine adenosine antagonist. J. Pharmacol. Exp. Ther. *241*, 415–420.

Witts, E., Nascimento, F., and Miles, G. (2015). Adenosine-mediated modulation of ventral horn interneurons and spinal motoneurons in neonatal mice. J Neurophysiol *114*, 2305–2315.

Wolpowitz, D., Mason, T.B., Dietrich, P., Mendelsohn, M., Talmage, D.A., and Role, L.W. (2000). Cysteine-rich domain isoforms of the neuregulin-1 gene are required for maintenance of peripheral synapses. Neuron *25*, 79–91.

Wu, L.-G., and Saggau, P. (1994). Adenosine inhibits evoked synaptic transmission primarily by reducing presynaptic calcium influx in area CA1 of hippocampus. Neuron *12*, 1139–1148.

Wu, L.-G., and Saggau, P. (1997). Presynaptic inhibition of elicited neurotransmitter release. Trends Neurosci *20*, 204–212.

Xiao, L., Hu, C., Yang, W., Guo, D., Li, C., Shen, W., Liu, X., Aijun, H., Dan, W., and He, C. (2013). NMDA receptor couples Rac1-GEF Tiam1 to direct oligodendrocyte precursor cell migration. Glia *61*, 2078–2099.

Xiao, L., Ohayon, D., McKenzie, I., Sinclair-Wilson, A., Wright, J., Fudge, A., Emery, B., Li, H., and Richardson, W. (2016). Rapid production of new oligodendrocytes is required in the earliest stages of motor-skill learning. Nature Neuroscience *19*, 1210–1217.

Yao, C., Vanderpool, K., Delfiner, M., Eddy, V., Lucaci, A., Soto-Riveros, C., Yasumura, T., Rash, J., and Pereda, A. (2014). Electrical synaptic transmission in developing

zebrafish: properties and molecular composition of gap junctions at a central auditory synapse. Journal of Neurophysiology *112*, 2102–2113.

Yu, R.C., Power, J., Barnea, G., O'Donnell, S., Brown, H.E., Osborne, J., Axel, R., and Gogos, J.A. (2004). Spontaneous neural activity is required for the establishment and maintenance of the olfactory sensory map. Neuron *42*, 553–566.

Zhang, P., Bannon, N.M., Ilin, V., Volgushev, M., and Chistiakova, M. (2015). Adenosine effects on inhibitory synaptic transmission and excitation-inhibition balance in the rat neocortex. The Journal of Physiology *593*, 825–841.

Zhang, Y., Chen, K., Sloan, S., Bennett, M., Scholze, A., O'Keeffe, S., Phatnani, H., Guarnieri, P., Caneda, C., Ruderisch, N., et al. (2014). An RNA-sequencing transcriptome and splicing database of glia, neurons, and vascular cells of the cerebral cortex. The Journal of Neuroscience *34*, 11929–11947.

Zhou, Q., Choi, G., and Anderson, D.J. (2001). The bHLH transcription factor Olig2 promotes oligodendrocyte differentiation in collaboration with Nkx2.2. Neuron *31*, 791–807.

Zhu, Y., Matsumoto, T., Nagasawa, T., Mackay, F., and Murakami, F. (2015). Chemokine Signaling Controls Integrity of Radial Glial Scaffold in Developing Spinal Cord and Consequential Proper Position of Boundary Cap Cells. The Journal of Neuroscience *35*, 9211–9224.

Zimmermann, H. (2000). Extracellular metabolism of ATP and other nucleotides.

Naunyn-Schmiedeberg's Arch of Pharmacol *362*, 299–309.

Ziskin, J., Nishiyama, A., Rubio, M., Fukaya, M., and Bergles, D. (2007). Vesicular release of glutamate from unmyelinated axons in white matter. Nature Neuroscience *10*, 321–330.

Zuchero, J.B., and Barres, B.A. (2015). Glia in mammalian development and disease. Development *142*, 3805–3809.